



**FIRST MINING
GOLD**



APPENDIX L

HYDROGEOLOGY TECHNICAL SUPPORT DOCUMENTS

- L-1 Baseline Hydrogeology Report
- L-2 Hydrogeological Modeling Report**



Hydrogeological Modelling Report

Springpole Gold Project

First Mining Gold Corp.

ONS2104

Prepared by:
WSP Canada Inc.

October 2024



Hydrogeological Modelling Report

Springpole Gold Project

Red Lake District, Northwest Ontario
Project #ONS2104

Prepared for:

First Mining Gold Corp.
Suite 2070, 1188 West Georgia Street
Vancouver, British Columbia, V6E 4A2

Prepared by:

WSP Canada Inc.
6925 Century Avenue, Suite 600
Mississauga, Ontario, L5N 7K2
Canada
T: (905) 567-4444

Copyright

The contents and layout of this report are subject to copyright owned by WSP Canada Inc.

EXECUTIVE SUMMARY

First Mining Gold Corp. proposes to develop, operate and eventually decommission / close an open pit gold and silver mine and ore process plant with supporting facilities known as the Springpole Gold Project (Project). The Project is located in a remote area of northwestern Ontario, approximately 110 kilometres (km) northeast of the Municipality of Red Lake and 145 km north of the Municipality of Sioux Lookout (Figure 1–1).

An environmental assessment pursuant to the *Canadian Environmental Assessment Act, 2012* (SC 2012, c. 19, s. 52) and the Ontario *Environmental Assessment Act* (RSO 1990, c. E.18) is required to be completed for the Project. This report is one of a series of Technical Support Documents prepared by WSP Canada Inc. on behalf of First Mining Gold Corp. to describe the predicted environmental effects of the Project.

During the consultation process, Project-specific input from regulatory agencies and Indigenous communities was considered at key milestones of the environmental assessment process including baseline studies, alternatives, assessment approach, mitigation and monitoring where appropriate. An overview of the consultation input that was considered during the assessment in relation to this assessment will be summarized in the final Environmental Impact Statement / Environmental Assessment.

The proposed Project is situated between two prominent lakes, Birch Lake and Springpole Lake. The physiography of the area consists of subdued and undulating hills characteristic of glaciated landscapes with thin and sparse overburden deposits overlying bedrock. A zone of very low rock quality designation (RQD) rock and unconsolidated granular material (UGM), associated with the primary zone of mineralization, corresponds to the deepest section of the north basin of Springpole Lake. Both of these low RQD and UGM zones exhibit relatively higher permeabilities compared to the surrounding host bedrock, which is generally of lower permeability. This contrast is especially evident for the area west of the low RQD and UGM zones, which consists of competent and low permeability andesite rock.

The Project site plan includes an open pit of approximately 300 metres (m) depth that coincides with the deepest section of the north basin of Springpole Lake. The pit will be isolated from Springpole Lake by two dikes to the south and southeast of the open pit.

A co-disposal facility (CDF) for tailings and mine rock materials is proposed to be built to the west of the open pit, corresponding to the area of competent andesite bedrock. The CDF features two cells: north and south. The south cell features a design concept to maintain high saturations, with the aid of a geosynthetic clay liner placed on the upstream side embankment around the perimeter, to resist the ingress of oxygen to mitigate acid generation. The CDF also includes a collection ditch around its perimeter to collect / manage runoff and CDF seepage.

A numerical groundwater model has been developed to simulate conditions at the proposed Project site to assess the potential of effects of mine development on the local groundwater environment and support environmental reporting activities. The model was developed and calibrated using information gathered as part of baseline characterization activities. Once calibrated, the model was used to conduct predictive simulations for two phases of mine life: 1) end of mine operations, representing conditions immediately following mine closure, 2) and post-closure, representing conditions long after closure. Simulations were conducted to estimate effects of mine infrastructure / operation on the surrounding groundwater environment. In addition to base case simulations for each of these mine phases, a suite of sensitivity simulations was run to assess the effects of model input parameter uncertainty on the model simulation results.

Simulations for the end of mine operations case focused on the estimation of groundwater inflow rates to the dewatered open pit and the overall effects on groundwater–surface interactions (i.e., groundwater flow budgets). Based on these simulations:

- The simulated groundwater inflow rate to the fully developed open pit for the base-case is 3,034 cubic metres per day (m^3/d). This ranges from 3,095 to 10,612 m^3/d in the sensitivity analyses, with the greatest groundwater inflow rate corresponding to the case where the low RQD zone is increased in spatial extent by 200 m.
- Groundwater flow budget analysis indicates that Springpole Lake and Birch Lake contribute the bulk of groundwater flow into the dewatered open pit. The effects on these are both most sensitive to the hydraulic conductivity of host bedrock (excluding the CDF area) and the extent of the low RQD zone. Water budgets for other smaller surface water features are also affected by open pit dewatering. Though the total effects for these smaller features are small compared to the larger features, the relative changes are comparable or greater in some cases.
- The open pit captures the majority CDF of seepage that bypasses the perimeter collection ditches. For the combined north and south cells, approximately 20 percent (%) of the total seepage is captured by the open pit and 73% discharges to the perimeter collection ditches, resulting in a combined capture of 93%.

Simulations for post-closure conditions focused on the estimation of groundwater seepage rates discharging from the CDF to surrounding surface water features. Based on these simulations:

- Overall, simulated seepage bypass rates from the CDF to nearby surface water receivers are very low in comparison to the overall water balance for the primary receivers (i.e., Springpole Lake and Birch Lake). Simulated seepage rates for these features are generally in the tens of cubic metres per day range, while the overall water budgets are hundreds of thousands of cubic metres per day.
- For the base-case model, approximately 90% of the groundwater seepages from both the north and south cells of the CDF discharge at the downstream toes of the perimeter CDF dams (i.e., “capture,” which would subsequently runoff to the perimeter collection ditches).
- Predicted groundwater seepage from the north cell is driven by the applied 200 millimetres per year (mm/yr) of infiltration and is most sensitive to this infiltration value.
- Seepage from the south cell is driven by the constant head boundary condition applied to the top surface (representing the assumed shallow groundwater depth conditions in the south cell). Sensitivity analysis for the south cell shows that the total seepage is most sensitive to the permeability of tailings in the south cell. The amount of bypass, however, is most sensitive to the hydraulic properties of a potential east-west trending bedrock structure underlying the south cell (corresponding to a topographic lineament, simulated as a zone of increased permeability for sensitivity analysis).
- Sensitivity analysis was conducted on the south cell embankment liner to assess liner performance, based on a range of assumed liner permeabilities in a two-dimensional cross sectional model. Simulation results indicate that, while increased liner permeability results in increased total seepage, there is only a very minor increase in the total amount of bypass to the environment since seepage penetrating / exfiltrating the liner enters the dams and subsequently discharges at the toe of the dam, which is captured by the perimeter collection ditches. Separate two-dimensional simulations were also conducted to assess the effect of introducing a liner at the base of the CDF south cell on amount of seepage emanating from the south cell, which are discussed under separate cover

(Appendix V-1). Results from this modelling indicated that the incorporation of a basal liner to the CDF south cell (i.e., in addition to the liner along the embankments) results in only a minimal decrease in seepage bypass compared to the case with the liner only on the dam embankments.

Numerical groundwater model simulations and sensitivity runs presented in this report highlight the following hydrogeological features which are of primary interest:

1. The hydraulic conductivity of the bedrock surrounding the open pit, represented conceptually by both / either of the extent of the low RQD zone or the overall hydraulic conductivity of the host bedrock zone outside of the CDF area, has the most influence on the simulated groundwater inflow rate to the open pit and the effects on groundwater–surface water balance.
2. The hydraulic conductivity of bedrock immediately underlying the CDF influences the total rate of seepage emanating from the south cell. Changes in the assumed hydraulic conductivity of shallow bedrock exert a similar level of control on predicted seepage rates as changes in the assumed hydraulic properties of the tailings themselves.

TABLE OF CONTENTS

	PAGE
1.0 INTRODUCTION	1-1
1.1 Background	1-1
1.2 Proposed Mining and Dewatering	1-1
2.0 SITE SETTING	2-1
2.1 Physiographic Setting.....	2-1
2.2 Geological Setting	2-1
2.3 Surface Water Features.....	2-2
3.0 HYDROGEOLOGICAL SETTING.....	3-1
3.1 Hydrostratigraphy.....	3-1
3.2 Hydraulic Conductivity.....	3-1
3.2.1 Overburden Hydraulic Conductivity	3-1
3.2.2 Bedrock Hydraulic Conductivity	3-1
3.3 Groundwater Levels.....	3-2
3.4 Groundwater Recharge.....	3-2
4.0 CONCEPTUAL HYDROGEOLOGICAL MODEL	4-1
4.1 Pre-mining Phase Conditions.....	4-1
4.2 Mining Phase Conditions	4-2
5.0 GROUNDWATER MODEL DEVELOPMENT	5-1
5.1 Model Construction	5-1
5.1.1 Domain, Discretization and Numerical Setup.....	5-1
5.1.2 Simulated Hydrostratigraphy.....	5-2
5.1.3 Boundary Conditions for Pre-mining Phase Simulation	5-2
5.2 Pre-mining Phase Model Calibration (baseline conditions).....	5-3
5.3 Model Limitations	5-5
6.0 MINING PHASE SIMULATIONS	6-1
6.1 End of Mine Operations Phase Simulations	6-2
6.1.1 End of Mine Operations Phase Simulation Results.....	6-3
6.2 Post-closure Phase Simulations	6-4
6.2.1 Post-closure Phase Simulation Results	6-4
7.0 SENSITIVITY ANALYSIS	7-1
7.1 End of Mine Operations (Variants 0 to 5).....	7-1
7.2 Post-closure (Variants 6 to 10)	7-1
7.3 South Cell Embankment Liner Effectiveness (Variant 11)	7-2
8.0 SUMMARY AND CONCLUSIONS	8-1
9.0 CLOSING	9-1
10.0 REFERENCES	10-2

LIST OF TABLES

Table 3-1: Site Hydrostratigraphic Units	3-4
Table 3-2: Estimated Hydraulic Conductivity Data Summary	3-5
Table 3-3: Measured Water Level Data (fall 2022)	3-6
Table 5-1: Model Numerical Setup	5-6
Table 5-2: Simulated Hydrostratigraphic Units with Initial Input Hydraulic Conductivities	5-6
Table 5-3: Simulated Boundary Conditions	5-6
Table 5-4: Post-calibration Pre-mining Model Parameters	5-7
Table 6-1: End of Mine Operations Model Simulated Water Budgets.....	6-6
Table 6-2: Simulated End of Mine Operations Seepage Rates	6-6
Table 6-3: Post-closure Model Simulated Water Budgets.....	6-7
Table 6-4: Simulated Post-closure Seepage Rates.....	6-7
Table 7-1: Sensitivity Simulation Variants.....	7-4
Table 7-2: Simulated Groundwater Budgets for End of Mine Operations Sensitivity Analysis	7-4
Table 7-3: Simulated Groundwater Budgets for Post-closure Sensitivity Analysis	7-4
Table 7-4: Summary of Post-closure Variant Seepages	7-5
Table 7-5: Simulated South Cell Seepages for Model Variants (post-closure)	7-5
Table 7-6: Simulated North Cell Seepages for Model Variants (post-closure)	7-5
Table 7-7: 2D Model Simulated Flows for Variant 11	7-5

LIST OF FIGURES

Figure 1-1: Project Location.....	1-3
Figure 1-2: EIS / EA Site Plan	1-4
Figure 2-1: Site Topography and Springpole Lake Bathymetry	2-3
Figure 2-2: Local Geologic Setting	2-4
Figure 2-3: Site Hydrological Map	2-5
Figure 3-1: Bedrock Zones	3-8
Figure 3-2: Measured Bedrock Hydraulic Conductivity Data	3-9
Figure 3-3: Measured Groundwater Levels and Contours (October 2022).....	3-10
Figure 4-1: Hydrostratigraphic Cross Section – Transverse to Open Pit.....	4-4
Figure 4-2: Conceptual Diagram for End of Mine Operations Conditions (CDF South Cell)	4-5
Figure 4-3 : Conceptual Diagram for Post-Closure Conditions (CDF South Cell)	4-6
Figure 5-1: Model Domain and Mesh.....	5-8
Figure 5-2: 3D Model Domain and Layers	5-9
Figure 5-3: Interpolated Overburden Thickness.....	5-10
Figure 5-4: Interpolated Lakebed Organic Thickness for Springpole Lake.....	5-11
Figure 5-5: Model Layers Cross Section.....	5-12
Figure 5-6: Bedrock Layers Plan View (26 mbgs)	5-13
Figure 5-7: Pre-mining Model Boundary Conditions	5-14
Figure 5-8: Calibration Scattergram	5-15
Figure 5-9: Simulated and Measured Heads with Residuals	5-16
Figure 5-10: Simulated and Measured Host Bedrock Hydraulic Conductivity	5-17
Figure 6-1: Mining Phase 3D Model View.....	6-8
Figure 6-2: Sub-watershed of Hydrological Nodes.....	6-9
Figure 6-3: Simulated Boundary Conditions for EoMO Model.....	6-10
Figure 6-4: Simulated Shallow Bedrock Head Contours for End of Mine Operations Model.....	6-11

Figure 6–5: Simulated Shallow Bedrock Drawdown Contours for End of Mine Operations Model.....	6-12
Figure 6–6: Simulated Budgets at Birch Lake Shoreline.....	6-13
Figure 6–7: Simulated Budgets at Springpole Lake Dikes.....	6-14
Figure 6–8: Simulated Boundary Conditions for Post-Closure Model	6-15
Figure 6–9: Simulated Shallow Bedrock Head Contours for Post-closure Model	6-16
Figure 6–10: Simulated Co-disposal Facility Seepage Pathway for Post-closure Model	6-17
Figure 7–1: E-W Fault SW-2 Location for Sensitivity Simulations	7-6
Figure 7–2: Variant 10 Shallow Bedrock Head Contours (masl)	7-7
Figure 7–3: 2D Model for Variant 11 Simulations	7-8

LIST OF ABBREVIATIONS

%	percent
2D	two-dimensional
3D	three-dimensional
CDF	co-disposal facility
DEM	digital elevation model
EIS	Environmental Impact Statement / Environmental Assessment
EoMO	end of mine operations
GCL	geosynthetic clay liner
ha	hectare
K	hydraulic conductivity
K _H	horizontal hydraulic conductivity
km	kilometre
km ²	square kilometre
K _V	vertical hydraulic conductivity
LiDAR	light detection and ranging
m	metre
m/s	metres per second
m ³ /d	cubic metres per day
m ³ /d/m	cubic metres per day per metre
MAE	mean absolute error
ME	mean error
m amsl	metres above mean sea level
mbgs	metres below ground surface
mm/yr	millimetres per year
MW	monitoring well
Project	Springpole Gold Project
RMSE	root-mean-square error
RQD	rock quality designation
UGM	unconsolidated granular material
VWP	vibrating wire piezometer
WSP	WSP Canada Inc.

1.0 INTRODUCTION

First Mining Gold Corp. (FMG) proposes to develop, operate and eventually decommission and close an open pit mine and ore process plant with supporting facilities known as the Springpole Gold Project (Project). The Project is located in a remote area of northwestern Ontario, approximately 110 kilometres (km) northeast of the Municipality of Red Lake and 145 km north of the Municipality of Sioux Lookout, shown in Figure 1–1.

An environmental assessment pursuant to the *Canadian Environmental Assessment Act, 2012* (SC 2012, c. 19, s. 52) and the Ontario *Environmental Assessment Act* (RSO 1990, c. E.18) is required to be completed for the Project. This document is part of a series of modelling / assessment reports prepared by WSP Canada Inc. (WSP) on behalf of FMG to describe the changes in environmental conditions.

During the consultation process, Project-specific input from regulatory agencies and Indigenous communities was considered at key milestones of the environmental assessment process including baseline studies, alternatives, assessment approach, mitigation and monitoring where appropriate. An overview of the consultation input that was considered during the effects assessment in relation to this report will be summarized in the Environment Impact Statement / Environmental Assessment (EIS/EA). The updated hydrogeological modelling, presented in this report, includes additional simulations, outputs and discussion based on the additional field data/information collected since the preparation of the draft EIS/EA.

The intent in this report is to describe groundwater modelling activities that have been conducted in support of the EIS/EA. This report supersedes the groundwater modelling report prepared for the draft EIS/EA (Wood 2022). This report is accompanied by an updated baseline hydrogeological conditions report (Appendix L-1), which provides a comprehensive summary of the hydrogeological data on which the groundwater flow model described in this report are based. Section 2.0 and Section 3.0 of this report provide a brief summary of the relevant hydrogeological field data related to the development of the numerical model. This report also includes additional analyses and discussion based on feedback provided by government agencies and Indigenous communities.

1.1 Background

Gold exploration at the Project has been carried out during two main periods, with the first period being in the 1920s to 1940s, and the second period from 1985 to the present.

The first period of exploration included trenching and prospecting activities carried out followed by advancement of 10 shallow boreholes totaling about 450 metres (m) in depth. After this, the site lay dormant until the second phase of exploration began in the mid-1980s and continues to the present day.

Work conducted in the second period of exploration has consisted of both airborne and ground based geophysical surveys as well as significant advancement of diamond drill holes across the Project site. Information collected during this work led to the identification of the currently understood prospect areas.

1.2 Proposed Mining and Dewatering

The proposed open pit and relevant site features are shown in Figure 1–2. The proposed Project will consist of an open pit that is to be developed in phases. The ultimate open pit is roughly oval in shape trending northwest–southeast and following the mineralization zone. The open pit will be approximately 1.7 km long with a maximum width of 1 km and approximately 120 hectares (ha) in size. The pit footprint extends under the north basin of Springpole Lake and will be about 300 m deep at its deepest point.

Two dikes will be built to isolate the open pit from the lake. These dikes are expected to be approximately 38 m wide and have a combined length of 940 m.

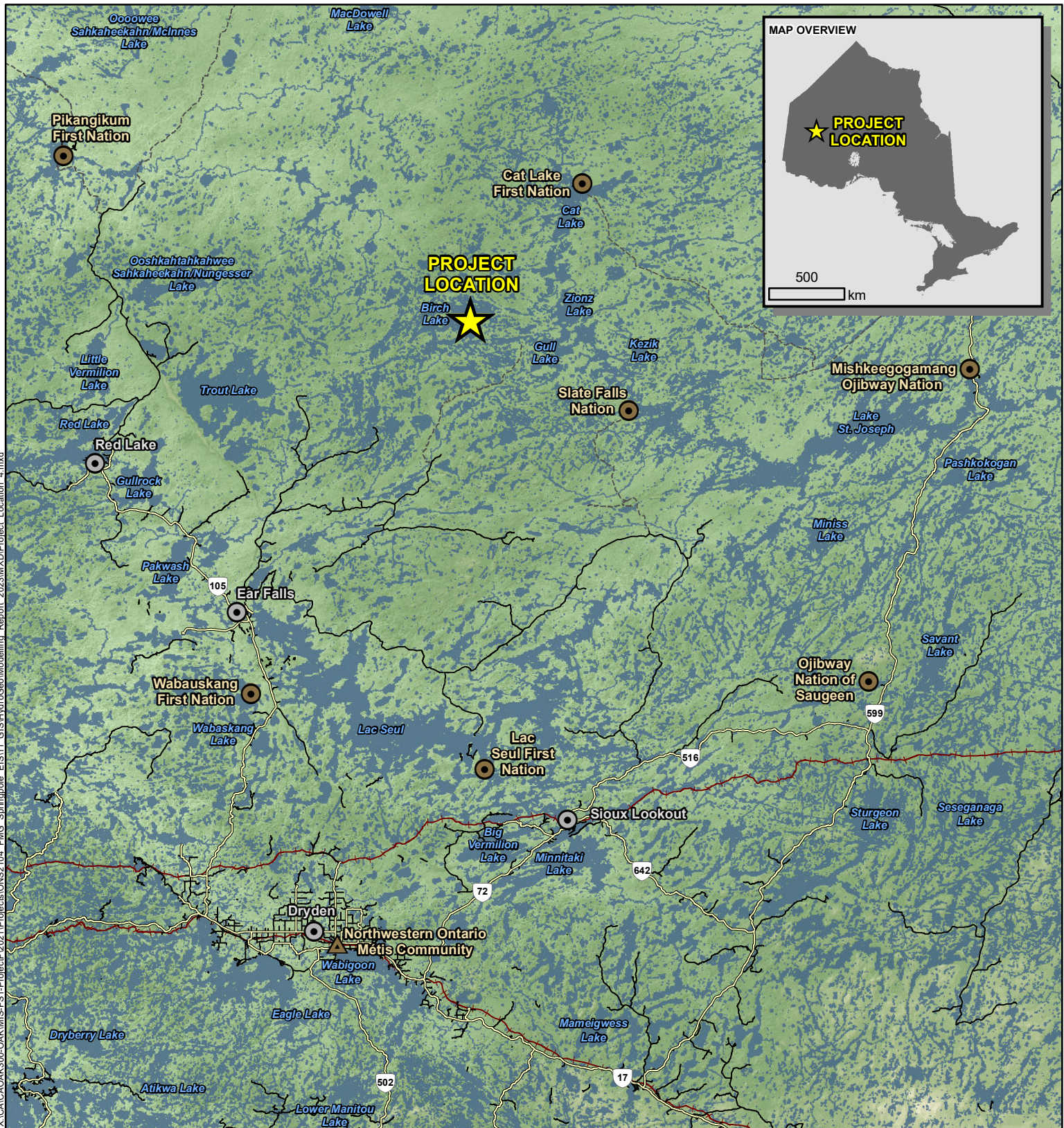
In addition to the open pit, a fish habitat development area will be excavated near the plant location during the pre-production period.











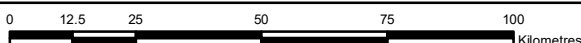
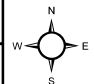
The proposed low grade ore stockpile area straddles the surface water flow divide between Birch Lake and Springpole Lake. The medium and high grade ore stockpile is located adjacent Springpole Lake.

A single co-disposal facility (CDF) will be constructed west of the open pit for storage of tailings from ore processing and mine rock from mining. The CDF will contain two cells: the south cell containing primary potentially acid generating slurry tailings and the north cell containing thickened non-acid generating tailings and mine rock. Details on the conceptual design of the CDF facility are provided in Appendix V-1.

The design of the CDF includes maintaining a high water table or near saturated conditions to avoid oxygenation of the mine rock that will be stored within the facility, and therefore prevent acid generation from minerals within the mine rock. The tailings will go through a sulphide removal process in the plant, before discharge to the CDF, to prevent or reduce their potential to become acid generating.

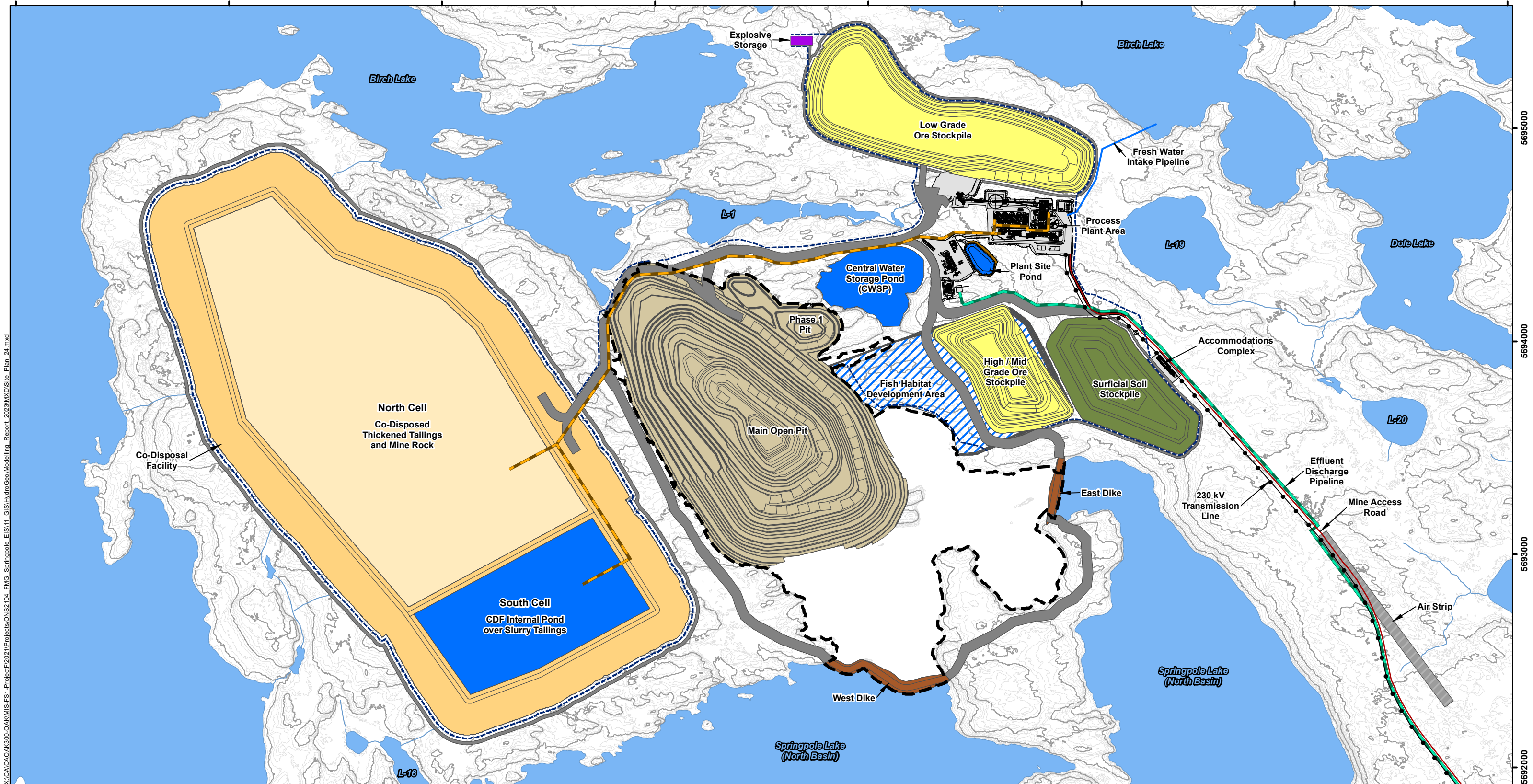
X:\CA\CA0300-OAK\MIS-FS1-Project\ONS2104-FMG_Springpole_EIS\11 GIS\HydroGeoModelling_Report_2023\MXD\Project_Location_4.mxd



LEGEND		NOTES: - Topographic information extracted from LIO, MNRF.		 FIRST MINING GOLD 	
 Project Location	 Railway			SPRINGPOLE GOLD PROJECT	
 Town				Project Location	
 First Nation Reserve					
 Northwestern Ontario Métis Community					
 Highway					
 Secondary Road					
 Resource / Winter Road					
		Datum: NAD83 Projection: UTM Zone 15N		PROJECT N ^o : ONS2104	FIGURE: 1-1
				SCALE: 1:1,500,000	DATE: September 2024

546000 547000 548000 549000 550000 551000 552000 553000

X:\CA\CAOAK300-OAKMIS-FS1-Project\2021\Projects\ONS2104_EMG_Springpole_EIS\11 GIS\HydroGeo\Modelling_Report_2023\MXD\Site_Plan_24.mxd



LEGEND

Watercourse

Waterbody

Major Contours (5 m interval)

Minor Contours (1 m interval)

Proposed Mine Features

Open Pit

Open Pit Basin

Ore Stockpile

Surficial Soil Stockpile

Co-Disposal Facility

Co-Disposed Thickened Tailings and Mine Rock

Process Plant Area

Dike

Pond

Haul / Access Road

Explosives Storage

Air Strip

Mine Access Road

Seepage / Runoff Collection System

230 kV Transmission Line

Fresh Water Intake Pipeline

Effluent Discharge Pipeline

Tailings Pipeline Corridor

Fish Habitat Development Area

NOTES:

- Contours extracted from 2020 LiDAR survey.

- Proposed site plan provided by Ausenco, drawing number 104496-GX-03000-31344-003, Rev 1. 26 June 2023 and modified by WSP July 2023.

- 230 kV transmission line provided by First Mining Gold, April 2024.

Datum: NAD83

Projection: UTM Zone 15N

N

W

E

S

FIRST MINING GOLD

WSP

SPRINGPOLE GOLD PROJECT

EIS / EA Site Plan

PROJECT N°: ONS2104

SCALE: 1:17,000

FIGURE: 1-2

DATE: September 2024

0

0.5

1

2

3

4

5

Kilometres

2.0 SITE SETTING

Detailed discussions on the site physiographic and geological setting are provided in the 2023 Baseline Hydrogeological Conditions report (Appendix L-1). The following sub-sections provide a brief summary of this information.

2.1 Physiographic Setting

The proposed mine site is situated within the western Superior Province of the Canadian Shield physiographic region where the landscape is dominated by recent glacial activity. The undulating and subdued topography clearly shows the effects of glaciation, whereby cyclical ice advances and retreats eroded ancient mountain ranges and generally deposited and reworked sediment in low-lying areas. The climate at the Project site can be classified as subarctic with cold winters and mild summers. The bulk of precipitation at the Project site occurs as rain in the warmer months although winter snowfall amount can be substantial.

Site topography is shown in Figure 2–1. The topography is typical of northern Ontario and can be characterized as moderately rugged. The elevation of Springpole Lake is 391 metres above mean sea level (m amsl), based on site light detection and ranging (LiDAR) data, and increases 35 m to a topographic high area located northwest of Lake L-3 with an elevation 426 m amsl.

The topography east of the proposed open pit is similar to the topographic high area, at 414 m amsl elevation separating the catchment of Dole Lake / South Dole Lake, which drains into Birch Lake, from that of Springpole Lake.

Existing land cover at site consists almost exclusively of forested area, with a combination of deciduous, coniferous and mixed forest. Aside from the forested area, a minimal footprint associated with the existing exploration camp is present.

2.2 Geological Setting

The characterization of Project site overburden is based on stratigraphic information gathered as part of site characterization activities, as detailed overburden geology mapping from the Ontario Geological Survey is not available for the Project site. Treatment of overburden in the numerical model is described in Section 3.1 and Section 5.1.

Detailed discussion on the regional bedrock setting is provided in the 2023 Baseline Hydrogeological Conditions report (Appendix L-1). Generally, the Project area comprises a zone of weak bedrock associated with the ore zone (i.e., the Portage Zone) and the surrounding host bedrock which consists of metasedimentary and metavolcanic rock, as well as numerous intrusions, which is shown in Figure 2–2. The Portage Zone is further divisible between a zone of unconsolidated granular material (UGM), termed the UGM zone, and the adjacent rock which has low rock quality designation (RQD), called the low RQD zone. Lithologies of the host bedrock consist primarily of mafic to felsic metavolcanic rock and metasedimentary rock, the primary rock type in the area of the CDF being relatively competent andesite. Several bedrock structures have been mapped in the area of the ore zone (SRK 2013, 2024). The primary feature of interest is an east-west trending fault SW-2 which intersects the open pit and correlates to a topographic lineament that underlies the CDF. The potential effects of this on groundwater seepage are described in Section 7.0.

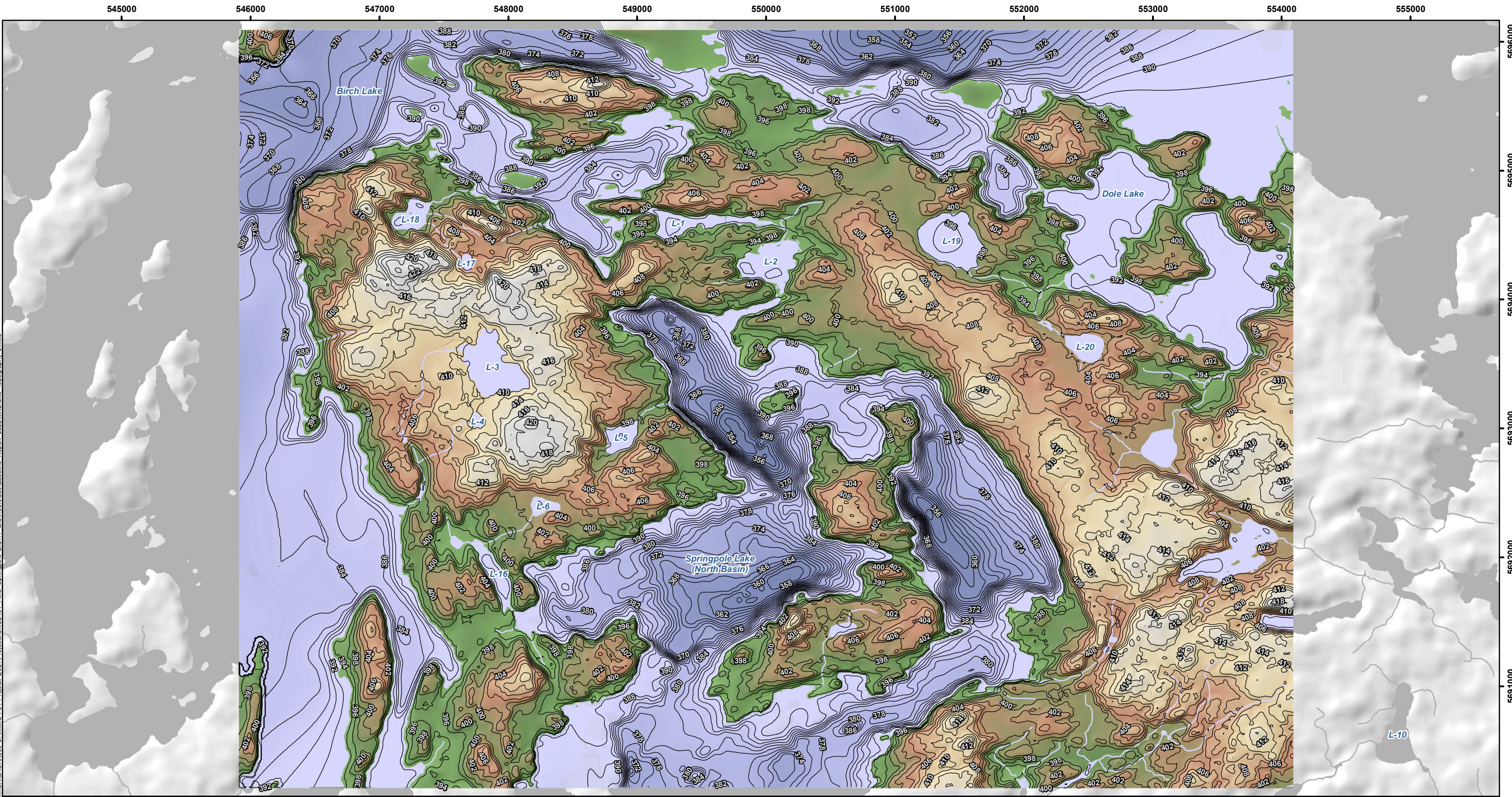
2.3 Surface Water Features

Detailed discussion of the surface water features and hydrology of the Project area can be found in the Hydrology Baseline Report (Appendix M-1). Major surface water features relevant to the Project are summarized briefly here. The Project site area falls between two major watersheds, including Birch Lake and Springpole Lake. These are shown in Figure 2–3.

Birch Lake is a large lake that is located upstream of Springpole Lake. It has a watershed area of approximately 1,050 square kilometres (km²). The elevation of Birch Lake is approximately 393 m amsl and is about 2 m higher than Springpole Lake, depending on the season.

The local Springpole Lake watershed is approximately 98 km²; however the total area reporting to the Springpole Lake outlet is approximately 1,370 km². The water surface elevation of Springpole Lake near the Project is approximately 391 m, although levels fluctuate between seasons.

Within the Springpole Lake surface water catchment area, there are a number of smaller ponds and creeks which drain into both Birch Lake and Springpole Lake. In the northern portion of Springpole Lake, these smaller watershed features generally contribute relatively little flow to Springpole Lake. Along the northern shore of the southeast portion of Springpole Lake, many of the smaller creeks are ephemeral in nature. The south shore of the southeast arm of Springpole Lake accepts surface runoff from several catchments of interconnected ponds that are permanent in nature although the surface water inputs are relatively small compared to the inflow from Cromarty Lake (which accepts surface flow from Birch Lake). Smaller lakes near the Project area include 20 L-series lakes / ponds (e.g., L-2). Of these features, L-3 to L-18 will be overprinted by the CDF and L-2 will be managed as a water storage pond during mine operations.



LEGEND

— Contours (2 metre interval)

Elevation (masl)

424


352


0 0.5 1 2 3 4 5 Kilometres

NOTES:

Datum: NAD83
Projection: UTM Zone 15N

N
W E
S

 **FIRST MINING GOLD**



SPRINGPOLE GOLD PROJECT

Site Topography and Springpole Lake Bathymetry

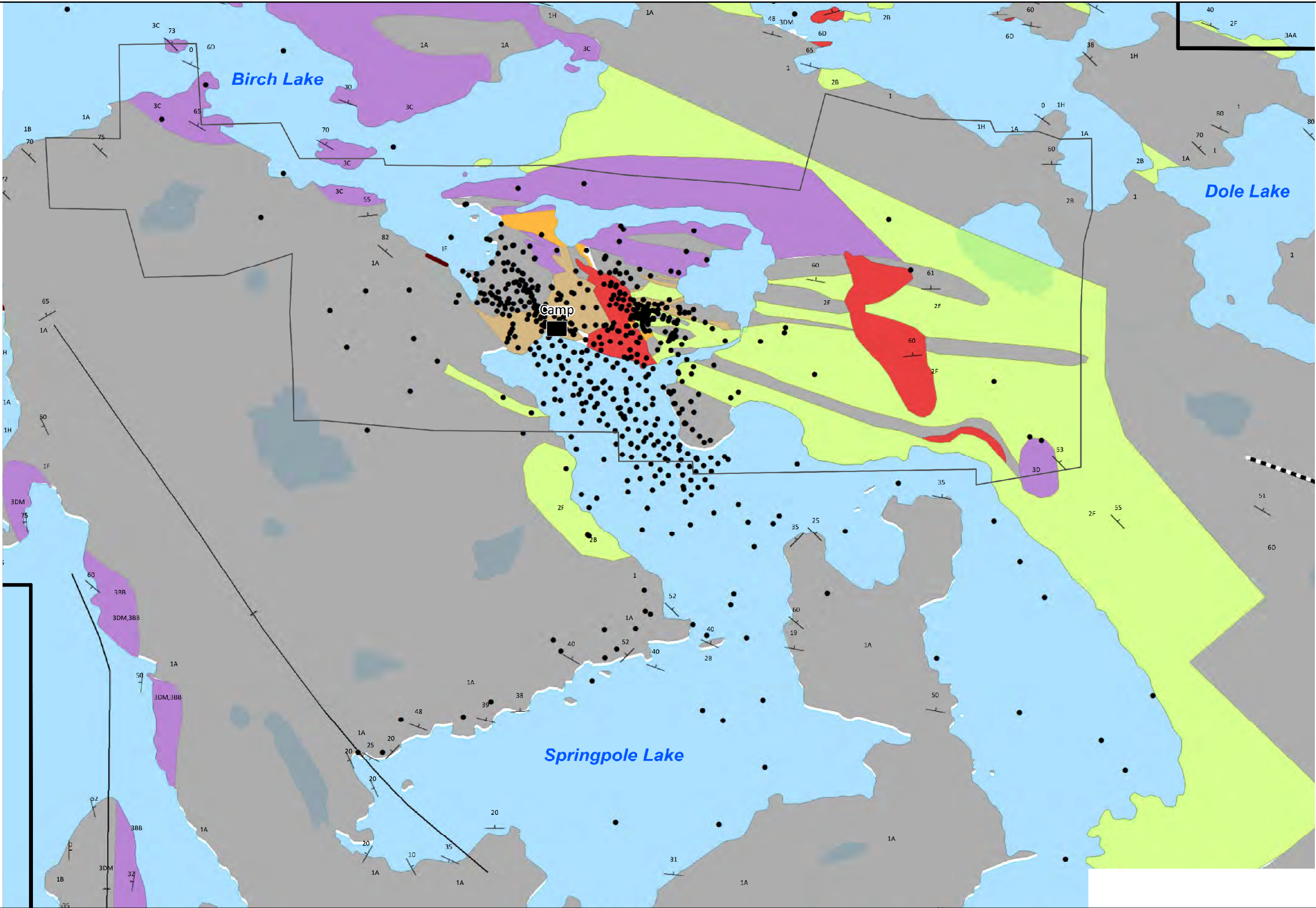
PROJECT N^o: ONS2104

SCALE: 1:28,000

FIGURE: 2-1

DATE: October 2023

X:\CA\CAOAK300-OAK\MS-FS1-ProjectF\2021\Projects\ONS2104_FMG_Springpole_EIS11_GIS\HydroGeoModelling_Report_2023\MXD\Site_Bedrock_Geology_1.mxd



LEGEND

- Drillhole Collar
 - Camp
 - ▭ Property Outline
 - ▭ Patents Outline
- Geology Mapping 20k Scale**

1-Mafic to Intermediate Metavolcanics; 1A-Massive Lava	2A-Rhyolite	6B-Quartz Porphyry	— BIF
2-Intermediate to Felsic Metavolcanics; 2B-Intermediate to Felsic Tuff	3AA-Clastic Sediment; 3C-Conglomerate; 3DM-Metasediments; 3BB-Siltstone and Greywacke; 3	6D-Feldspar Porphyry	▬▬▬ Shear
		B	— Anticline
		O	— Syncline
		Lithology Observation	
		Structure Strike/Dip	

NOTES:
- Site bedrock geology provided by FracFlow Consultants Inc., Hydrogeology Baseline Report 19 February 2021.

Datum: NAD83
Projection: UTM Zone 15N



SPRINGPOLE GOLD PROJECT

Local Geologic Setting

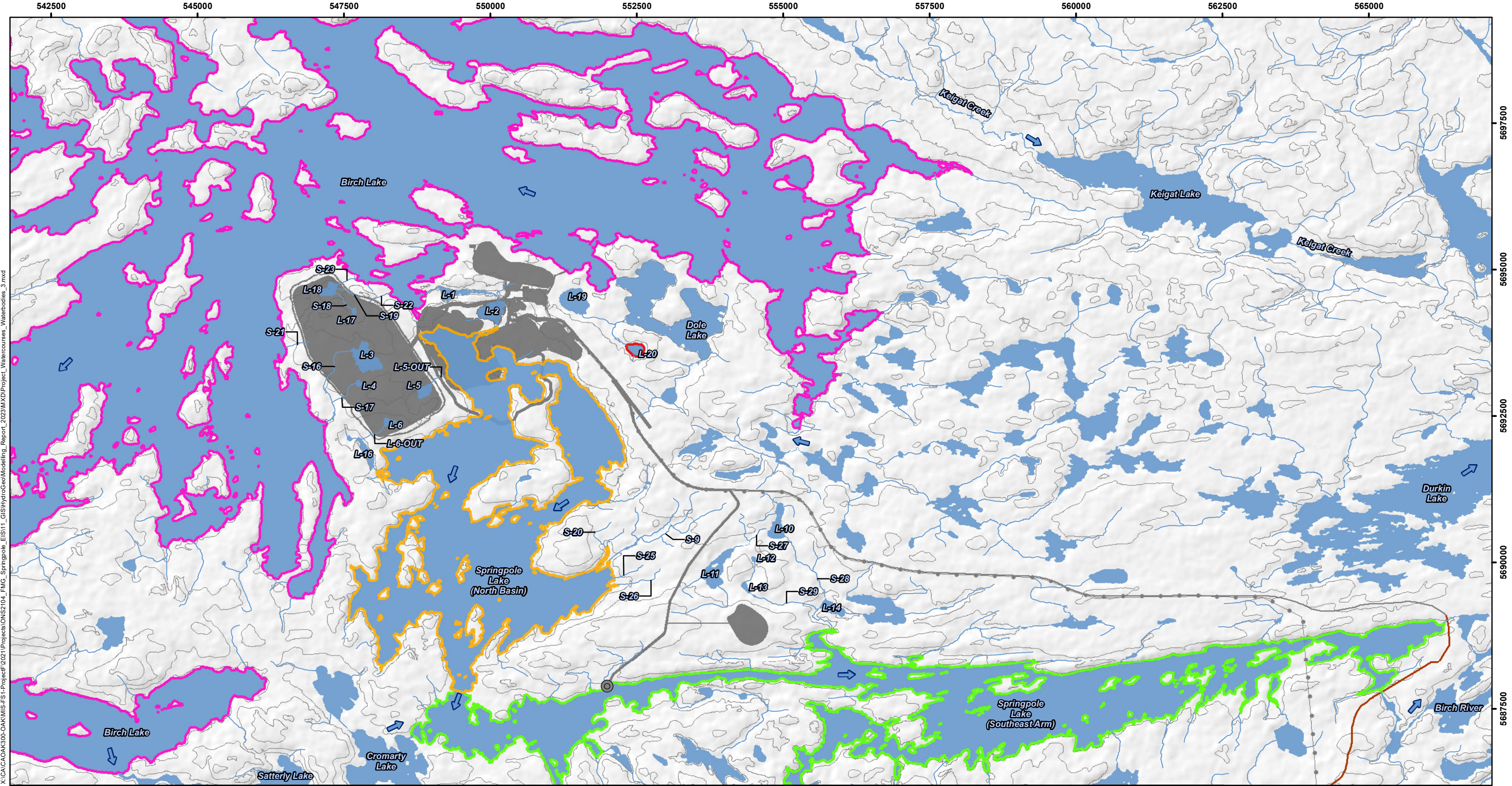
PROJECT N°: ONS2104

FIGURE: 2-2

SCALE: 1:21,000

DATE: October 2023





X:\CA\CAOAK300-CAKMIS-FS1-Project\2021\Projects\ONS2104_FMG_Springpole_EIS11_GIS\HydroGeoModelling_Report_2023MXD\Project_Watercourses_Waterbodies_3.mxd

LEGEND

Proposed Mine Feature

Proposed Effluent Discharge Location

Wenasaga Forestry Road

Contour (10 m intervals)

Existing Watercourse

Existing Waterbody

Flow Direction

Birch Lake

Springpole Lake (North Basin)

Springpole Lake (Southeast Arm)

Small Inland Waterbodies

NOTES:

- Topographic information extracted from LIO, MNRFP
- Proposed site plan provided by Ausenco, drawing number 104496-GX-03000-31344-003, Rev 1. 26 June 2023 and modified by WSP July 2023.
- 230 kV transmission line provided by First Mining Gold, April 2024.

Datum: NAD83
Projection: UTM Zone 15N

FIRST MINING GOLD

SPRINGPOLE GOLD PROJECT

Site Hydrological Map

PROJECT N°: ONS2104

SCALE: 1:61,000

FIGURE: 2-3

DATE: September 2024



3.0 HYDROGEOLOGICAL SETTING

Hydrogeological conditions at site have been assessed as part of several site hydrogeological and geotechnical investigation programs, the bulk of which have been conducted since 2019. This information is described in detail in the 2023 Baseline Hydrogeological Conditions report (Appendix L-1) and is briefly summarized below.

3.1 Hydrostratigraphy

Site-specific hydrostratigraphic conceptualization has been developed through the synthesis of borehole data (821 points, including data from exploration drilling and investigation programs [including 208 geotechnical boreholes]), test pits (106 points), outcrop mapping (458 points) and general observations from shoreline mapping.

Based on this information, five site hydrostratigraphic units have been demarcated and are described in Table 3-1. Justification for the demarcation of these units, and additional subdivision of them based on hydraulic testing, is provided in Section 3.2. The simplification of these units for simulation in the numerical groundwater model and additional information on model layer development are described in Section 5.1.

3.2 Hydraulic Conductivity

Hydraulic conductivity (K) for overburden and bedrock materials found at site have been assessed as part of several site investigations and programs, with the majority of site work having been conducted since 2019. Measured K data for hydrostratigraphic units are given in Table 3-2. In total, 232 hydraulic conductivity tests have been completed at the site, including one 30-day pumping test.

3.2.1 Overburden Hydraulic Conductivity

Hydraulic conductivity values for overburden and interface materials (i.e., the overburden and bedrock surface interface), excluding the lake bed organics, show a relatively narrow range, with values ranging from 1.0×10^{-6} to 6.0×10^{-5} metres per second (m/s), with an overall geometric mean of 5.9×10^{-6} m/s. This contrasts with the two values available for lake bed organics (obtained from laboratory tests), which both yielded very low values. For the purpose of developed numerical model, the overburden conceptualization is, therefore, simplified as being a two-layer system whereby lake bed organics (low hydraulic conductivity) are differentiated from the remainder of the other lumped overburden sub-units (higher hydraulic conductivity). This simplification is justified based on the limited thickness and sparse distribution of overburden materials at site, the narrow range of test values and the anticipated removal of overburden beneath the CDF dams during construction. Further details on this are provided in the 2023 baseline hydrogeology report (Appendix L-1).

3.2.2 Bedrock Hydraulic Conductivity

Hydrogeological characterization investigations at the Project site have primarily focused on bedrock. The current database of hydraulic conductivity estimates has been supplemented with results from field programs conducted in 2021 and 2022 (WSP 2023), and now includes 220 unique estimates of bedrock hydraulic conductivity obtained through analysis of rising / falling head tests in monitoring wells and packer tests in boreholes. Of the 220 bedrock hydraulic conductivity estimates, available at the time of report preparation, 99 are associated with either the CDF or are directly adjacent to the CDF / open pit, 72 are located within or near to the proposed open pit, 31 are located across the eastern portion of the Project site and 18 hydraulic conductivity estimates are available at the proposed dike locations.

Bedrock at site is broadly grouped into three zones, including: host rock, the UGM zone and the low RQD zone. Utilizing the three-dimensional (3D) hydrostratigraphic conceptual model developed for the Project using Leapfrog, hydraulic conductivity measurements for bedrock have been grouped into each of these three categories by querying the corresponding bedrock model unit where each test interval was located (as described in Appendix L-1).

The host rock in the vicinity of the CDF (primarily andesite) differs from host rock across the rest of site, which includes a range of other rock types including other / different metavolcanics, metasedimentary rock and various intrusions (i.e., "other" host rock). Within this other host rock zone, the highly altered and weak rock of the UGM and low RQD zones contrast starkly with the surrounding other host rock (as well as the CDF area andesite). Hydraulic conductivity estimates of bedrock hydrostratigraphic units have, thus, been grouped between: 1) CDF area host rock, 2) other site area host rock, 3) the low RQD zone and 4) the UGM zone. The approximate locations of these zones and corresponding hydraulic conductivity data are shown in Figure 3-1 and Figure 3-2, respectively.

3.3 Groundwater Levels

Groundwater level monitoring has been conducted at site to support baseline characterization and design activities. This has included "snapshot" water level monitoring rounds as well as automated datalogging in screened monitoring wells, select open boreholes and grouted-in vibrating wire piezometers (VWPs).

A snapshot water level monitoring event was conducted at site between October 8 and 17, 2022. This included manual water level measurements in 52 screened monitoring wells and four open holes and was also supplemented by VWP readings from 26 monitoring ports (at 10 multi-levels installations) between September 25 and 29, 2022, for a total of 82 measurements. These water level data were subsequently processed and are provided in Table 3-3. Shallow groundwater level contours were generated by co-kriging the measured water level data against the site digital elevation model (DEM) on a 20 by 20 m grid using Surfer (version 23), with breaklines (i.e., fixed elevations) being assigned along the shorelines of site waterbodies. In instances where multi-level data are available, the shallow monitoring port was generally used in the kriging. The resulting contours and measured data are shown in Figure 3-3. The water level contours and measured data illustrate that groundwater levels generally decrease from topographic high areas (e.g., BH-WSF2-06 at 417.9 m amsl) towards the topographic low areas and surface water features. Locations of shallow groundwater levels close to the surface at topographic highs are likely indicative of a tendency for local bedrock to not readily drain and are an indication of low permeability / limited fracture connectivity.

Additional details on site groundwater level monitoring are provided in the 2023 baseline hydrogeology report (Appendix L-1).

3.4 Groundwater Recharge

Groundwater recharge for the Project area will generally be highest during the spring freshet and late fall, when snowmelt and rainfall have their respective peaks and evapotranspiration is reduced. Groundwater recharge will typically be focused on locations where the landscape is favourable, those areas that are flat to gently sloping, have minimal interception / transpiration (and are yet shaded from evaporation) and have permeable soil types. As such, localized infiltration / recharge rates can vary considerably within a given watershed depending on immediate local conditions. Overall, recharge is generally best informed by catchment-scale stream flow monitoring and, as such, can likely be approximated for the site utilizing streamflow data from local sub-watersheds.

Stream flow monitoring has been conducted at site as part of baseline hydrological characterization (Appendix M-1). Based on the measured low flows, groundwater recharge rates range from approximately 25 to 76 millimetres per year (mm/yr). Given that the average annual precipitation is 696 mm/yr, this represents a small proportion of the overall hydrologic cycle and, therefore, this system is mostly runoff controlled. This is generally consistent with findings from regional studies on groundwater recharge in northern Ontario, completed by Singer and Cheng (2002). Conclusions from this study indicated, on average, that groundwater recharge in similar settings ranged from 27.6 to 57.9 mm/yr on an average annual basis.

Table 3-1: Site Hydrostratigraphic Units

Layer	Unit	Description
Overburden	Surficial organics	The Project site is generally covered by a thin layer of dark brown to black peat / organics which is typically less than 1 m on land (average of 0.39 m, excluding outcrop locations). Lower ground surface elevations tend to show increasing organics depth. The thickest organics at site are often found adjacent to the various lakes / ponds.
	Lake bed organics	Lake bed organics form the shallowest substrate of the various lakes around site. The thickest lake bed organics are likely to be present in the deepest part of Springpole Lake (average thickness of 1.4 m). Note that the substrate material of Springpole Lake also includes silt / clay and till deposits, in addition to the shallow lake bed organics.
	Glaciolacustrine silt/clays	Glaciolacustrine silts / clays are sparsely distributed at site, with average thicknesses being approximately 0.68 m. A small decrease in thickness with increasing elevation is apparent based on the measured data.
	Glacial till	A thin layer of till with variable composition covers most of the existing ground surface, with an average thickness of 1.1 m. The till thickness does not change appreciably with elevation, on-land, suggesting that the topography is covered with a consistent, thin, veneer of till.
	Coarse deposit	A sand / gravel deposit of limited spatial extent is located along the eastern shoreline of Springpole Lake. This material primarily consists of sand and gravel. Due to its very limited spatial extent, it is not expected to represent a unit of hydrogeological significance for this study.
Bedrock	UGM zone	The UGM zone consists of highly altered / disintegrated rock lending to a "sand-like" texture due to its apparent granularity. This zone is located primarily within / adjacent to the extents of the proposed open pit and is largely encapsulated by a zone of low RQD rock (see next), which together form the portage zone.
	Low RQD zone	A zone of very low RQD bedrock (defined as less than 25% based on structural modelling) is present in the area of the proposed open pit. This zone largely encapsulates the UGM zone, combined with which it forms the portage zone. Due to the persistence of low rock qualities in this zone, bedrock structures are not expected to enhance its already high permeability. This zone represents a modelled / interpolated volume based on rock mechanics modelling being conducted to support open pit slope stability analyses.
	Host rock	Host / country rock surrounding the pit area (i.e., the UGM zone and low RQD zone, or together the portage zone), consists of a varying lithologies. Bedrock in the area of the CDF consists primarily of andesite, while other areas of site have more varied lithology. Several structures have been mapped in the area of the open pit which may extend into the host rock zone, particularly in area of the CDF.

% = percent.

Table 3-2: Estimated Hydraulic Conductivity Data Summary

Unit	Location	Depth (mbgs)	Number of Hydraulic Tests	Geometric Mean - K (m/s)
Overburden		N/A	12	5.9×10^{-6}
Lake bed organics		N/A	2	Low ⁽¹⁾
Host rock	CDF area	0–25	30	5.7×10^{-8}
		25–200	13	1.6×10^{-8}
		>200	3	2.3×10^{-9}
	Other area	0–25	49	8.5×10^{-7}
		25–125	48	5.9×10^{-7}
		125–350	39	1.1×10^{-7}
		>350	1	1.0×10^{-10}
Low RQD		N/A	33	2.9×10^{-6}
UGM		N/A	4	5.0×10^{-6}

Notes:

(1) Two lab tests yielding values of 1.7×10^{-9} and 3.0×10^{-10} m/s.

mbgs = metres below ground surface; N/A = not applicable; > = greater than.

Table 3-3: Measured Water Level Data (fall 2022)

Station ID	Type ⁽¹⁾	Easting	Northing	Date	Water Level (m amsl)	Water Depth (mbgs)
SH22-MW-003A	MW	548425	5692154	October 6, 2022	395.6	4.2
SH22-MW-003B	MW	548426	5692154	October 6, 2022	395.6	4.2
BL-0334D	MW	548847	5692194	October 6, 2022	392.8	5.2
BL-0334S	MW	548847	5692194	October 6, 2022	392.8	5.2
BL-0357	Open hole	549473	5692455	October 6, 2022	393.4	3.2
MW5	MW	549556	5692429	October 6, 2022	390.4	1.6
SH22-MW-001B	MW	548477	5694283	October 6, 2022	406.9	3.6
SH22-MW-001A	MW	548477	5694283	October 6, 2022	408.8	2.3
SGH20-001	MW	549339	5693015	October 6, 2022	395.6	7.9
BL-0143S	MW	549041	5693629	October 6, 2022	394.7	2.7
BL-0143D	MW	549041	5693629	October 6, 2022	397.3	0.05
BH-TMF-04D	MW	548122	5693471	October 6, 2022	411.0	1.3
BH-TMF-04S	MW	548122	5693471	October 6, 2022	410.6	1.7
BH-WSF2-06	MW	548012	5694089	October 6, 2022	417.9	2.4
BH-TMF-05	MW	547428	5694198	October 6, 2022	413.1	0.2
BH-WSF2-13D	MW	547290	5694515	October 6, 2022	399.1	2.4
BH-WSF2-13S	MW	547290	5694515	October 6, 2022	400.6	0.9
SGH20-004	MW	548811	5694076	October 6, 2022	393.5	15.1
MW2	MW	548946	5694468	October 7, 2022	393.3	1.7
SGH20-008D	MW	549328	5694167	October 7, 2022	392.3	8.5
SGH20-008S	MW	549328	5694167	October 7, 2022	397.3	3.5
BH-PS-07-R1S	MW	550473	5694184	October 7, 2022	401.5	3.4
BH-PS-07-R1D	MW	550473	5694184	October 7, 2022	400.6	4.3
BH-PS-08-R1S	MW	550666	5693923	October 7, 2022	399.7	1.1
BH-PS-08-R1D	MW	550666	5693923	October 7, 2022	399.6	1.2
BH-PS-09-R1S	MW	550747	5693841	October 7, 2022	399.2	1.2
BH-PS-09-R1D	MW	550747	5693841	October 7, 2022	399.3	1.1
BH-WSF1-03S	MW	550726	5694431	October 7, 2022	403.1	1.5
BH-WSF1-03D	MW	550726	5694431	October 7, 2022	402.3	2.3
BH-WSF1-11S	MW	551085	5694725	October 7, 2022	398.5	0.8
BH-WSF1-11D	MW	551085	5694725	October 7, 2022	398.5	0.8
SH22-MW-008B	MW	551001	5694632	October 7, 2022	399.7	0.2
SH22-MW-008A	MW	551001	5694632	October 7, 2022	399.6	0.3
SH22-MW-004D	MW	549885	5694812	October 8, 2022	401.1	1.6
SH22-MW-004C	MW	549885	5694812	October 8, 2022	401.0	1.7
BH-WSF1-02S	MW	550399	5694977	October 8, 2022	399.1	0.9
BH-WSF1-02D	MW	550399	5694977	October 8, 2022	399.1	0.9
SH22-MW-007A	MW	550823	5695082	October 8, 2022	399.6	0.6
BH-WSF1-01S	MW	549772	5695076	October 8, 2022	398.0	0.8
BH-WSF1-01D	MW	549772	5695076	October 8, 2022	398.1	0.7
BH-WSF1-12D	MW	549785	5695494	October 8, 2022	394.5	0.7
BH-WSF1-12S	MW	549785	5695494	October 8, 2022	394.5	0.7
MW3	MW	550320	5694013	October 9, 2022	397.8	0.2
SH22-MW-009B	MW	551192	5694354	October 9, 2022	399.5	0.4
SH22-MW-009A	MW	551192	5694354	October 9, 2022	398.0	1.9
SG22-042	Open hole	546581	5694466	October 10, 2022	401.6	0.4
SG22-038	Open hole	547337	5693631	October 10, 2022	409.0	0.5
BH-WSF2-14D	MW	547152	5692980	October 10, 2022	403.4	0.8

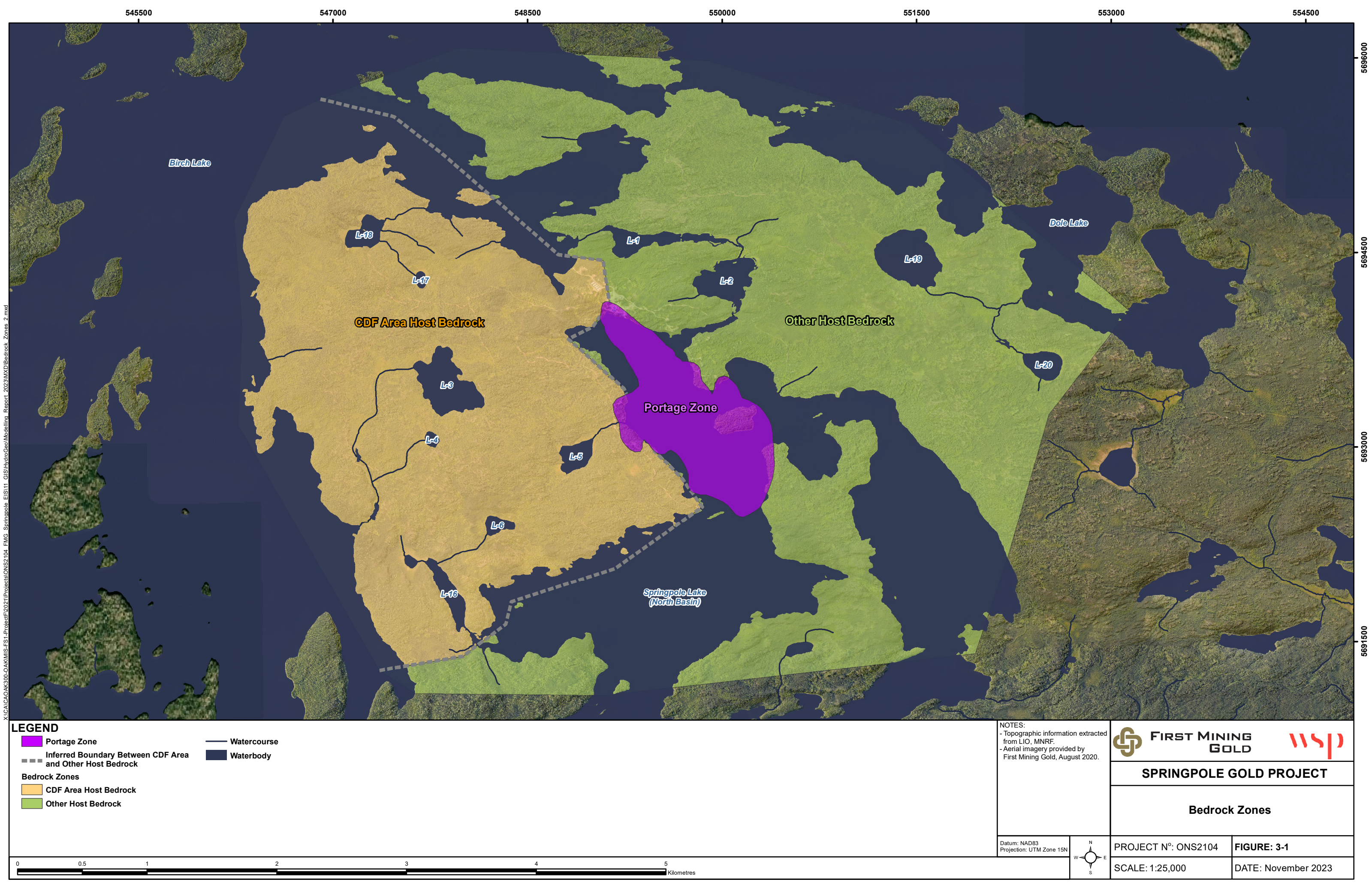
Table 3-3: Measured Water Level Data (fall 2022)

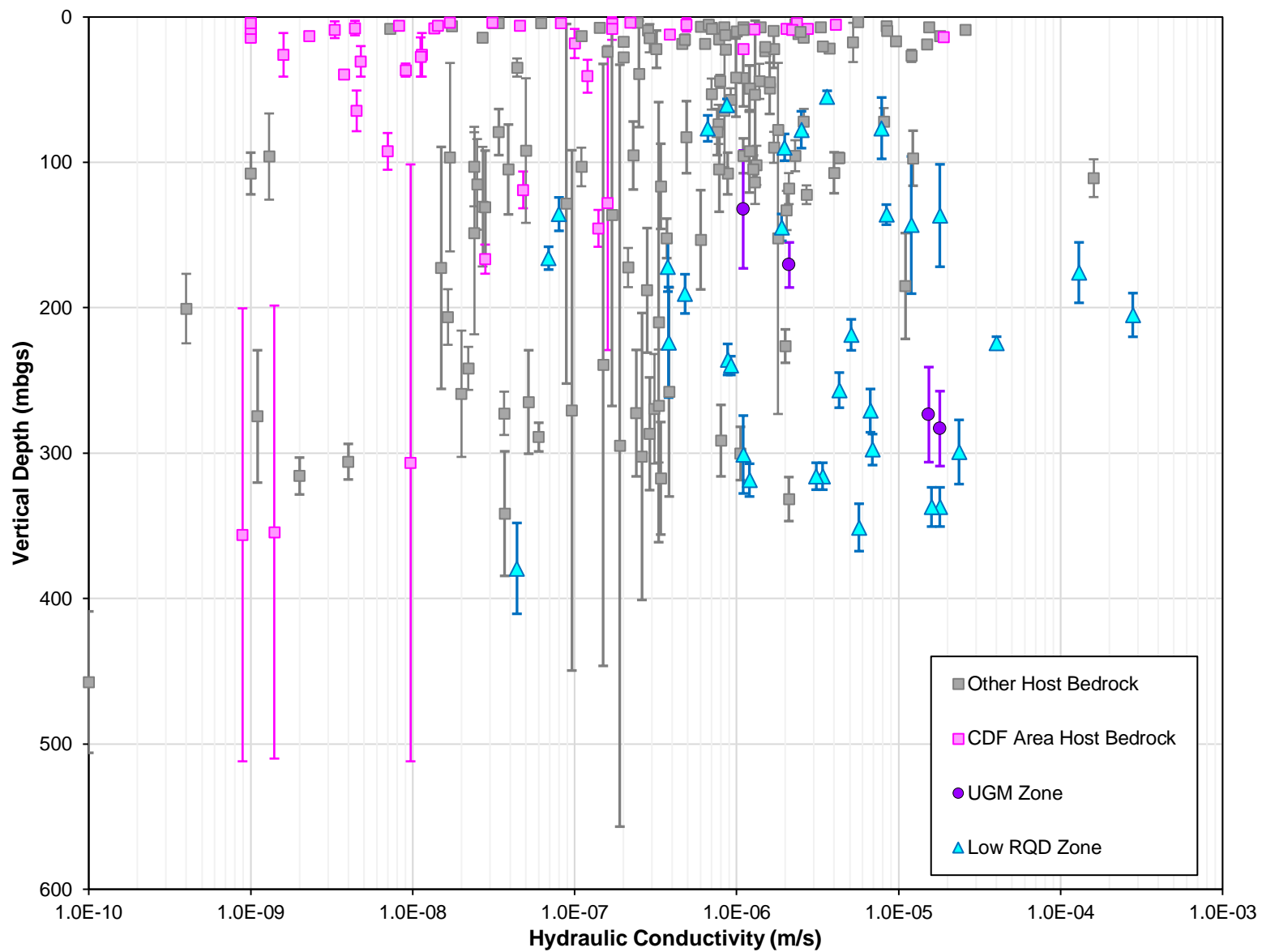
Station ID	Type ⁽¹⁾	Easting	Northing	Date	Water Level (m amsl)	Water Depth (mbgs)
BH-WSF2-14S	MW	547152	5692980	October 10, 2022	403.5	0.7
SH22-MW-006B	MW	547526	5694692	October 12, 2022	402.1	-0.3
SGH22-MW-006A	MW	547532	5694692	October 12, 2022	402.0	-0.2
BH-TMF-15S	MW	549463	5692557	October 12, 2022	394.9	0.9
BH-TMF-15D	MW	549463	5692557	October 12, 2022	394.1	1.7
SG22-033	Open hole	547686	5692276	October 16, 2022	395.1	0.3
SH22-MW-002B	MW	546868	5694900	October 17, 2022	405.0	5.2
SH22-MW-002A	MW	546868	5694900	October 17, 2022	403.6	7.3
SCH21-049-380	VWP	547341	5694275	September 29, 2022	413.7	6.9
SCH21-049-306	VWP	547341	5694275	September 29, 2022	410.9	9.7
SCH21-049-236	VWP	547341	5694275	September 29, 2022	409.5	11.1
SGH21-006-381	VWP	549171	5693255	September 28, 2022	390.5	9.3
SGH21-006-343	VWP	549171	5693255	September 28, 2022	390.5	9.3
SGH21-006-260	VWP	549171	5693255	September 28, 2022	389.2	10.6
SGH21-006-147	VWP	549171	5693255	September 28, 2022	387.8	12.0
SGH21-006-43	VWP	549171	5693255	September 28, 2022	388.0	12.0
SH22-002-377	VWP	548721	5694325	September 25, 2022	395.6	1.1
SH22-002-347	VWP	548721	5694325	September 25, 2022	395.6	1.1
SH22-002-277	VWP	548721	5694325	September 25, 2022	395.6	1.1
BH-CAMP-32-403	VWP	551360	5693903	September 25, 2022	407.8	0.2
BH-TMF-35-397	VWP	548125	5694343	September 29, 2022	405.4	1.7
BH-TMF-35-367	VWP	548125	5694343	September 29, 2022	408.9	-1.8
BH-TMF-36-394	VWP	548764	5693368	September 27, 2022	405.1	-1.3
BH-TMF-36-363	VWP	548764	5693368	September 27, 2022	406.1	-2.3
BH-TMF-37-405	VWP	546937	5693579	September 26, 2022	413.1	1.9
BH-TMF-37-374	VWP	546937	5693579	September 26, 2022	413.0	2.0
BH-TMF-38-400	VWP	547046	5694790	September 29, 2022	407.1	3.3
SG22-008-299	VWP	549200	5693446	September 27, 2022	387.5	6.6
SG22-008-223	VWP	549200	5693446	September 27, 2022	391.8	2.3
SG22-008-121	VWP	549200	5693446	September 27, 2022	390.7	3.4
SG22-017-259	VWP	549975	5693214	September 28, 2022	388.9	5.0
SG22-017-193	VWP	549975	5693214	September 28, 2022	389.8	4.1
SG22-017-128	VWP	549975	5693214	September 28, 2022	385.7	8.2
SG22-017-071	VWP	549975	5693214	September 28, 2022	386.5	7.4

Notes:

(1) MW indicates monitoring well, VWP indicates vibrating wire piezometer.

(2) ID = identification; mbgs = metres below ground surface.





**FIRST MINING
GOLD**

Figure No: 3-2

Project No: ONS2104

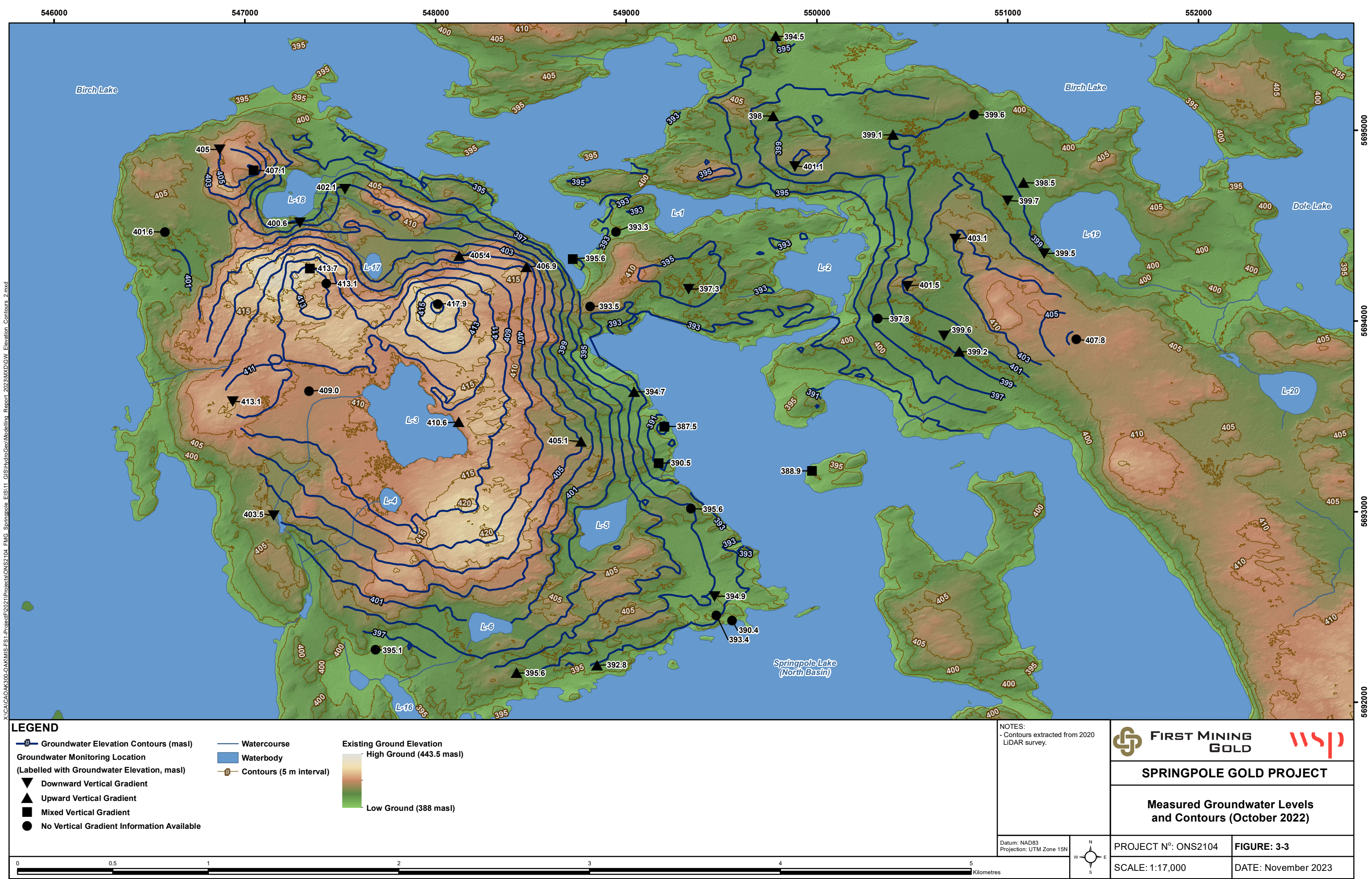
Springpole Gold Project – 2023 Hydrogeological Modelling Report



Date: 29-Jun-23

Rev: 0

Measured Bedrock Hydraulic Conductivity Data



4.0 CONCEPTUAL HYDROGEOLOGICAL MODEL

A conceptual hydrogeological model has been developed for the site using data / information gathered as part of the various field investigation programs and insights from desktop analyses based on these data. Section 4.1 and Section 4.2 present conceptual hydrogeological conditions for pre-mining and mining phase conditions.

4.1 Pre-mining Phase Conditions

There are several important elements in the hydrogeological conceptual model for the Project, including surface water features, overburden cover, bedrock geology, structural setting and geologic history. This section briefly summarizes the site conceptual hydrogeological model for the pre-mining phase.

Stream flow gauging suggests that the groundwater regime may have limited groundwater flow and provides minimal baseflow to creeks in the immediate vicinity of the Project as indicated by a number of the creeks that appear to essentially stop flowing at certain times of the year.

In areas of competent bedrock, groundwater flow through the bedrock will be mostly restricted to flow through those open fractures that are part of a connected fracture network. Outside of the low RQD and UGM zones (i.e., the portage zone proximal to the open pit) bedrock fractures are generally sparse and poorly connected at site, leading to typically low permeabilities in the rock. Andesite bedrock in the area of the CDF has fewer well-connected fractures as compared to the rest of host bedrock at site, which is exhibited by its higher competence observed during drilling. Within the host bedrock, it is anticipated that open fractures will be less common with depth as is consistent with the patterns of fracturing typically seen in Archean rock in northern Ontario, creating a trend of reduced bulk hydraulic conductivity within the host bedrock with depth.

A transverse stratigraphic section through the open pit, showing bedrock zones, is shown in Figure 4–1. The heart of the Project deposit (i.e., the low RQD and UGM zones which together comprise the portage zone) show markedly higher hydraulic conductivity than the surrounding host bedrock. Based on hydraulic conductivity estimates shown in Figure 3–2, hydraulic conductivity within the low RQD and UGM zones does not appear to decrease with depth in the same manner that is seen in surrounding host rock. Higher permeabilities in the low RQD and UGM zones reflect the presence of weak rock in this zone, which appears more prone to fracturing and weathering than either the metavolcanic (andesite) host rock to the southwest, or the metasediment to the northeast of the proposed open pit. The fracturing within this zone is focused on several structural features identified by SRK Consulting (SRK 2013). The initial structures allowed for greater fluid movement, resulting in higher alteration in the core of the UGM zone. The fracturing within the low RQD zone, which surrounds the UGM, developed in response to the rock within the UGM becoming weaker due to the alteration progressing over time in the geologic past and the surrounding rock in what is now the low RQD zone lost confining support from the UGM zone.

Under the current existing conditions, most of the local groundwater flow is driven by recharge in higher elevation areas and subsequent discharge to surface water features in low-lying areas. Thin pockets of overburden overlying the fractured rock act as recharge buffers, whereby shallow infiltration is stored in porous overburden following rainfall / snowmelt events and slowly percolates into the fractured rock system which will have comparatively little storage. What limited groundwater flow that exists is preferential through the overburden and shallow fractured bedrock, towards surface water features such as Birch Lake and Springpole Lake. The degree of hydraulic connectivity between the groundwater flow system and surface water features is largely location specific. For example, groundwater levels in the immediate vicinity of Springpole Lake are close to the lake elevation, indicating a good hydraulic connection, which is attributed to the prevalence of fracturing in the low RQD zone. Conversely, groundwater levels away from

the low RQD zone show little relation to the levels in Springpole Lake or local surface water features as they generally remain much higher than local surface water features.

The overall slow rate of groundwater movement through the fractured bedrock is demonstrated by the presence of a high water table in the higher elevation ground, which does not drain quickly after the spring freshet over dry periods, such as the summer, and is insufficient to support year round flow (i.e., several small creeks appear to flow intermittently, ceasing to flow during the summer months).

The low porosity of bedrock, where groundwater is found in a sparse fracture network, indicates that the bedrock fracture network contains very little water on a per volume of material basis compared to the overburden. Groundwater recharge across the Project area migrates mostly to Springpole Lake and Birch Lake, but given the size of these lakes, does not make an appreciable contribution to the lake water balance.

4.2 Mining Phase Conditions

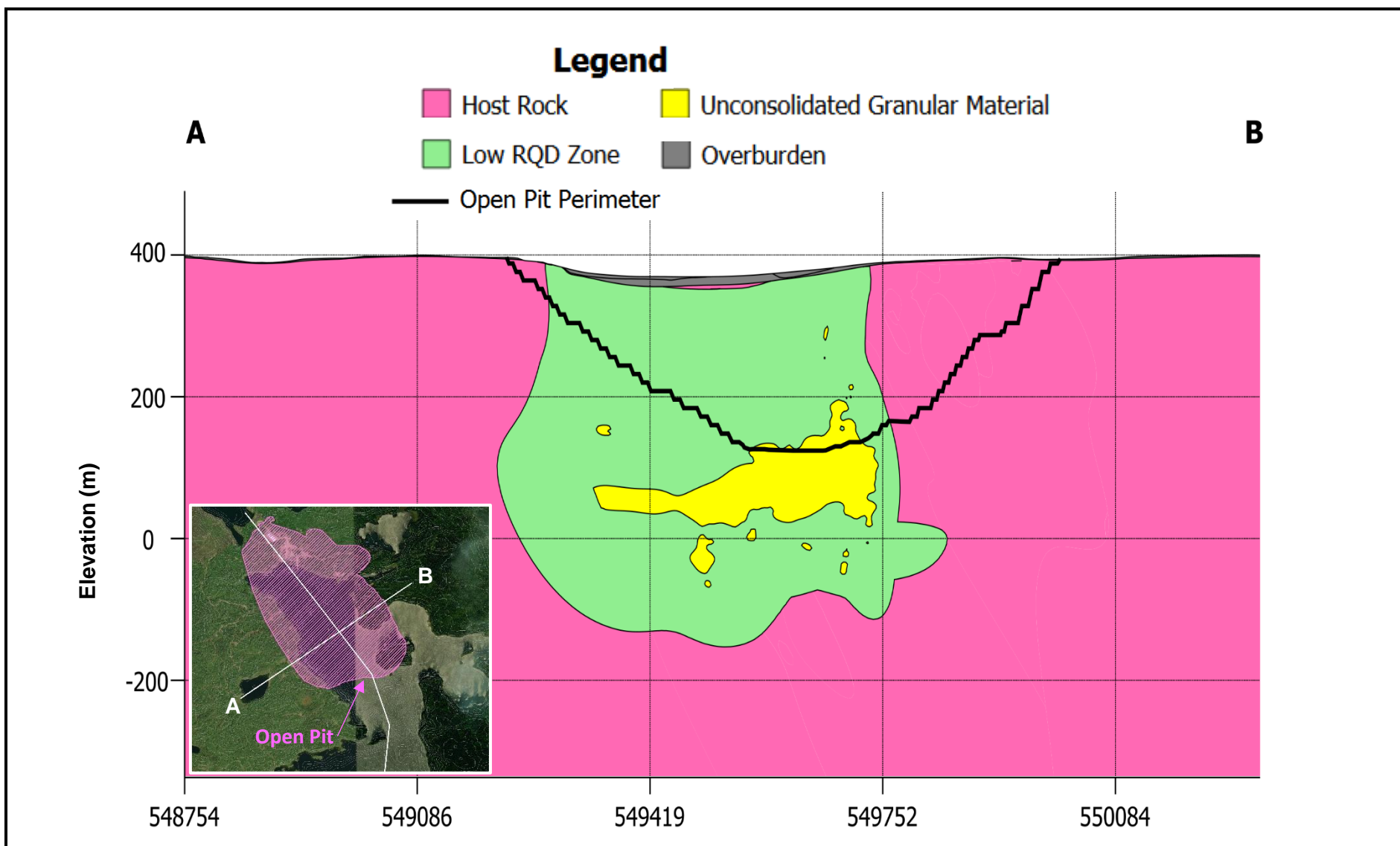
The conceptual hydrogeologic characteristics noted for the pre-mining phase conditions in Section 4.1 are largely consistent for mining phase conditions. During mining, the most relevant changes to the groundwater flow system include the development of the open pit and construction of the CDF. Two primary phases of mine development are considered in this report: 1) end of mine operations (EoMO), which represents conditions immediately after (i.e., the first day of) closure and 2) post-closure conditions, which represents conditions long after closure (after which the groundwater system has reached its long-term conditions following open pit filling).

A diagram depicting conceptual subsurface flow pathways for EoMO conditions is presented as Figure 4-2 and for post-closure conditions is presented as Figure 4-3. These figures illustrate a conceptual east-west cross section transecting the CDF south cell and open pit, with the surface water feature on the left side representing a nearby surface water receiver (Birch Lake). Overburden is differentiated from the bedrock, which is sub-divided between host rock, the low RQD zone and the UGM zone. The CDF includes tailings that are overlain by a cover and surrounded by the perimeter dams, which include a liner on the upstream face of the perimeter embankments. The CDF is surrounded by shallow collection ditches. In Figure 4-2, the open pit is shown in its fully dewatered state, while Figure 4-3 illustrates the fully filled open pit basin.

The water table is indicated in Figure 4-2 and Figure 4-3 by the dashed blue line. The water table within the CDF south cell is shown as very shallow for both cases, which is a feature of the current conceptual design of the facility (Appendix V-1a). The water table corresponds to local topographic conditions within the perimeter dams and generally will be quite flat. Outside of the CDF, water levels will more closely resemble pre-mining conditions, depending on local fracture connectivity and whether increased heads at depth under the CDF are able to dissipate outside of the CDF. Under EoMO conditions, a drawdown cone will emanate radially from the open pit. Drawdowns will be largest within the low RQD zone (and UGM zone), as this zone is expected to drain readily.

Seepage pathways in Figure 4-2 and Figure 4-3 are depicted by the blue flow arrows. For the purpose of visibility, these are not scaled to the relative amounts of seepage in these figures (e.g., the arrows showing bypass would likely be associated with flows that are much smaller than the amounts reaching the ditches). Seepage from the CDF can follow three main pathways: 1) directly through the embankment liner into the perimeter dam, 2) upwelling under the liner through the shallow bedrock into the perimeter dams, or 3) diffuse seepage / percolation into the bedrock underlying the CDF. Flows within the dams will accumulate and converge towards topographic low points within the dams, at which point flows would seep / discharge from the dam toes and runoff to the perimeter collection ditch. Flows within the shallow rock are likely to

move sub-laterally within the most permeable zone of rock. Depending on local conditions, a component of this flow may discharge to the surrounding perimeter collection ditch. Otherwise, flows bypassing the perimeter collection ditch would eventually discharge to surrounding surface water features. Due to the low permeability of bedrock, it is expected that only a minimal amount of seepage would penetrate deep enough into the bedrock to bypass the perimeter dams and collection ditches and subsequently discharge to nearby receivers. For the EoMO conditions (Figure 4–2), it is anticipated that the primary pathway for seepage bypass would be the open pit, due to the large drawdown cone imposed by the dewatered open pit.



**FIRST MINING
GOLD**

Figure No: 4-1

Project No: ONS2104

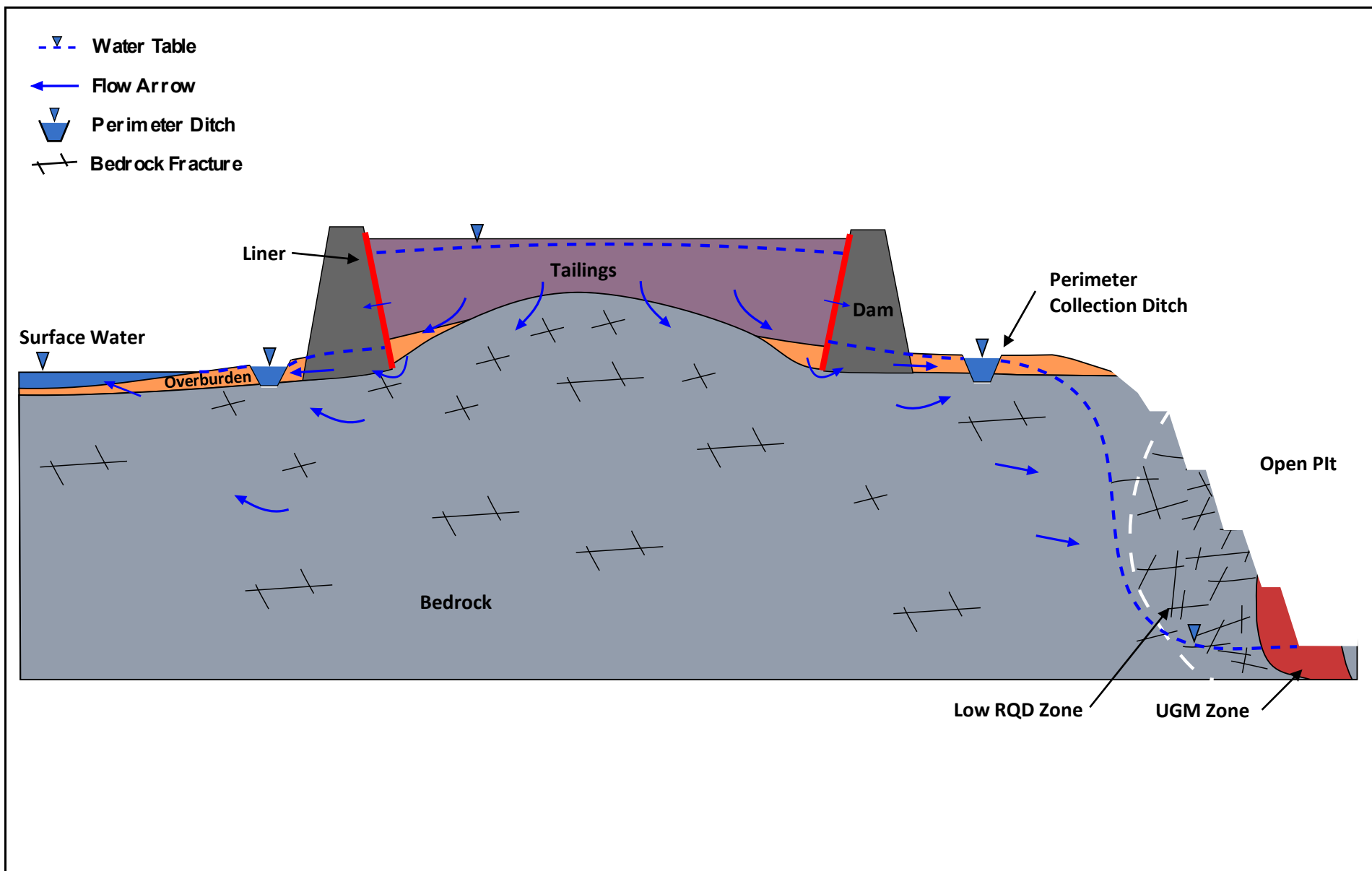
Springpole Gold Project – 2023 Hydrogeological Modelling Report





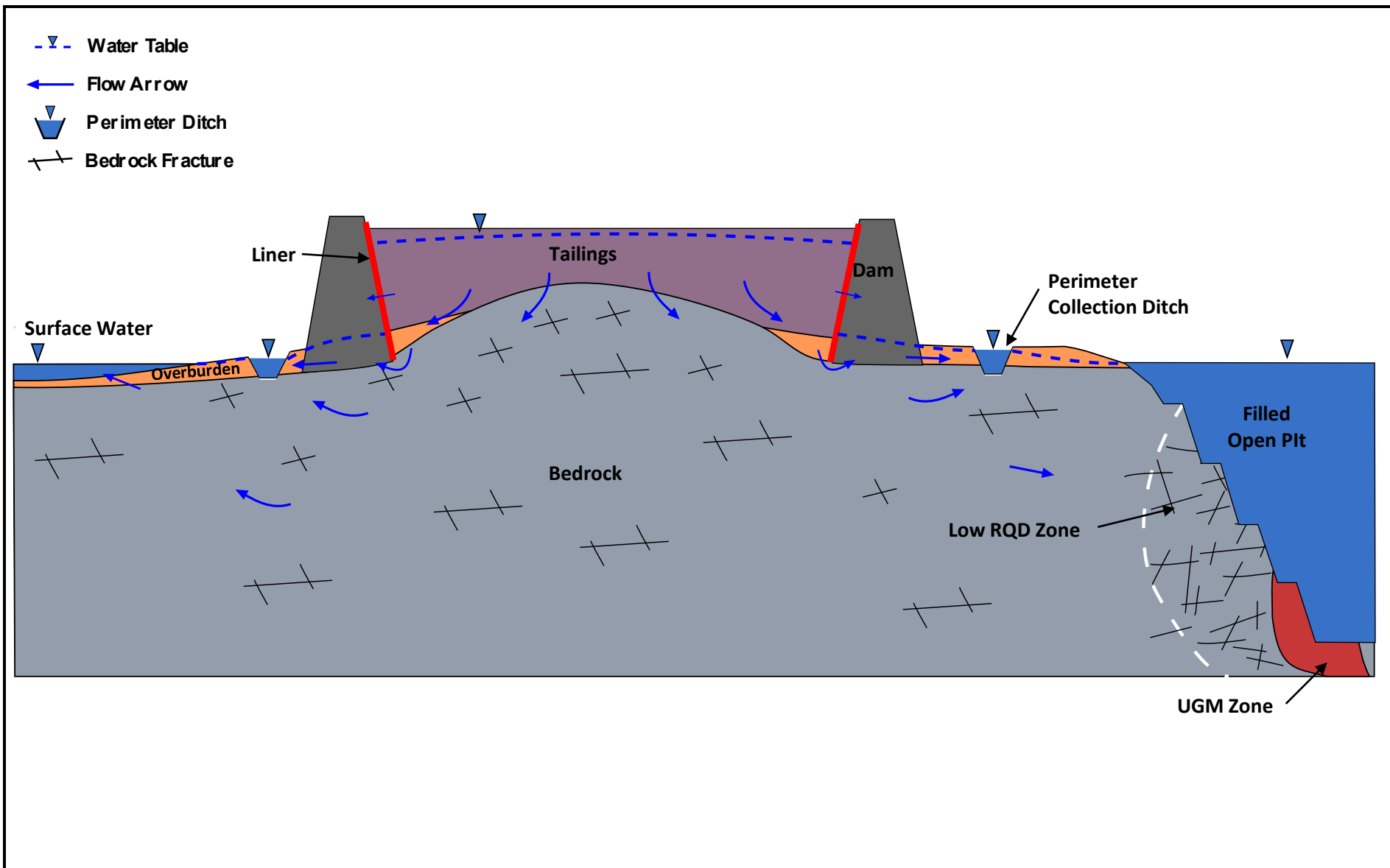
Date: 29-Jun-23

Rev: 0

Hydrostratigraphic Cross Section – Transverse to Open Pit



 FIRST MINING GOLD	Figure No: 4-2	Springpole Gold Project – 2023 Hydrogeological Modelling Report
	Project No: ONS2104	
	Date: 29-Jun-23	Conceptual Diagram for End of Mine Operations Conditions (CDF South Cell)
	Rev: 0	



**FIRST MINING
GOLD**

Figure No: 4-3

Project No: ONS2104

Springpole Gold Project – 2023 Hydrogeological Modelling Report



Date: 29-Jun-23

Rev: 0

Conceptual Diagram for Post-Closure Conditions (CDF South Cell)

5.0 GROUNDWATER MODEL DEVELOPMENT

Groundwater modelling was conducted for three mine development conditions, corresponding to key hydrogeological conditions during the lifespan of the mine. The numerical groundwater flow model represents 3D steady-state flow conditions with bedrock layers represented using an equivalent porous media approach. Three conditions were simulated:

- **Pre-mining conditions:** Existing (baseline) site conditions were simulated first for model development and calibration purposes. Hydraulic conductivity and recharge values were initially set based on the available field data described in Section 2.0 and Section 3.0 and then incrementally adjusted, within reasonable ranges based on the field measurements, to calibrate the model. Further discussion on model calibration is provided in Section 5.2.
- **End of mine operations (EoMO):** This condition represents the first day of mine closure, where the CDF is constructed to its maximum elevation, the open pit is developed to its maximum depth and the open pit is fully dewatered. Further discussion on EoMO simulations is provided in Section 6.1.
- **Post-closure:** This case represents conditions long after closure, where the open pit has fully filled and the groundwater levels in the vicinity of site have reached their long-term state. Further discussion on post-closure simulations is provided in Section 6.2.

5.1 Model Construction

The commercial groundwater modelling code FEFLOW (version 8.0), developed by WASY GmbH, was selected to develop the site groundwater flow model. FEFLOW uses finite element techniques to solve the groundwater flow equations (Diersch 2014). Model construction was conducted using data / information gathered from historical and recent site investigation programs. This information is discussed in detail in the 2023 Baseline Hydrogeological Conditions report (Appendix L-1) and summarized in Sections 2.0 through 4.0.

5.1.1 Domain, Discretization and Numerical Setup

The groundwater model domain is shown in Figure 5–1. The domain covers an area of approximately 31 km². The perimeter of the model is primarily bound by Birch Lake to the west, north and east, and Springpole Lake to the south. A no-flow boundary condition formed along the inferred groundwater flow divide, which is assumed to correspond to the local topographic high ground immediately west and east of Springpole Lake, forms the southwest and southeast model domain extents.

The numerical mesh is shown in plan view in Figure 5–1. The horizontal dimension of the finite elements generally ranges from less than 1 m to approximately 150 m, with typical element sizes near the open pit and CDF being approximately 15 m and 15 to 30 m, respectively. Elements were generally refined along surface water feature shorelines, within the CDF and in the open pit area.

The model domain and numerical model mesh, illustrating the vertical discretization in a 3D view (on a 5:1 vertical exaggeration), are shown in Figure 5–2. Vertically, the model is divided into 129 numerical layers ranging from 0.75 to 39 m in thickness (thickest elements corresponding to the deepest numerical layers). The uppermost 44 numerical layers represent layers above the existing / pre-mining surface. These layers are included to simulate the CDF during EoMO and post-closure simulations (Section 6.0) and are set to inactive for the pre-mining model calibration simulation. For the pre-mining model, the uppermost active model layer (i.e., the bottom of layer 44 or slice 45) corresponds to the DEM for the site which includes the bathymetries of Birch Lake, Springpole Lake, L-1, L-2 and L-5 (shown in Figure 5–1) The deep numerical layers in the model were vertically distributed to accommodate the open pit shell. The base of the model

domain was formed at a depth of 500.5 metres below ground surface (mbgs) (between -76 and -148 m amsl), representing a depth below which groundwater discharge was assumed to be negligible.

The numerical setup for model simulations is provided in Table 5-1. Further to the information provided in Table 5-1, a 1 % error acceptance criterion was taken for the model flow balance.

5.1.2 Simulated Hydrostratigraphy

The site hydrostratigraphy utilized in the numerical groundwater model as well as the corresponding justifications for these demarcations are discussed in detail in the baseline hydrogeology report (Appendix L-1) and summarized in Section 3.0. Hydrostratigraphic layers in the numerical groundwater model, along with the corresponding measured geometric averages that were used as initial estimates for model calibration, are summarized in Table 5-2.

The 3D hydrostratigraphic layers for the numerical model were generated using a combination of Leapfrog (Seequent 2020), Surfer (version 24) and Feflow's internal 3D layer generator. These include borehole data (821 points, including data from exploration drilling and investigation programs), test pits (106 points), outcrop mapping (458 points) and general observations from shoreline mapping (e.g., observations of bedrock outcropping, lake bed organics, other overburden layers). Control points were also added where necessary to constrain layer surfaces as required, generally at local topographic highs and at shoreline locations.

The total overburden thickness was interpolated utilizing the co-kriging scheme in Surfer, with the total overburden depths being co-kriged (10 m grid spacing) against the site DEM. The distribution of lake bed organics layers within the total overburden was interpolated in a similar fashion. The thickest sections of lake bed sediments generally correspond to the deepest sections of Springpole Lake. The interpolated thicknesses for the total overburden and lake bed organics are shown in Figure 5-3 and Figure 5-4, respectively. Overburden elements in the numerical model mesh were assigned based on the resulting interpolations for lake bed organics and other overburden layers. Lake bed organics elements were applied to the shallowest layers (i.e., layer 45) for the various smaller lakes / ponds around site, where no borehole data were available (e.g., L-1, L-2).

Differentiation of the UGM, host rock and low RQD zone bedrock layers in the numerical groundwater model were assigned based on the Leapfrog model, which was developed as part of rock mechanics investigations conducted by (SRK 2013, 202447). Host bedrock zones were further sub-divided based on location (CDF versus other host bedrock) and depth, as given in Table 5-2 and described in the 2023 baseline hydrogeology report (Appendix L-1). A cross section through the numerical groundwater model showing the resulting model layers is given in Figure 5-5. The horizontal extents of simulated bedrock types at a depth of 64 m, showing a typical bedrock distribution at depth, is shown in Figure 5-6.

Adjustments made to model layers for mining phase simulations are provided in Section 6.0.

5.1.3 Boundary Conditions for Pre-mining Phase Simulation

Pre-mining model boundary conditions are shown in Figure 5-7. Three types of boundary conditions were implemented in the baseline condition model:

- **Recharge (2nd type):** Two zones of groundwater recharge were applied corresponding to the footprints of the simulated host bedrock zones (i.e., CDF area and other host bedrock). Initial estimates of recharge were assigned based on the estimated ranges summarized in Section 3.4 and discussed in detail in Appendix L-1. Both were initially taken as 50 mm/yr.

- **Fluid transfer (3rd type):** Fluid transfer boundary conditions were applied for the various, generally small, streams present at site. The fluid transfer-rate for these was set to one per day (representing a high value such that groundwater – surface water exchange would not be impeded), with a reference head equal to the DEM at each groundwater model node.
- **Constant head (1st type):** Constant head conditions were applied to each of the lakes / ponds at site. The simulated values were generally based on surface water level measurements acquired at site where available, otherwise the approximate values from the DEM were taken. These values are given in Table 5-3.

Adjustments made to model boundary conditions for mining phase simulations are described in Section 6.0.

5.2 Pre-mining Phase Model Calibration (baseline conditions)

The baseline conditions model was calibrated to the measured groundwater levels from site monitoring wells and vibrating wire piezometers from the fall 2022 monitoring event (Section 3.3). Calibration was conducted by incrementally adjusting the model input hydraulic conductivity and recharge values, within reasonable limits defined by field measurements, until simulated groundwater levels provided an acceptable match to the observed values as indicated by goodness-of-fit parameters.

Figure 5–8 displays the calibration scattergram for the simulated versus observed groundwater levels. Horizontal error bars are shown on this figure for several data points at the lower end of the range of values. These error bars represent the range in uncertainty in VWP measurements due to the greater depths at which these particular VWPS have been installed. The “raw” observed values (blue markers) are used for goodness-of-fit calculations, although the true difference between the measured and simulated values for these points is likely better represented by the position of the right-hand extent of the error bar in the plot. Further discussion on this is provided in Appendix L-1.

The simulated heads show generally good agreement with the measured values. All parameters fall within the target calibration acceptance criterion of 10% of the measured water table relief, indicating a satisfactory model calibration (Wels et al. 2012; Anderson et al. 2015). Goodness-of-fit parameters based on the 82 measurements points (N) for the calibration are, thus:

- **Mean-error (ME) = +0.54 m (+1.7%):** The ME is the average difference between simulated and observed values, which therefore represents the overall tendency for a model to either under or over simulate heads relative to the measured data. The positive value for the ME indicates a slight tendency for the model to over-simulate the measured head values; however, this is likely affected by offsets in VWP measurements noted above (adjusting the VWP measured values would shift the ME to +0.23 m/+0.8%). As such, the true value is likely smaller. Despite this, +0.54 m is still considered sufficient in this context.
- **Mean-absolute error (MAE) = 2.07 m (6.4%):** The MAE represents the average absolute difference between simulated and observed water levels. As such, it is not affected by potential high positive and negative residuals that serve to balance each other across the dataset. Inspection of the calibration scattergram suggests that the largest MAE values are not associated with any specific range of head values, and are rarely greater than 5 m.
- **Root-mean-square error (RMSE) = 2.67 m (8.1%):** The RMSE is similar to the MAE in that it describes the typical difference between simulated and observed head values. The degree to which RMSE exceeds the MAE is an indicator of the extent to which outliers exist in the dataset. The RMSE for the calibrated groundwater flow model is 8.1%, indicating a satisfactory calibration.

Simulated and inferred water level contours as well as the spatial distribution of simulated residuals are shown in Figure 5–9. A comparison of the simulated and inferred head contours shows a reasonable agreement between the overall trends of groundwater flow. Groundwater highs are typically associated with local topographic highs and decrease towards the lows and local surface water features.

Residuals data points in Figure 5–9 do not appear to show any consistent spatial bias of residuals, except for the general tendency for simulated water levels in VWPs adjacent to Springpole Lake to underpredict the measured values; however, this can be attributed to the relative accuracy and resolution of VWP measurements at greater depths noted above. The residual values range from -6.49 m in BH-CAMP-32-403 (VWP located in the exploration camp area at site) to +5.5 m in SG22-017-128 (VWP adjacent to Springpole Lake).

The resulting calibrated model input parameters are given in Table 5-4 (geometric means of field data given in Table 5-2). The lake bed organics were simulated with a low isotropic K value of 10^{-8} m/s. Given that only two lab measurements of hydraulic conductivity were available for this layer (both with low values), this layer was selected for sensitivity analysis (Section 7.0). Overburden K_H was decreased from an initial input value of 5.9×10^{-6} to 1.0×10^{-6} m/s as a result of model calibration. This represents the largest shift from initial value to final calibration. Given this, assumed overburden hydraulic conductivity was also selected for sensitivity analysis (although overburden is expected to have limited influence on simulated seepages and open pit groundwater inflows) (Section 7.0). The UGM zone remained unchanged from initial to final calibration, largely due to its relatively small volumetric extent and proximity to Springpole Lake resulting in limited influence on the overall calibration results. Similar to the UGM zone, the low RQD zone was adjusted from 2.9×10^{-6} to 2.0×10^{-6} m/s during calibration, which represents a relatively minor change. The influence of the spatial extent of the low RQD zone is assessed in sensitivity analysis discussed in Section 7.0.

The calibrated host bedrock K_H values are shown relative to the measured values in Figure 5–10 (geometric means for the corresponding depth intervals are given in Table 5-2). Calibrated bedrock K_H values generally agree well with the measured mean values for each depth interval (excluding the deepest section of other host rock, which only has a single corresponding measurement), with most intervals being within a factor of three of the measured mean value. Vertical hydraulic conductivity values were primarily established through model calibration, using the underlying assumption that the anisotropy ratio decreases with depth as fractures seal due to bedrock confining pressures and both horizontal and vertical hydraulic conductivity (K_H and K_V) values converge towards the bedrock matrix permeability. Given the importance of bedrock hydraulic conductivity in the context of this assessment, detailed sensitivity analyses for the influence of bedrock K values on model predictions were conducted and are discussed in Section 7.0.

Recharge values were adjusted incrementally for both zones during calibration. It was generally found that, given the difference in shallow zone K values for the host rock zones, 50 mm/yr for the other host rock and 32 mm/yr for the CDF area rock yielded the optimal calibration result. These values both fall within the estimated range of recharge based on stream flow gauging (Section 3.4; Appendix L-1).

5.3 Model Limitations

The objective of numerical groundwater modelling presented in this report is to estimate the potential long-term effects of mine development on the local groundwater environment. Specifically, the model has been constructed to assess the rate of groundwater inflow to the fully developed open pit and the rate/distribution of seepage emanating from the fully constructed CDF. The model has been constructed using data/information from recent and historic site investigation programs. This consisted of numerous investigations to assess the hydrogeological conditions of bedrock at site and groundwater levels, in addition to consideration of other aspects such as overburden and stream flows.

The numerical model assumes an equivalent porous medium, whereby flow through the dual-porosity system (i.e., bedrock matrix and fractures) is assumed to be consistent with the overall bulk properties of the rock. This is considered to be applicable over the scale of investigation for this work; however, is unlikely to capture effects of individual fractures over small spatial / temporal scales.

Model simulations were conducted using steady-state conditions, which assumes that groundwater flow conditions have equilibrated to local / applied conditions and do not change with time. This is considered appropriate at this scale of this analysis, which is modelling the potential long-term effects of mine development.

Bedrock hydraulic conductivity data used to support model parameterization are primarily based on single well hydraulic response tests and packer testing. These tests represent small-scale measurements (i.e., approximately tens of metres test zone sensitivity) and tend to overestimate bedrock hydraulic conductivity values over larger scales as bedrock fractures eventually expire (i.e., fracture networks have limited persistence / connectivity over large scales). Considering the spatial scale of the model / assessment (i.e., approximately thousands of metres scale), this means that the reference bedrock hydraulic conductivity values used to inform the model parameterization may be biased higher than the average in situ value over this scale. This results in increased seepage values from the CDF, increased effects on water balance for surface waterbodies and increased groundwater inflow rates to the open pit. As such, the groundwater model is considered to be conservative with respect to the selection of input hydraulic conductivity values.

Table 5-1: Model Numerical Setup

Parameter	Value
Flow conditions	Unconfined
Flow state	Steady
Free surface	Phreatic
Residual water depth	0.15 m
Head error tolerance	10^{-3} (pre-mining)
Error norm	Euclidean L2 (RMS)
Equation system solver	SAMG
Solver termination criteria	10^{-10}

Note:

RMS = root mean square.

Table 5-2: Simulated Hydrostratigraphic Units with Initial Input Hydraulic Conductivities

Layer	Depth Zone (mbgs)	Measured Geometric Mean (m/s) ⁽¹⁾
Lake bed organics	N/A	N/A ⁽²⁾
Overburden	N/A	5.9×10^{-6} (12)
UGM zone	N/A	5.0×10^{-6} (4)
Low RQD zone	N/A	2.9×10^{-6} (33)
CDF area host rock	0–25	5.7×10^{-8} (30)
	25–200	1.6×10^{-8} (13)
	200+	2.3×10^{-9} (3)
Other host rock	0–25	8.5×10^{-7} (49)
	25–125	5.9×10^{-7} (48)
	125–300	1.1×10^{-7} (39)
	300+	1×10^{-10} (1)

Notes:

- (1) Number of measurements provided in brackets.
(2) Two lab test values of 3.0×10^{-10} and 1.7×10^{-9} m/s.
N/A = not applicable.

Table 5-3: Simulated Boundary Conditions

Feature	Water Surface Elevation (m amsl)
Birch Lake	393.1
Springpole Lake	391.0
Dole Lake	393.1
L-1	393.4
L-2	392.5
L-3	410
L-4	410
L-5	398
L-6	400.5
L-16	393
L-17	404
L-18	397
L-19	398.5
L-20	402

Table 5-4: Post-calibration Pre-mining Model Parameters

Layer	Depth (mbgs)	K_H (m/s)	K_V (m/s)	Recharge (mm/yr)
Lake bed organics	N/A	1.0×10^{-8}	1.0×10^{-8}	N/A
Overburden	N/A	1.0×10^{-6}	5.0×10^{-7}	N/A
UGM zone	N/A	5.0×10^{-6}	5.0×10^{-6}	N/A
Low RQD zone	N/A	2.0×10^{-6}	2.0×10^{-6}	N/A
CDF area host rock	0–25	8.0×10^{-8}	2.9×10^{-8}	32
	25–200	3.7×10^{-8}	1.8×10^{-8}	N/A
	200+	8.0×10^{-9}	8.0×10^{-9}	N/A
Other host rock	0–25	6.0×10^{-7}	1.0×10^{-7}	50
	25–125	2.0×10^{-7}	7.0×10^{-8}	N/A
	125–300	7.0×10^{-8}	4.0×10^{-8}	N/A
	300+	1.0×10^{-8}	1.0×10^{-8}	N/A

Note:

N/A = not applicable.



Model Domain



**FIRST MINING
GOLD**



Figure No: 5-1

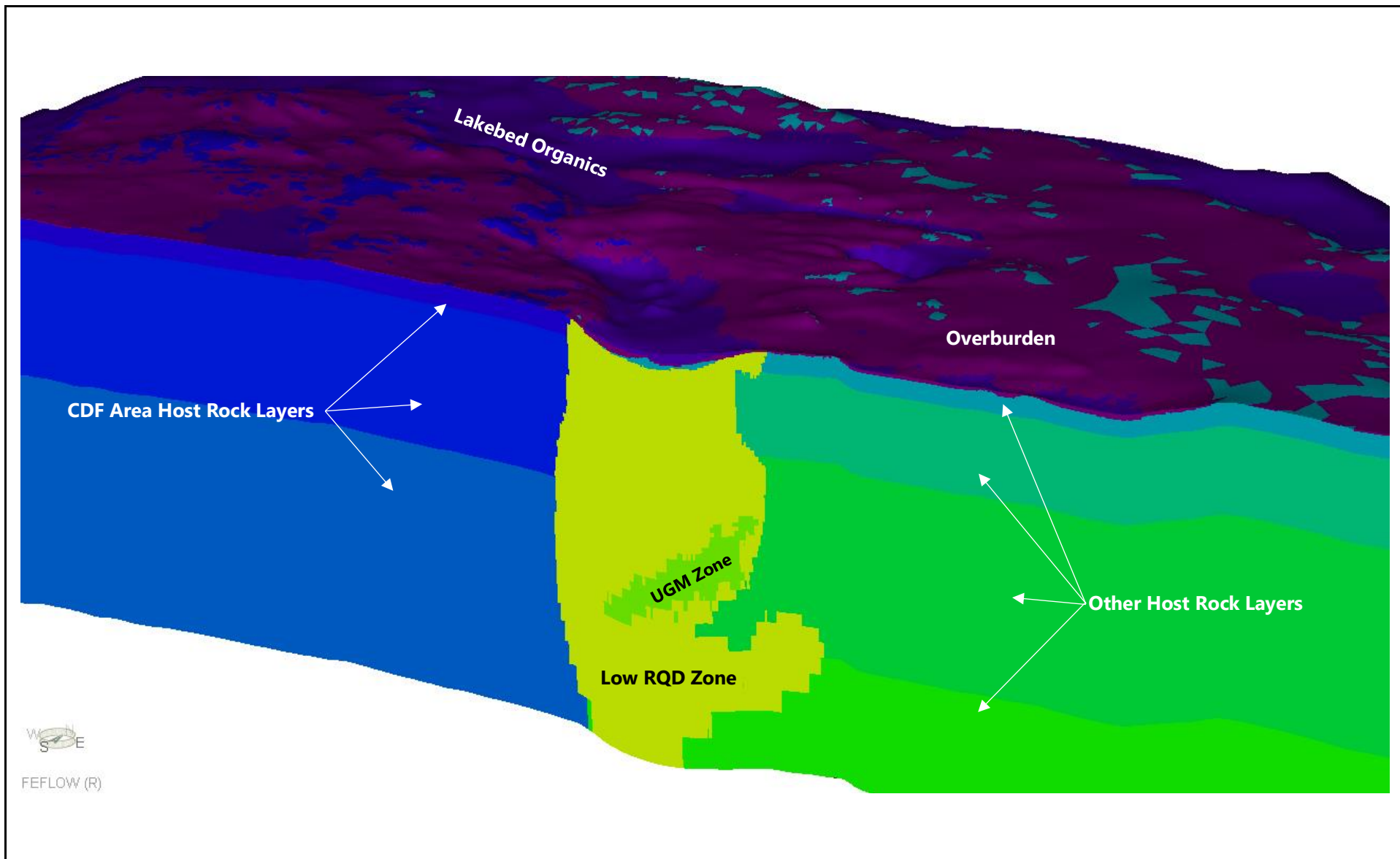
Project No: ONS2104



Date: 29-Jun-23

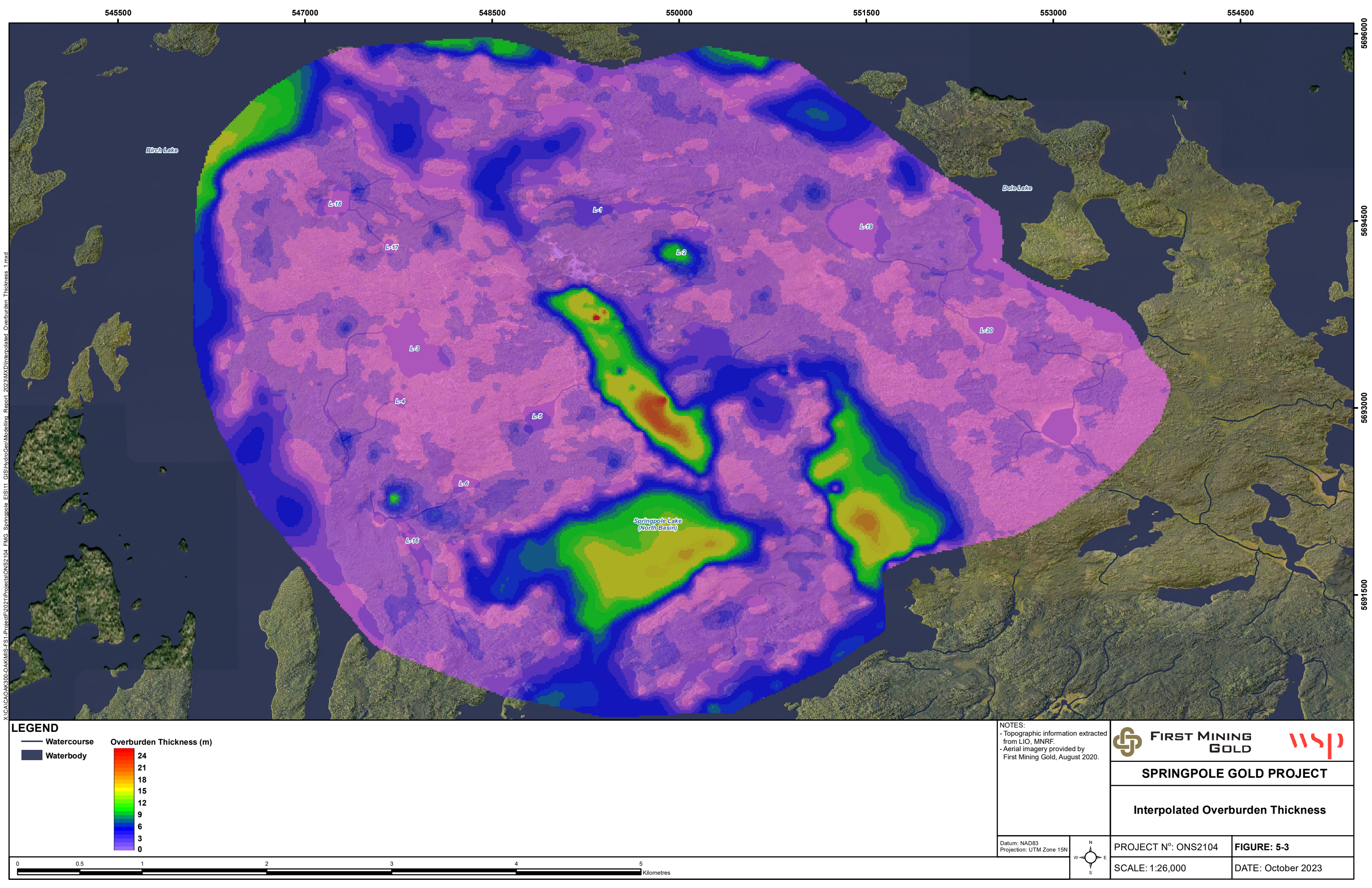
Rev: 0

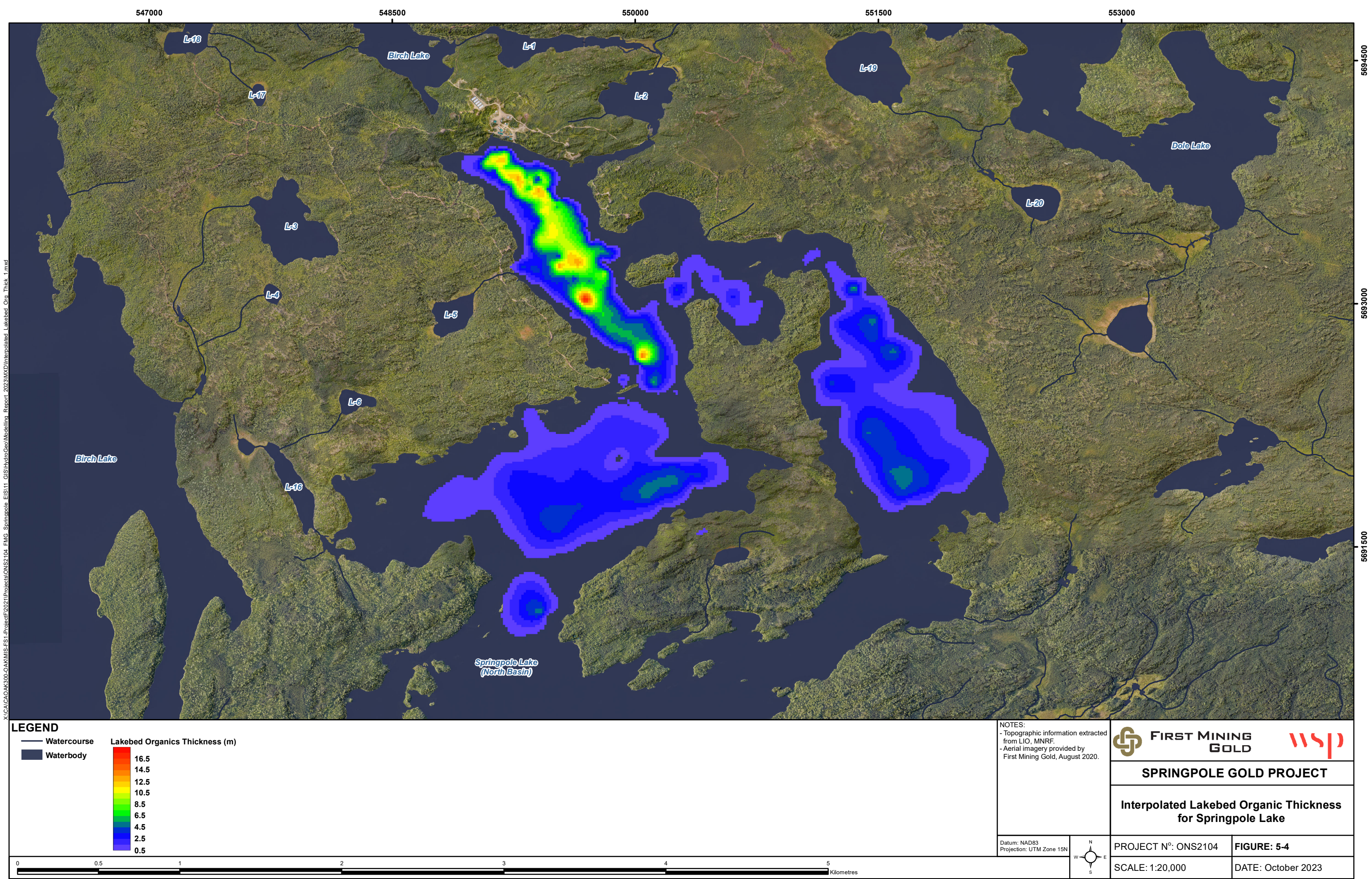
Springpole Gold Project – 2023 Hydrogeological Modelling Report

Model Domain and Mesh

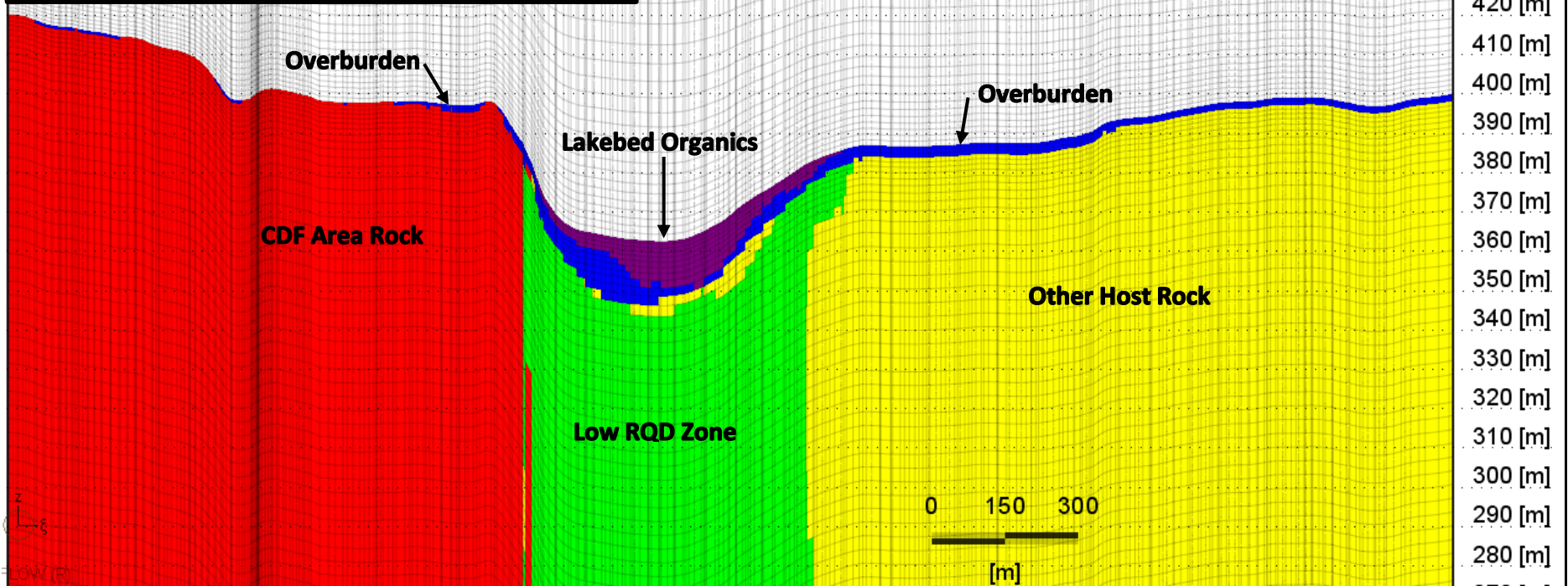
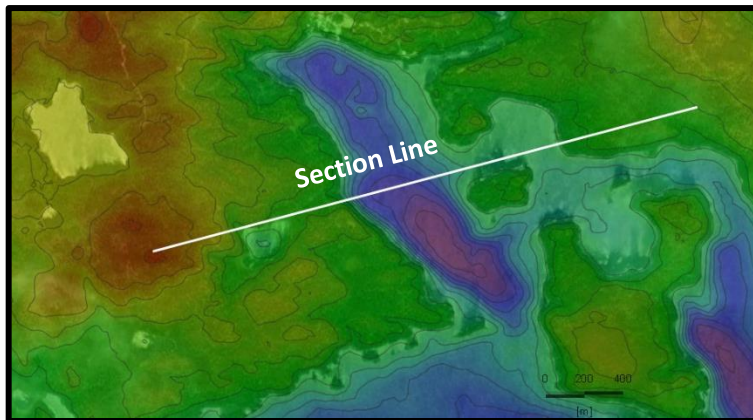


 FIRST MINING GOLD	Figure No: 5-2	Springpole Gold Project – 2023 Hydrogeological Modelling Report
	Project No: ONS2104	
	Date: 29-Jun-23	3D Model Domain and Layers
	Rev: 0	





X:\CA\CA\OAK300-OAKMIS-FS1-Project\2021\Projects\ONS2104_FMG_Springpole_EIS\11 GIS\HydroGeo\Modelling_Report_2023\MXD\Interpolated_Lakebed_Org_Thick_1.mxd



**FIRST MINING
GOLD**

Figure No: 5-5

Project No: ONS2104

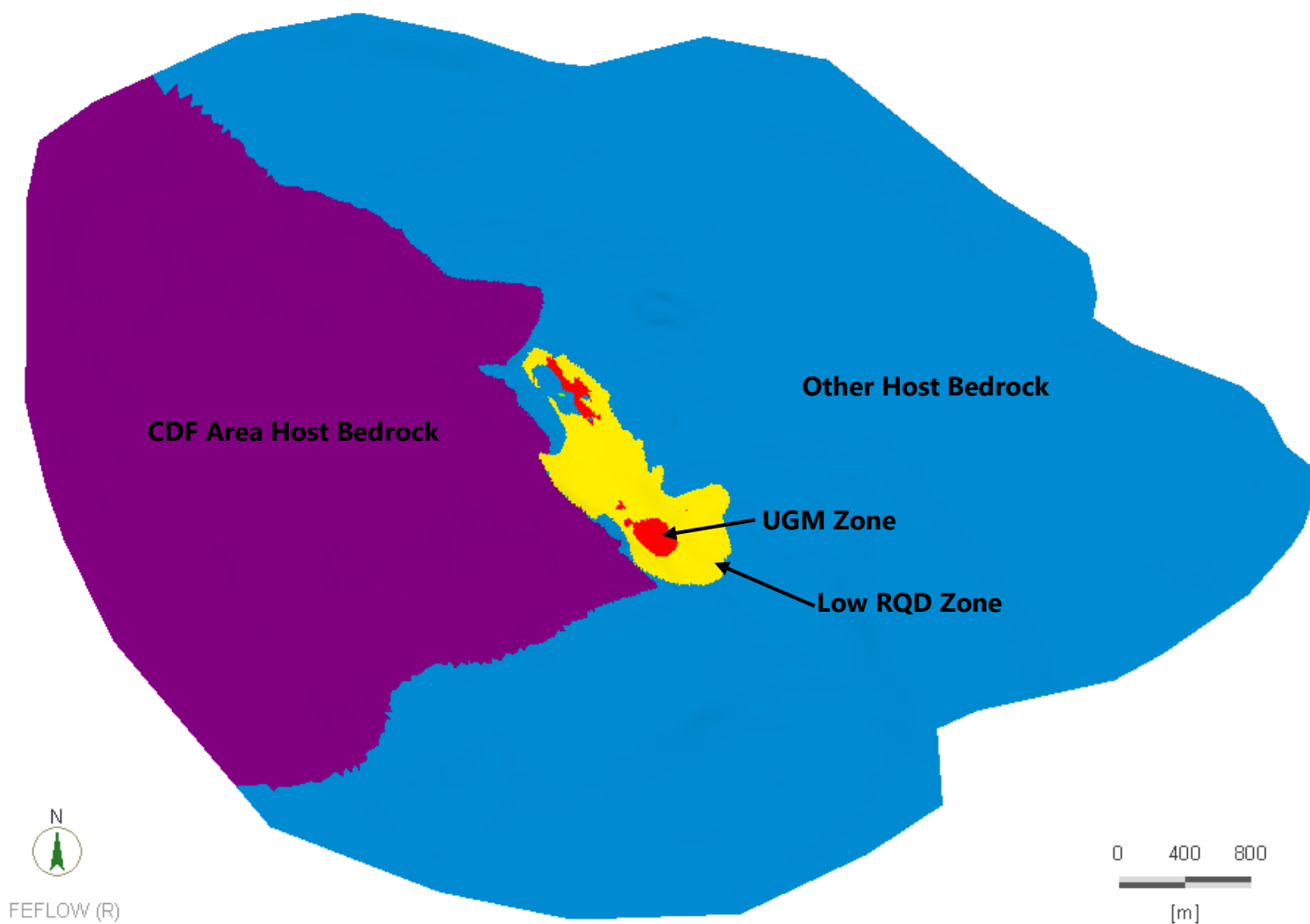
Springpole Gold Project – 2023 Hydrogeological Modelling Report



Date: 29-Jun-23

Rev: 0

Model Layers Cross Section



**FIRST MINING
GOLD**



Figure No: 5-6

Project No: ONS2104

Date: 29-Jun-23

Rev: 0

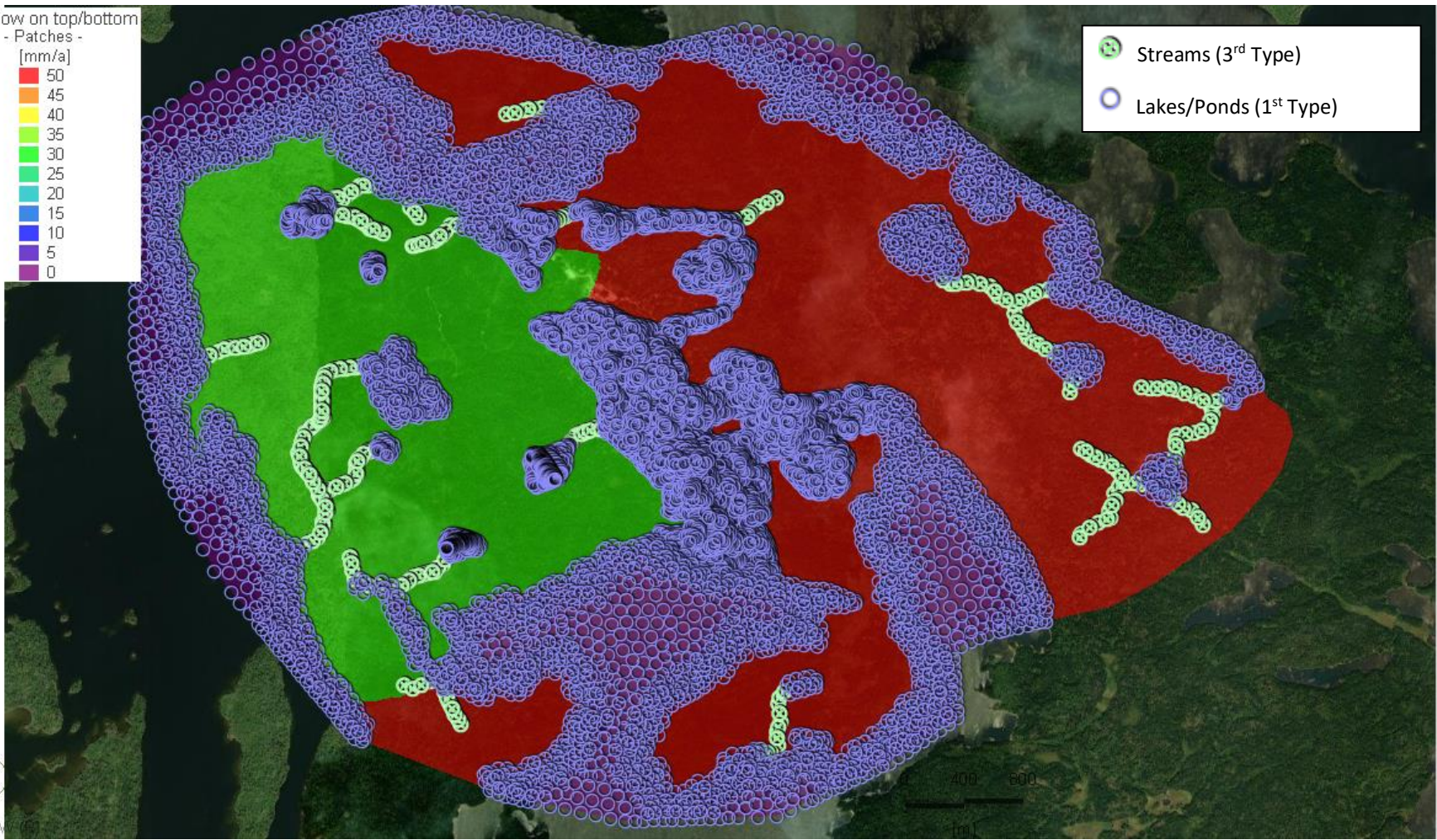
Springpole Gold Project – 2023 Hydrogeological Modelling Report



Bedrock Layers Plan View (26 mbgs)

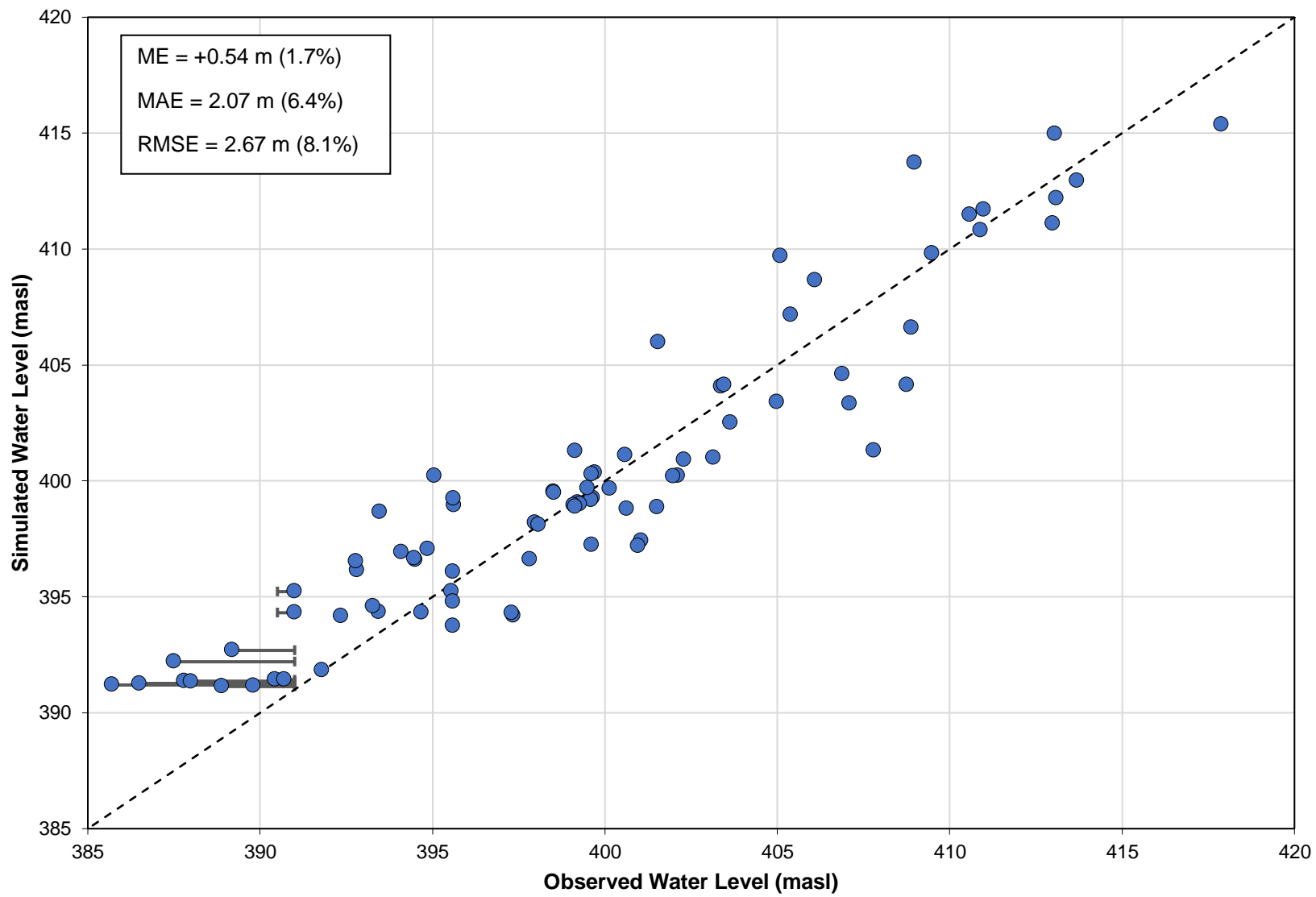
In/outflow on top/bottom
 - Patches -
 [mm/a]

50
45
40
35
30
25
20
15
10
5
0

- Streams (3rd Type)
- Lakes/Ponds (1st Type)



	Figure No: 5-7	Springpole Gold Project – 2023 Hydrogeological Modelling Report
	Project No: ONS2104	
	Date: 29-Jun-23	Pre-mining Model Boundary Conditions
	Rev: 0	



**FIRST MINING
GOLD**

Figure No: 5-8

Project No: ONS2104

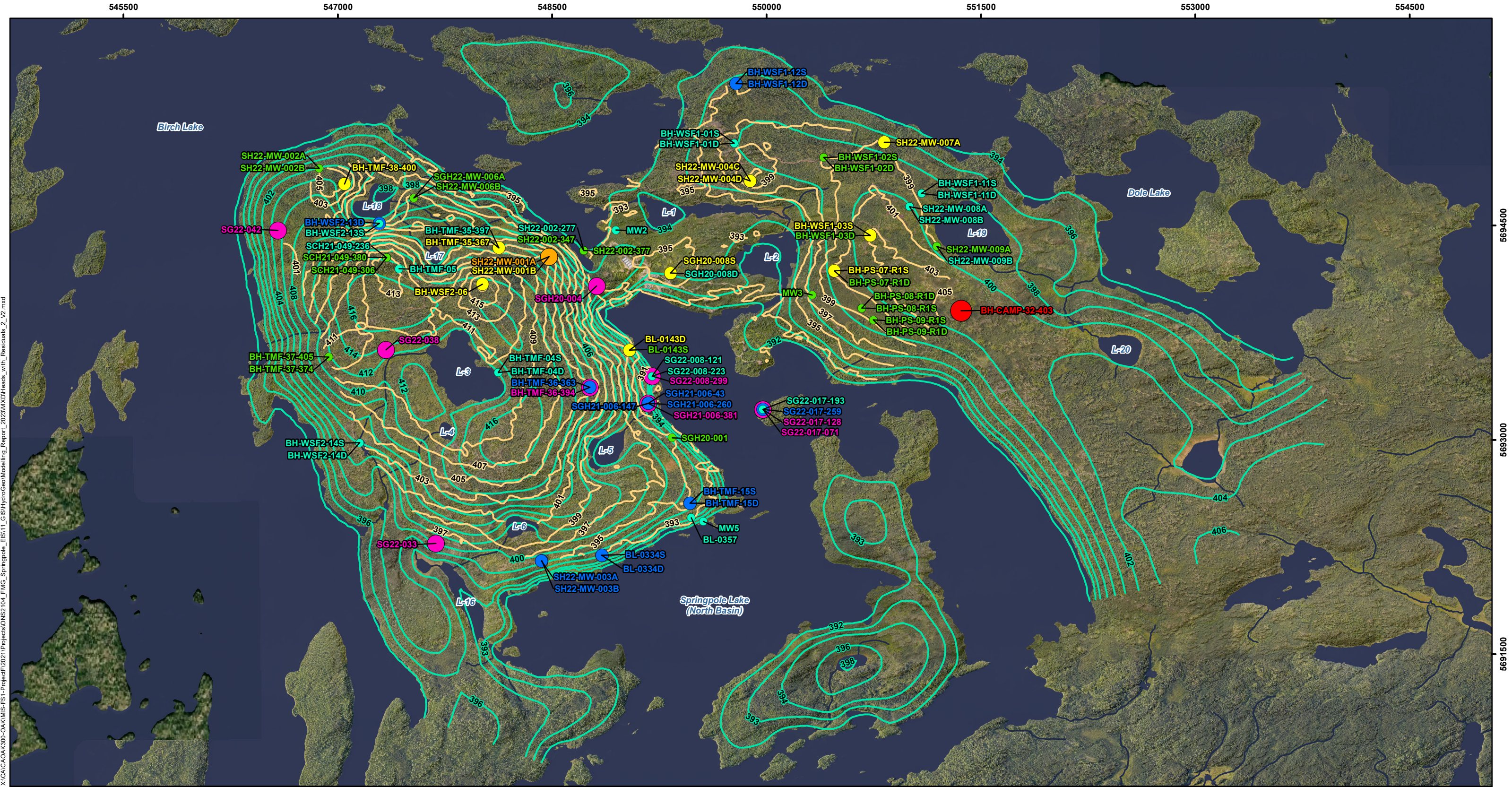
Springpole Gold Project – 2023 Hydrogeological Modelling Report



Date: 29-Jun-23

Rev: 0

Calibration Scattergram



LEGEND

- Measured Head Contour (masl)
- Simulated Head Contour (masl)
- Watercourse
- Waterbody

Residuals Points (m)

- <-6
- 6 to -4
- 4 to -2
- 2 to 0
- 0 to 2
- 2 to 4
- > 4

NOTES:

- Topographic information extracted from LIO, MNR.
- Aerial imagery provided by First Mining Gold, August 2020.

Datum: NAD83
Projection: UTM Zone 15N

FIRST MINING GOLD

SPRINGPOLE GOLD PROJECT

Simulated and Measured Heads with Residuals

PROJECT N°: ONS2104

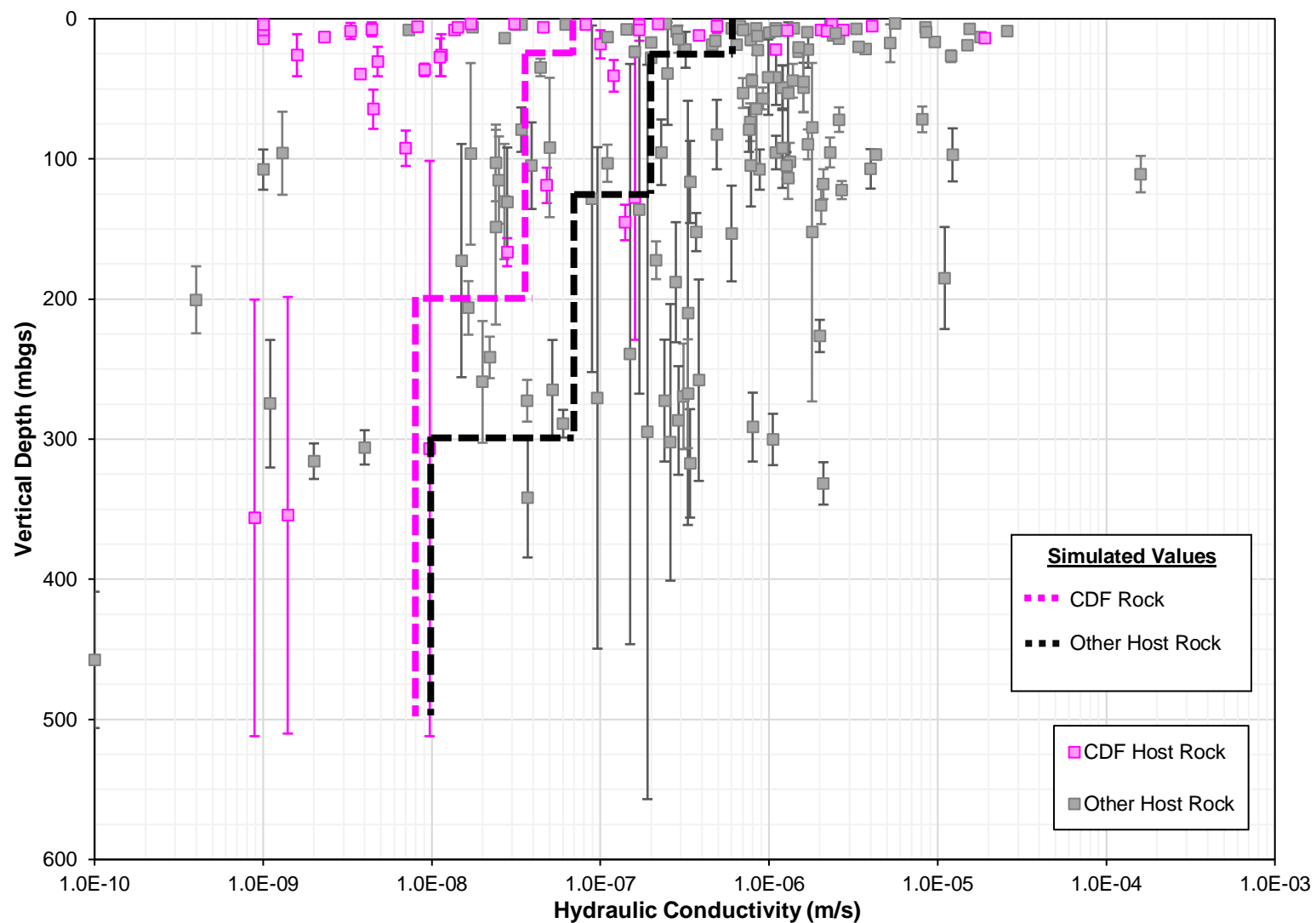
SCALE: 1:25,000

FIGURE: 5-9

DATE: November 2023

00.512345

Kilometres



**FIRST MINING
GOLD**

Figure No: 5-10

Project No: ONS2104

Springpole Gold Project – 2023 Hydrogeological Modelling Report



Date: 29-Jun-23

Rev: 0

Simulated and Measured Host Bedrock Hydraulic Conductivity

6.0 MINING PHASE SIMULATIONS

Following calibration, the model described above was modified and used to simulate EoMO conditions and post-closure conditions. A 3D view of the mining phase model is shown in Figure 6–1. Mining phase simulations were conducted with three primary objectives:

- Quantify seepage pathways from the CDF and the ore stockpiles for the EoMO and post-closure phases;
- Estimate the groundwater inflow rate to the open pit during the EoMO phase; and
- Predict changes in groundwater–surface water interactions for both phases.

Seepage and water balance analyses were conducted based on sub-watersheds corresponding to the hydrological and receiver water quality modelling for the site. The sub-watersheds of hydrological nodes used for the analyses are shown in Figure 6–2. Note that sub-watersheds for these nodes change from pre-development to post-development. This should be considered when interpreting changes in water balance between pre-mining and mining phase simulations.

To accomplish the objectives listed above, the following site features were introduced into the calibrated groundwater flow model:

Co-disposal Facility

The footprint of the proposed CDF is shown in Figure 1–2 and a 3D view of the numerical model CDF layers is shown in Figure 6–1. Generally, the CDF consists of two cells (north and south) which are bound at the perimeter by mine rock dams and separated by an internal mine rock dike. The south cell includes a geosynthetic clay liner (GCL) on the upstream embankment of the west, south and east dams. The crest elevation of the south cell is 480 m, while the crest of the north cell is 485 m.

The south cell will be maintained at nearly saturated conditions while the north cell will have variably saturated conditions. As such, the south cell top surface was simulated using a constant head boundary condition with an assumed water level of 480 m. The north cell was simulated using an assumed infiltration boundary condition of 200 mm/yr (this value was varied during the model sensitivity analysis). These boundary conditions were applied for both mining phase cases (i.e., EoMO and post-closure). A seepage face boundary condition (i.e., outflow-only constant head boundary condition with the reference head equal to the nodal elevation) was applied at the downstream dam toe around the perimeter of the CDF to allow for seepage discharge at the dam toes. In addition, seepage nodes (with an assumed reference elevation of 1 mbgs) were also applied 60 m away from the dam toes to simulate the perimeter seepage collection ditches. The various lakes / ponds within the footprint of the CDF were removed, including L-3, L-4, L-5, L-6, L-17 and L-18. For the purpose of base case simulations, the CDF south cell embankment liner was simulated as being impermeable (numerical elements representing the liner set to inactive). The effects of liner performance on seepage were subsequently assessed using a 2D cross sectional model for the south cell, which is presented in Section 7.3.

Tailings materials within the south cell are expected to have higher fines content compared to the north cell (which is to consist of co-mingled non-acid-generating tailings and mine rock materials); therefore, for both cases, the south cell was simulated with an assumed isotropic hydraulic conductivity of 10^{-7} m/s and the north cell was simulated with an anisotropic hydraulic conductivity of 10^{-6} m/s (with $K_H/K_V = 10$).

Open Pit

The proposed open pit footprint is shown in Figure 1–2 and is shown in 3D in Figure 6–1. The open pit is located at the northern basin of Springpole Lake and will require controlled dewatering of a section of the basin of the lake beyond two dikes during its development. Based on the current design, the open pit has a total depth of approximately 300 m, with a bottom elevation of 88 m asl. Boundary conditions for the open pit were applied based on the mining phase and are described in the following sections.

Dikes

Two dikes are to be placed to isolate the open pit area from Springpole Lake during mine development and operations (Figure 1–2). These are to consist of impermeable core dikes (i.e., plastic cement) and a zone of pressure grouted bedrock underneath the dikes to limit seepage through the shallow rock underlying the dikes. Details on their simulation for each case are provided below (see Section 6.1 and 6.2).

Fish Habitat Development Area

A fish habitat development area, shown in Figure 1–2, is planned to be implemented for the post-closure phase at the east of the pit. For post-closure conditions, this was assumed to have a constant water level equal to Springpole Lake (391 m asl).

Ore Stockpiles

Ore stockpiles are located adjacent to the plant site, including a low grade ore stockpile and a combined medium and high grade ore stockpile. Since ore within the stockpiles will be processed prior to site closure, the ore stockpiles are only considered as a potential source of seepage during the EoMO phase. Further, since the ore stockpiles will consist of cobbles to boulders sized material, groundwater mounding is not expected to occur within the stockpiles and subsurface seepage rates from facility would thus be limited to the natural groundwater flow rate. Thus, the ore stockpiles were not explicitly simulated using discrete model layers. Instead, seepage analysis was conducted by performing forward particle tracking from the footprint of the stockpiles to determine the fate and rate of seepage for the EoMO condition. Seepages from the ore stockpiles, therefore, correspond to the rate of groundwater recharge, prior to mine development (i.e., pre-mining conditions).

6.1 End of Mine Operations Phase Simulations

The EoMO model effectively represents conditions on the first day of closure. Overall, this case is expected to represent the most conservative with respect to effects on the water balance of the various surface water lakes / ponds in the vicinity of the site due to drawdown / withdrawals from the open pit dewatering. With respect to seepage from the CDF, however, this case is not likely to be the most conservative as the dewatered open pit is expected to act as a major captor of seepage emanating from the CDF, thereby mitigating seepages that would otherwise migrate to other nearby receivers.

Boundary conditions for this case are shown in Figure 6–3 For this case:

- The CDF is simulated as described above in Section 6.0.
- The open pit is simulated in its fully dewatered state. To achieve this in the EoMO model, cells within the open pit volume were set to inactive and the exterior nodes of the volume were assigned outflow-only seepage face boundary conditions.
- The dikes were implemented by removing the constant head cells representing Springpole Lake on the open pit side of the dikes. As such, flow from Springpole Lake to the open pit is possible whereby water enters the model at the Springpole Lake boundary and travels through the bedrock

toward the open pit (i.e., under the dike structure overlying the existing overburden and bedrock). The dewatered area of Springpole Lake (i.e., between the dikes and open pit) was assigned and assumed recharge / infiltration of 30 mm/yr.

6.1.1 End of Mine Operations Phase Simulation Results

Simulated shallow bedrock head contours and drawdown contours for the EoMO case are shown in Figure 6-4 and Figure 6-5, respectively. Contours in these plots show the following notable characteristics:

1. Simulated heads range from 480 m asl, which corresponds to the simulated south cell boundary condition level, to 88 m asl, which corresponds to the bottom of the dewatered open pit.
2. A drawdown cone emanates radially from the open pit. This drawdown cone extends outward from the open pit toward the nearest boundary conditions (mainly Springpole Lake and Birch Lake). A 2-m drawdown contour emanating from the open pit is shown in Figure 6-5, indicating an inferred zone of influence for the open pit.
3. Groundwater mounds within the CDF, but extends only as far as the perimeter dams downstream side toes and nearby collection ditches, which collect groundwater seepage.

Simulated groundwater flow budgets are shown as scaled spheres along the boundary conditions / shorelines at Birch Lake and Springpole Lake (i.e., the dike locations) in Figure 6-6 and Figure 6-7, respectively. The scaled spheres show the magnitude of inflow / outflow from the groundwater model at each model node (red = inflow, blue = outflow). In this case, model nodes at the edge of the boundary conditions show the highest rates of inflow. This concept holds true at most locations; interactions between groundwater and surface water tend to be focused along the shorelines of the various lakes / ponds.

Groundwater-surface water interactions were assessed by analyzing model computed flow rate budgets at the hydrological nodes. A summary of the water budgets for each hydrological node is given in Table 6-1. These budgets represent the net water budget for each hydrological node (i.e., the net value of gaining and losing components). This table also provides the simulated groundwater inflow rate to the open pit.

The simulated open pit groundwater inflow rate is 3,034 cubic metres per day (m^3/d) in the base case simulation. Inflows to the open pit are sourced from four general areas: the portion of Birch Lake immediately north of the open pit, Springpole Lake (on the lake side of both dikes), seepage from the CDF area and general groundwater recharge. The largest changes in groundwater budgets from pre-mining to EoMO conditions are for node 5 (Springpole Lake), node 1 (L-1) and nodes 6 to 8 (Birch Lake), with smaller changes for the various other lakes / ponds. The smallest change occurs at node 3 (lake L-20). It should be noted that the sub-watershed footprints for some hydrological nodes change from pre-mining to post-development conditions (e.g., node 5, Figure 6-2); therefore, a portion of the water budget change is a result of this change in sub-watershed footprints. For example, a portion of the node 5 (Springpole Lake) sub-watershed is replaced by the mine site and open pit area. While the largest overall changes in water budgets can be attributed to Birch Lake and Springpole Lake, these will generally be relatively minor compared to the overall water balance for these features. Smaller lakes and ponds in close proximity to the open pit show relative changes that are more significant. For example, Lake L-19 changes from a net gaining feature ($+9 \text{ m}^3/\text{d}$) to a net losing feature ($-49 \text{ m}^3/\text{d}$), representing a change of $58 \text{ m}^3/\text{d}$.

Seepage pathways and rates were assessed in the model using particle tracking to delineate source / receptor zones for seepage emanating from the CDF (as well as the ore stockpiles) in conjunction with the fluid budget analyzer tool. Using this method, particle tracking was conducted in the forward direction from the CDF to determine the discharge locations of CDF seepage. Reverse particle tracking was then conducted from the identified receivers back to the CDF to determine the corresponding CDF seepage rates (by

analyzing model mass balances for each zone). The resulting seepage bypass rates for each hydrological node are provided in Table 6-2 along with the total seepage rate and corresponding capture rates (i.e., the amount of flow reporting to the CDF dam downstream side toes and perimeter collection ditches).

The open pit is the primary receiver of seepages from both the north cell and south cell in this case. Combined, the open pit and seepage collection ditches are predicted to capture 91% of the total seepage from the north cell and 97% of the total seepage from the south cell. When considered as the total CDF, these represent a total of 93% seepage capture by either the open pit or seepage collection ditches. The primary receiver of the 9% bypass for the north cell is Birch Lake (nodes 6 to 8) while nodes 4 and 5 receive the remaining 3% bypass from the south cell. For the combined north and south cells, i.e., the total CDF, approximately 20% of the total seepage is captured by the open pit and 73% discharges to the perimeter collection ditches (i.e., a combined capture of 93%), with the remaining 7% discharging to surrounding receivers. Seepages emanating from the low grade ore stockpile are split between the open pit and Birch Lake (node 8), with approximately 87% of the seepage discharging to the open pit and 13% to Birch Lake, and all of the simulated seepage from the medium and high grade ore stockpile discharging to the open pit.

6.2 Post-closure Phase Simulations

The post-closure model simulates conditions long after mine closure, representing conditions where groundwater and surface water levels have recovered to their long-term states, post mine operations. This case is the most relevant for simulated CDF seepages, as it reflects the steady-state / long-term flow rates for seepage from the CDF.

Boundary conditions for the post-closure case are shown in Figure 6–8. In this model case:

- The CDF is simulated as described in Section 6.0. The perimeter collection ditches / dam toes seepage nodes are present in this model, as with the EoMO model.
- The open pit is simulated in its fully filled state. Elements previously set as inactive to simulate the excavation of the open pit are still inactive; however, the simulated water level for the open pit lake boundary condition is now set equal to Springpole Lake (391 m amsl).
- The area of Springpole Lake between the dikes and open pit that is desaturated in the EoMO model is now refilled. The fish habitat development area connected to Springpole Lake is also simulated in this case.
- For water budget and seepage accounting purposes, the refilled open pit, fish habitat development area and refilled section of Springpole Lake (noted in previous bullet) are referred to as the open pit area.

6.2.1 Post-closure Phase Simulation Results

Simulated head contours in the shallow bedrock for the post-closure model are shown in Figure 6–9. Similar to the EoMO case, simulated heads mound within the footprint of CDF in the post-closure case. Heads near the open pit, however, have reached their long-term conditions, which results in a much less pronounced gradient towards the former open pit / Springpole Lake.

As with the EoMO case, groundwater budgets were analyzed for each hydrological node. Simulated groundwater budgets for the post-closure case are provided in Table 6-3.

Aside from the changes in sub-watershed footprints for the post-closure conditions, the primary factor contributing to differences between the pre-mining and post-closure water budgets is the inclusion of the CDF and its associated boundary conditions (200 mm/yr for the north cell and a constant head of 480 m asl for the south cell). In the pre-mining / calibration model, the CDF is not present and groundwater recharge

in this area is simulated with a recharge value of 32 mm/yr, which generally discharges to the nearby streams and lakes / ponds. Although a greater amount of water is available for seepage in the post-closure case as compared to the corresponding footprint for the pre-mining case, most of this water is predicted to discharge at the dam toes / perimeter collection ditches; therefore, there is generally a net decrease in the amount of groundwater reporting to surface water features (Birch Lake being the primary example). Similar to the EoMO simulation, the largest relative changes in water budgets tend to be for the smaller lakes / ponds. Specifically, lake L-19 experiences an 11 m³/d change in groundwater budget from pre-mining, as a portion of groundwater flow is diverted toward the filled open pit / fish habitat development area.

Simulated seepages from the CDF were assessed for the post-closure case and are provided in Table 6-4. In addition, the final discharge locations of CDF seepage are shown in Figure 6-10. In this figure, the polygons within the CDF depict the source areas for CDF seepage relative to their eventual discharge locations. For example, the teal polygon in this figure depicts the source area for seepage within the CDF that eventually discharges to node 8 (Birch Lake).

Simulated seepages in Table 6-4 show several characteristics:

- Seepages are limited to features immediately surrounding the CDF. Nodes 1, 2 and 3, which are farther away, are not predicted to receive seepage from the CDF.
- Approximately 90% of north cell seepage is captured at the perimeter dam toes / perimeter collection ditch. Birch Lake (nodes 6 to 8) is the primary receiver of the 10% of north cell seepage that bypasses the perimeter collection ditch (71 m³/d). A negligible amount of seepage from the north cell discharges to nodes 4 or 5, while 21 m³/d is predicted to discharge to the open pit area.
- Approximately 91% of the south cell seepage is captured at the perimeter dam toes / perimeter collection ditch. Springpole Lake and the open pit area are the primary receivers of groundwater seepage emanating from the south cell that bypasses the seepage collection ditches (a total of 43 m³/d, combined). A negligible amount of seepage from the south cell discharges to nodes 6 to 8.

Fluid budget analysis and particle tracking results indicate that seepage flows from the south cell can be grouped into three main pathways: 1) upwelling of flows into the dams from / through the bedrock near the embankment liner, 2) seepage into the internal dike separating the north and south cells, and 3) diffuse seepage / percolation into the bedrock underlying the south cell. Upwelling under the liner and seepage into / through the internal dike both contribute flows to the perimeter dams, which discharge at the toes of the dams (i.e., these flows are generally captured). Conversely, diffuse seepage into the bedrock represents the main pathway by which seepage bypasses capture and discharges to nearby receivers. This is evident in Figure 6-10, which shows that seepage bypass for nodes 4 and 5 as well as the open pit area are sourced from the centroid of the south cell. Essentially, these flows migrate vertically from the south cell boundary condition through the south cell tailings then enter the underlying bedrock, at which point they start to move sub-laterally towards the surrounding receivers, deep enough that they bypass the capture zone of the perimeter collection ditches / dam toes.

Seepage pathways from the north cell are similar to the south cell in that the bypass seepages are generally derived from the centroid of the north cell (Figure 6-10). Flows accumulate at the base of the north cell above the bedrock (which has lower hydraulic conductivity compared to the overlying co-mingled tailings and mine rock) and flow through the tailings (and shallowest rock) towards the perimeter dams. Flows accumulate within the dams, converging and flowing towards the low points where they subsequently discharge at the dam toes / perimeter collection ditches.

Table 6-1: End of Mine Operations Model Simulated Water Budgets

Receiver Waterbody	Hydrological Node	Pre-mining Groundwater Budget (m ³ /d) ⁽¹⁾	EoMO Groundwater Budget (m ³ /d) ⁽¹⁾	Change (m ³ /d)
L-1	1	54	-235	-289
L-19	2	9	-49	-58
L-20	3	-10	-13	-3
L-16	4	61	42	-19
Springpole Lake	5	1,031	-657	-1,688
Birch Lake	6	234	-2	-236
	7	179	134	-45
	8	672	566	-106
Open pit	N/A	N/A	3,034	N/A

Notes:

(1) Sign convention taken with respect to surface water (+ = gaining; - = losing).

N/A = not applicable.

Table 6-2: Simulated End of Mine Operations Seepage Rates

Receiver Waterbody	Hydrological Node	Seepage from CDF North Cell (m ³ /d)	Seepage from CDF South Cell (m ³ /d)	Seepage from Low Grade Ore Stockpile (m ³ /d)	Seepage from Medium-High Grade Ore Stockpile (m ³ /d)
L-1	1	0	0	0	0
L-19	2	0	0	0	0
L-20	3	0	0	0	0
L-16	4	3	5	0	0
Springpole Lake	5	0	12	0	0
Birch Lake	6	5	0	0	0
	7	50	0	0	0
	8	28	0	10	0
Open pit	N/A	167	134	66	30
Collection ditch capture ⁽¹⁾		694	372	N/A	N/A
Total		947	523	76	30

Notes:

(1) Includes portion discharging at downstream side dam toes.

N/A = not applicable.

Table 6-3: Post-closure Model Simulated Water Budgets

Receiver Waterbody	Hydrological Node	Pre-mining Groundwater Budget (m ³ /d)	Post-Closure Groundwater Budget (m ³ /d)	Change (m ³ /d)
L-1	1	54	54	0
L-19	2	9	-2	-11
L-20	3	-10	-9	1
L-16 + L-6	4	61	38	-23
Springpole Lake	5	1,031	628	-403
Birch Lake	6	234	164	-70
	7	179	113	-66
	8	672	641	-31
Open pit area ⁽¹⁾	N/A	N/A	280	N/A

Notes:

(1) Open pit area represents the section of Springpole Lake on the open pit side of the two dikes which has since refilled following mine closure.

N/A = not applicable.

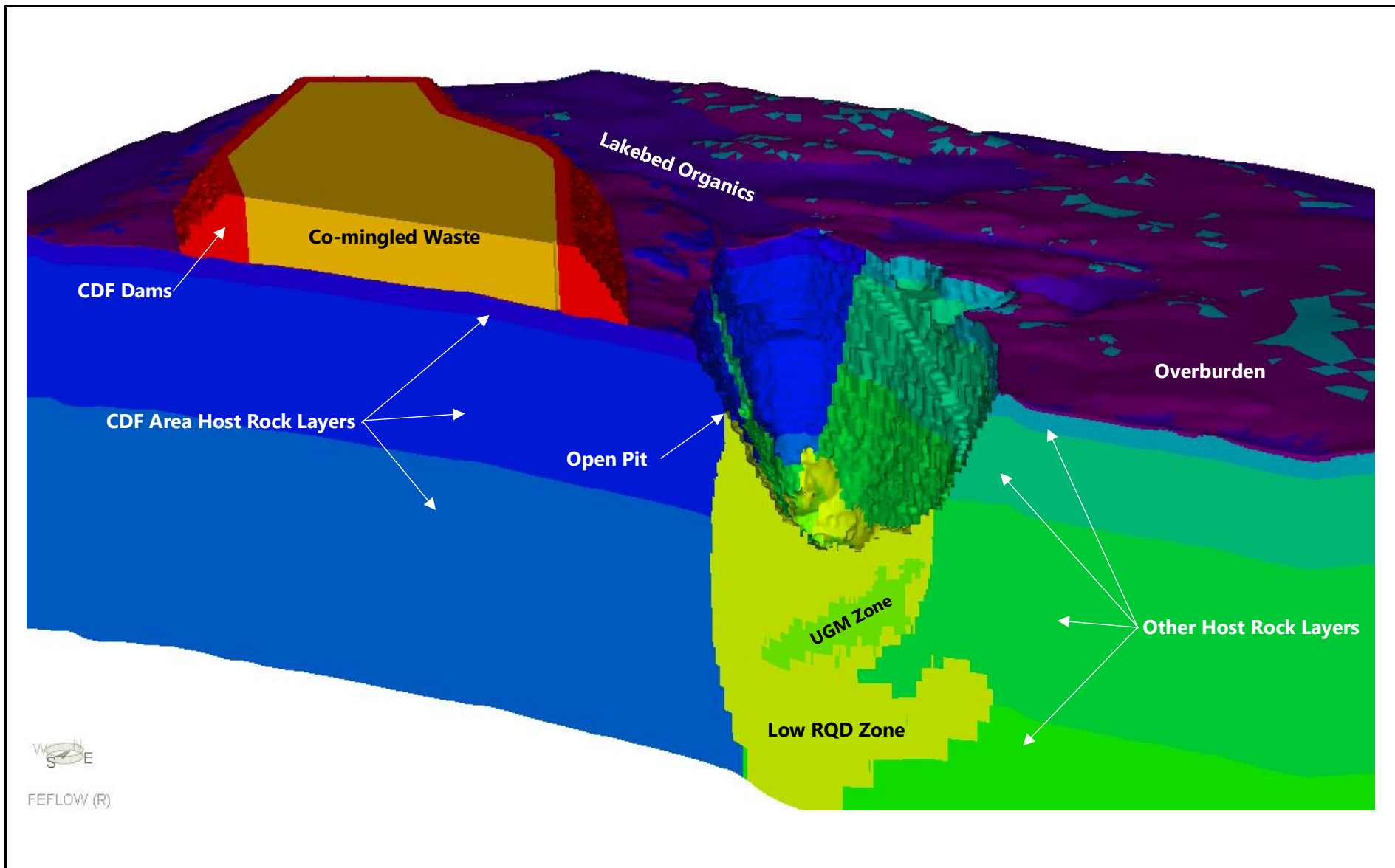
Table 6-4: Simulated Post-closure Seepage Rates

Receiver Waterbody	Hydrological Node	Seepage from CDF North Cell (m ³ /d)	Seepage from CDF South Cell (m ³ /d)
L-1	1	0	0
L-19	2	0	0
L-20	3	0	0
L-16 + L-6	4	0	5
Springpole Lake	5	0	24
Birch Lake	6	19	0
	7	26	0
	8	26	0
Open pit area ⁽¹⁾	N/A	21	19
Collection ditch capture ⁽¹⁾		855	475
Total		948	523

Notes:

(1) Open pit area represents the section of Springpole Lake on the open pit side of the two dikes which has since refilled following mine closure.

N/A = not applicable.



**FIRST MINING
GOLD**



Figure No: 6-1

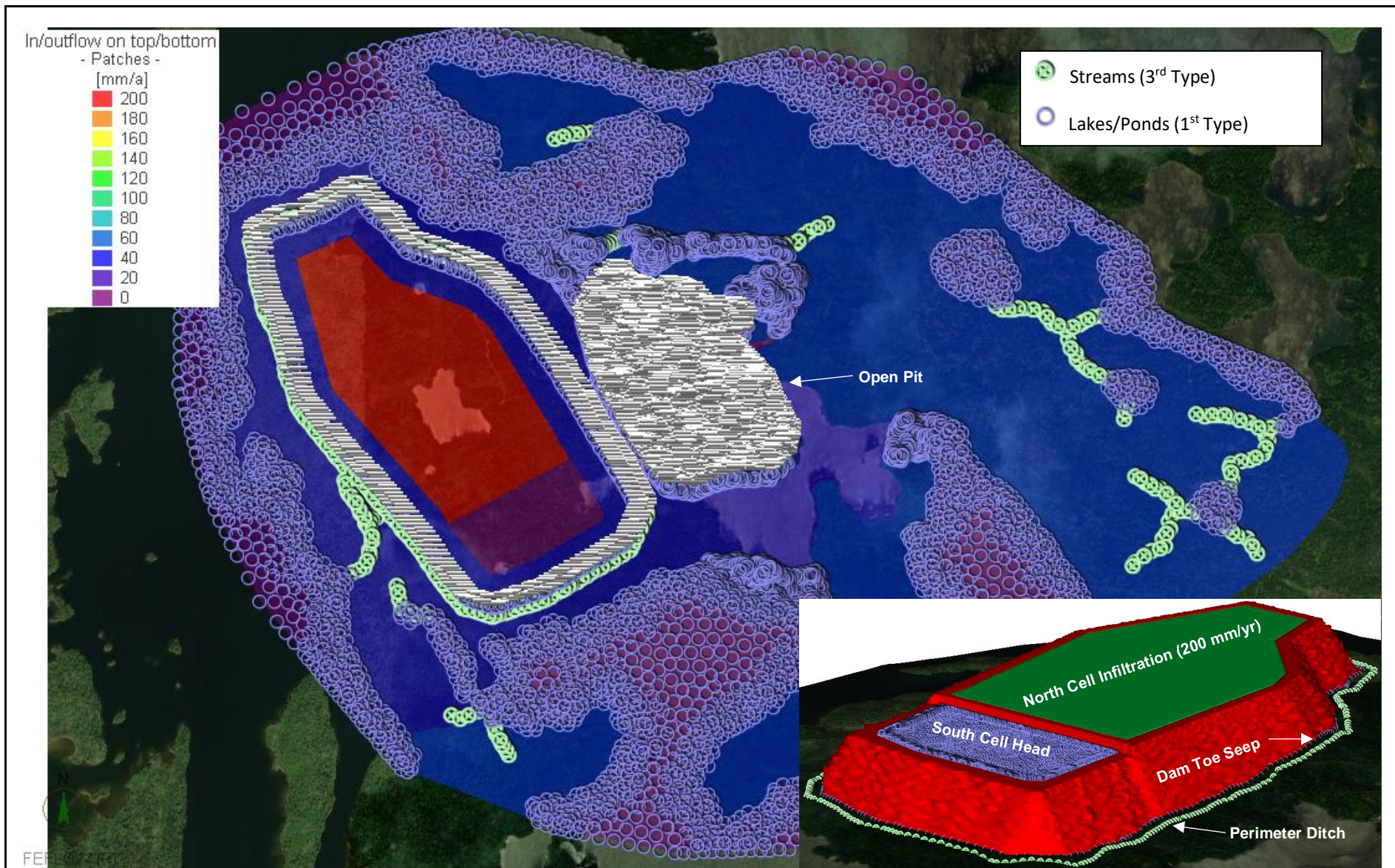
Project No: ONS2104

Date: 29-Jun-23

Rev: 0

Springpole Gold Project – 2023 Hydrogeological Modelling Report

Mining Phase 3D Model View



**FIRST MINING
GOLD**

Figure No: 6-3

Project No: ONS2104

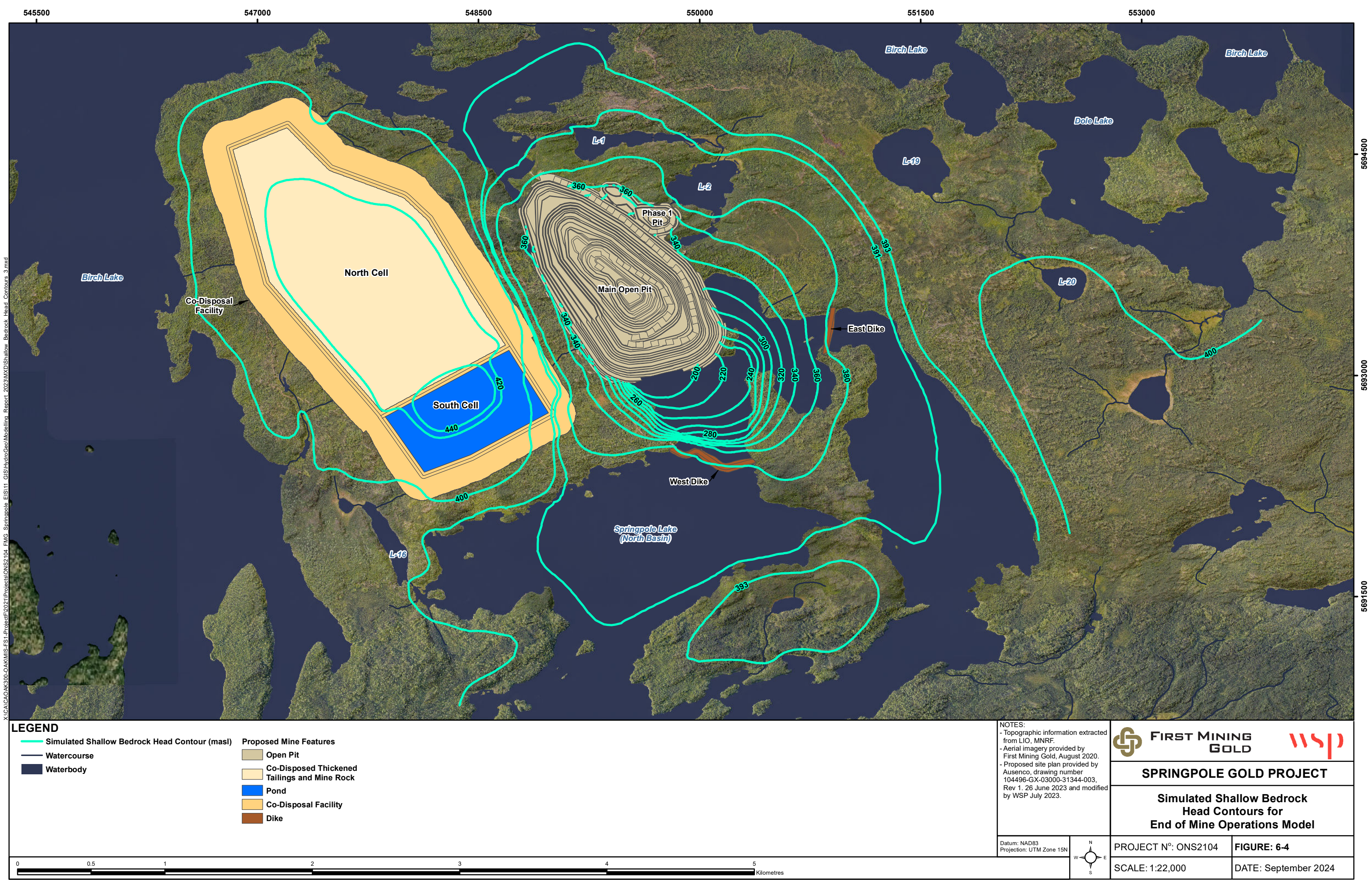
Springpole Gold Project – 2023 Hydrogeological Modelling Report

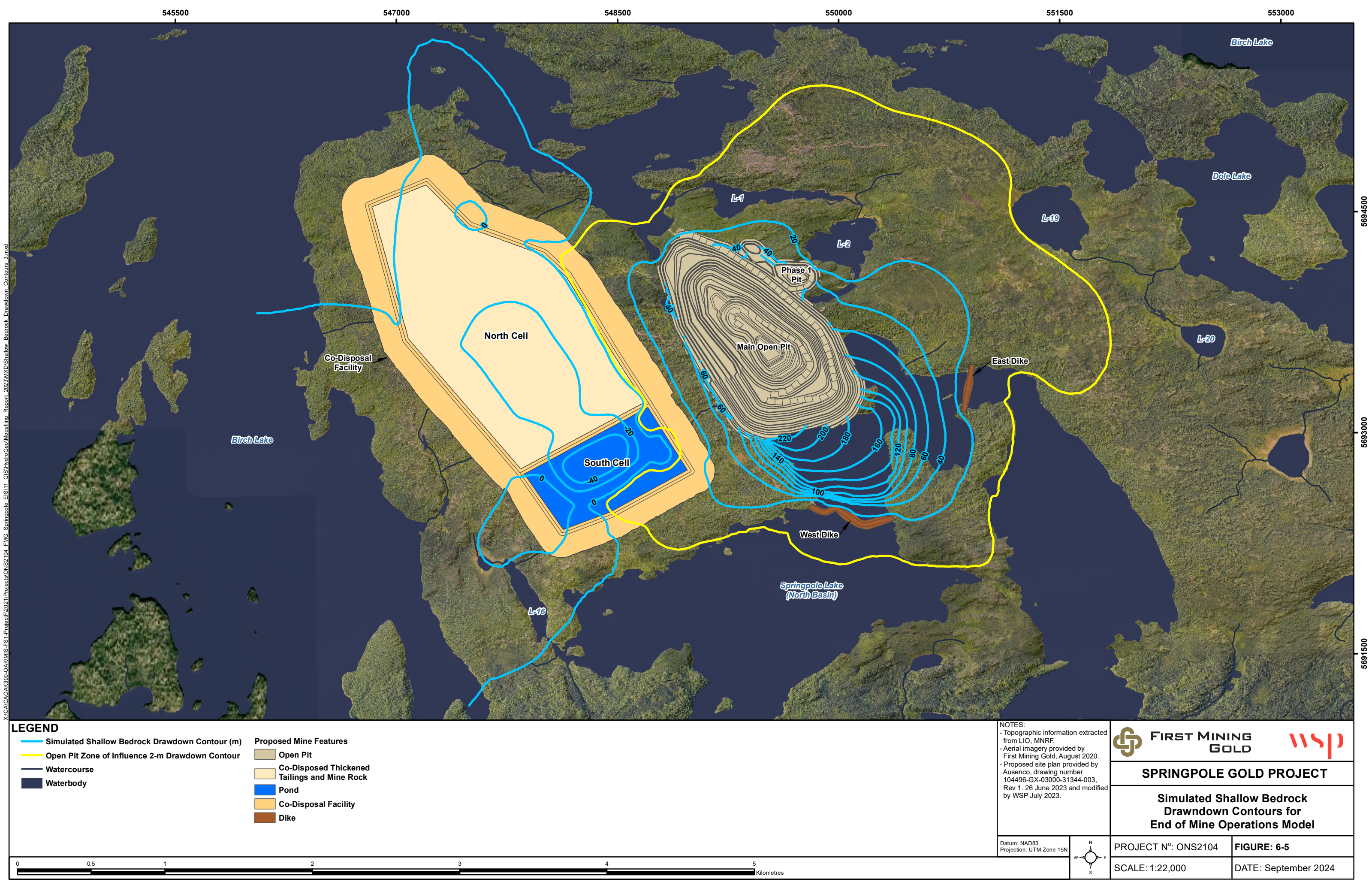


Date: 29-Jun-23

Rev: 0

Simulated Boundary Conditions for EoMO Model





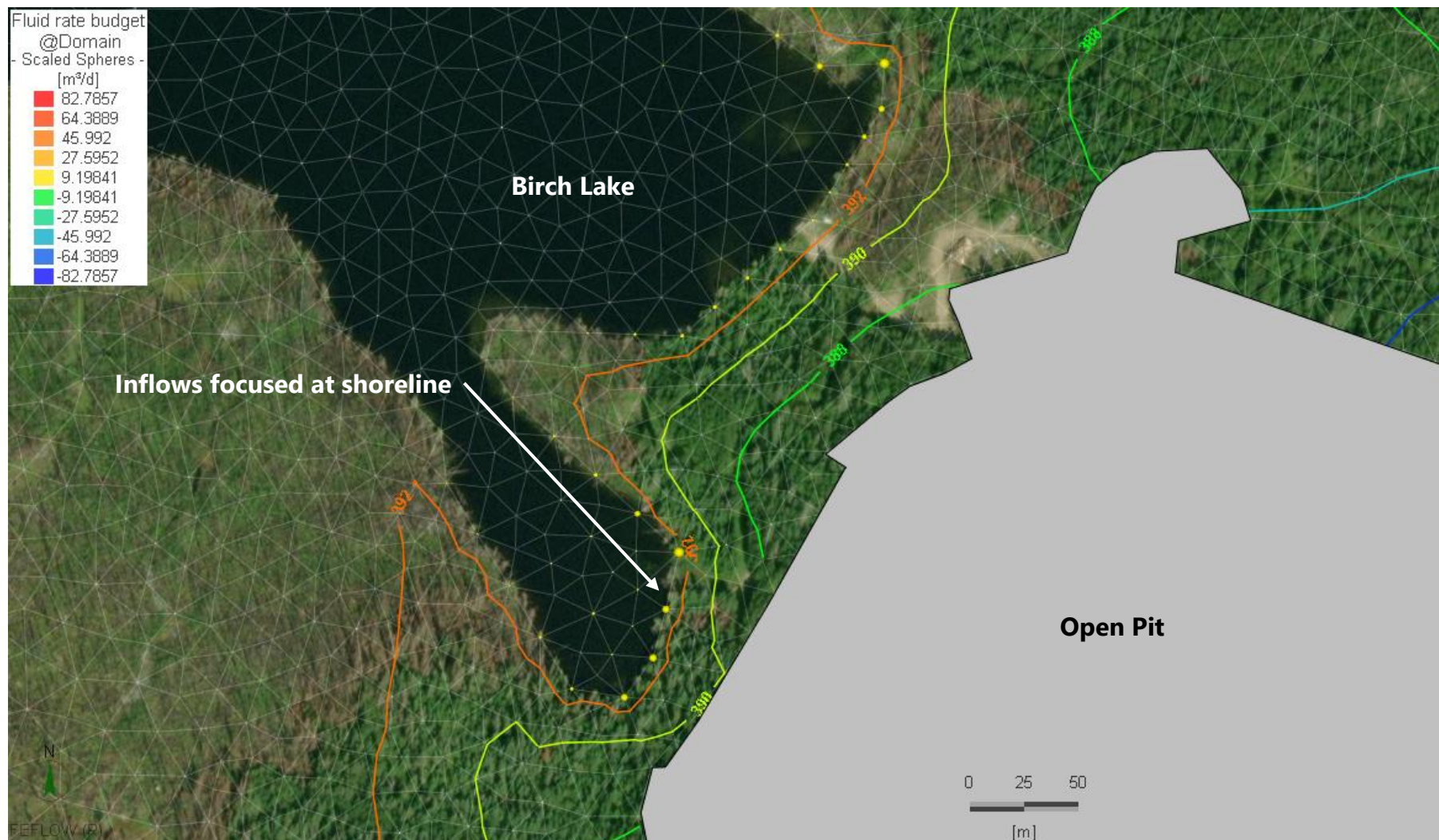


Figure No: 6-6

Project No: ONS2104

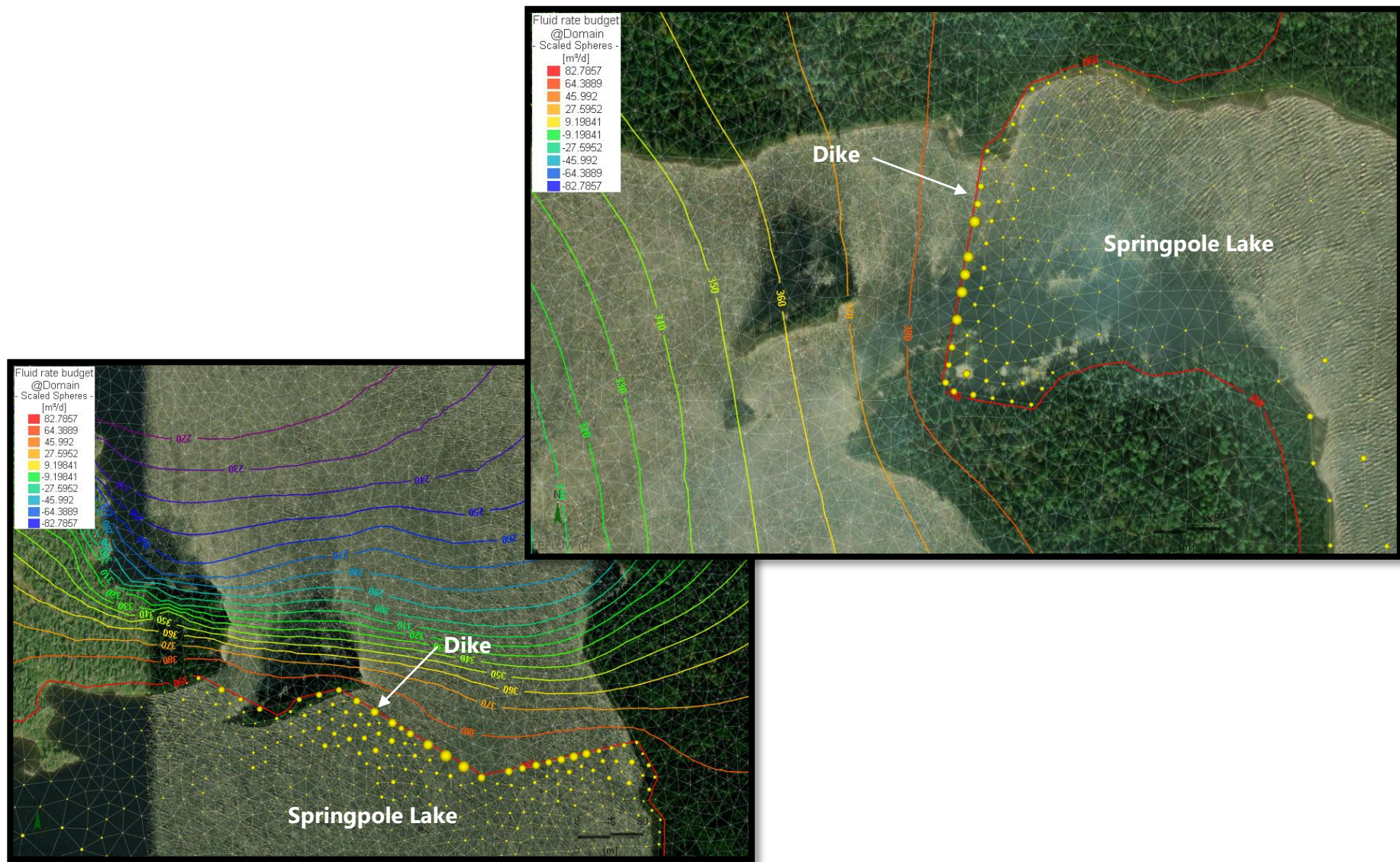
Springpole Gold Project – 2023 Hydrogeological Modelling Report



Date: 29-Jun-23

Rev: 0

Simulated Budgets at Birch Lake Shoreline



**FIRST MINING
GOLD**

Figure No: 6-7

Project No: ONS2104

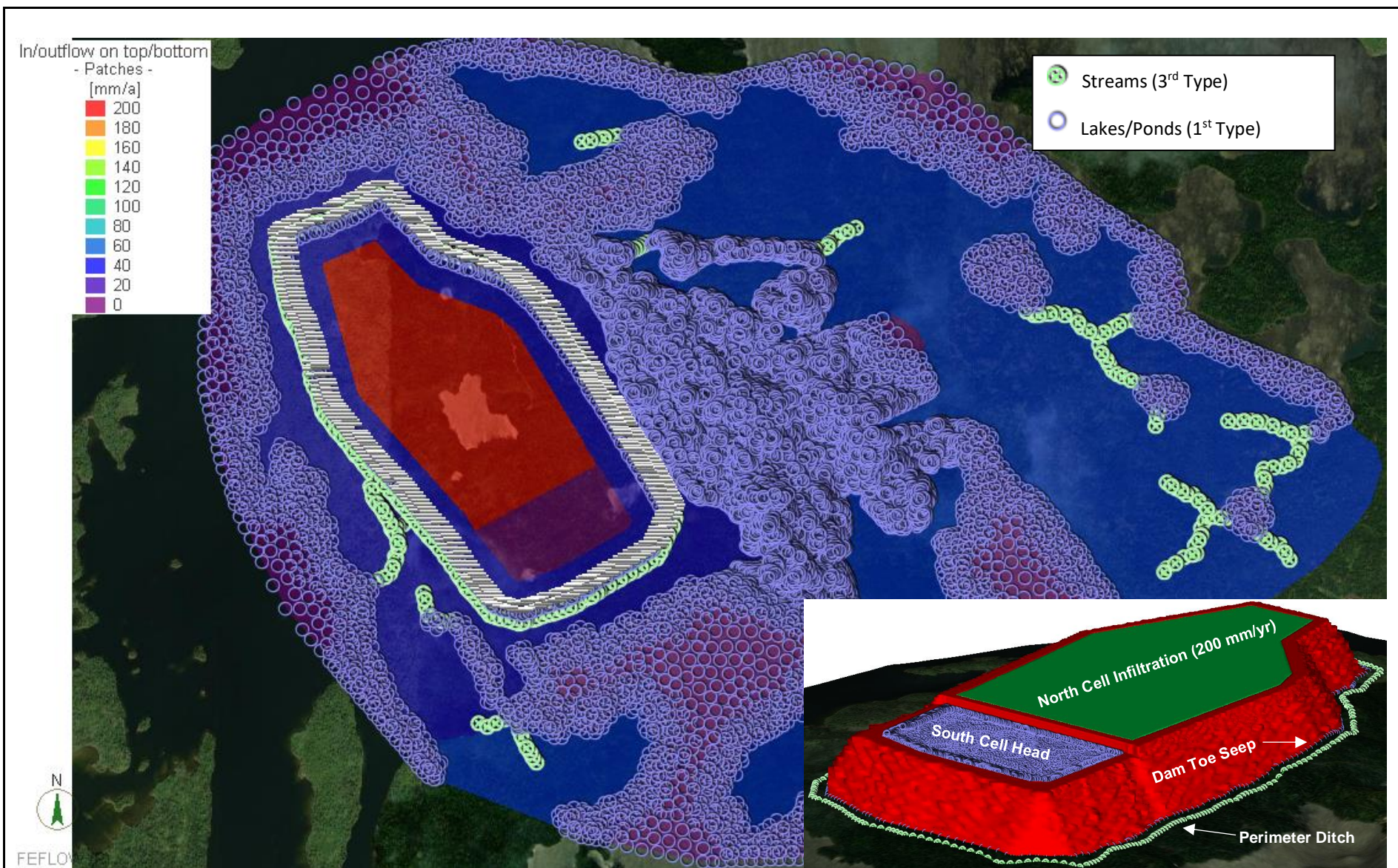
Springpole Gold Project – 2023 Hydrogeological Modelling Report



Date: 29-Jun-23

Rev: 0

Simulated Budgets at Springpole Lake Dikes



**FIRST MINING
GOLD**

Figure No: 6-8

Project No: ONS2104

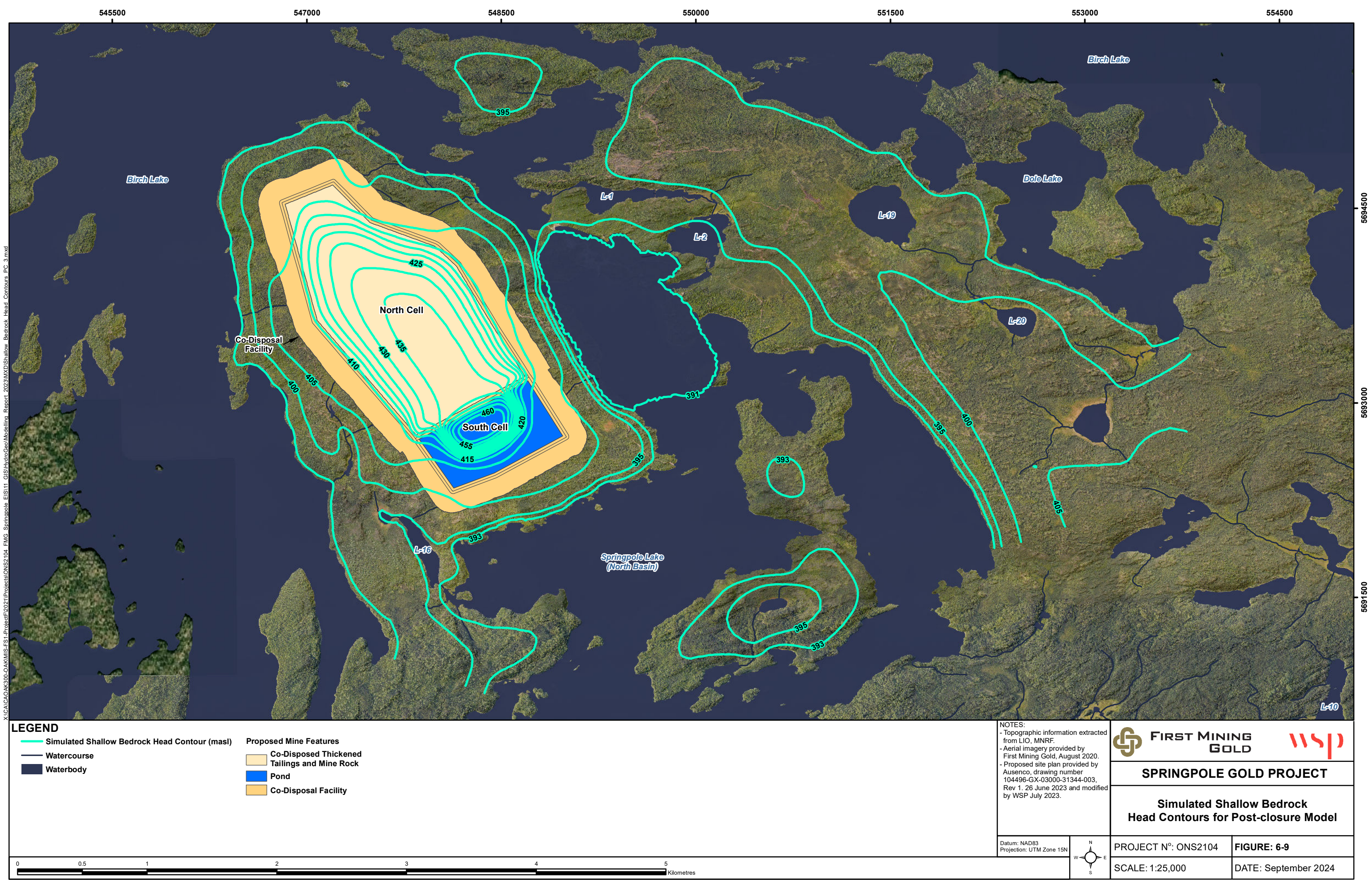
Springpole Gold Project – 2023 Hydrogeological Modelling Report



Date: 29-Jun-23

Rev: 0

Simulated Boundary Conditions for Post-Closure Model



547000

548000

549000

Birch Lake

Birch Lake

L-1

5695000

5694000

5693000

5692000

Springpole Lake
(North Basin)

L-16

North Cell

South Cell

Co-Disposal
Facility**LEGEND**

— Watercourse

■ Waterbody

Proposed Mine Features■ Co-Disposed Thickened
Tailings and Mine Rock

■ Pond

■ Co-Disposal Facility

■ Captured Seepage

Seepage Bypass Pathways

■ Node 4

■ Node 5

■ Node 6

■ Node 7

■ Node 8

■ Pit Area (North Cell)

■ Pit Area (South Cell)

NOTES:

- Topographic information extracted from LIO, MNRF.
- Aerial imagery provided by First Mining Gold, August 2020.
- Proposed site plan provided by Ausenco, drawing number 104496-GX-03000-31344-003, Rev 1. 26 June 2023 and modified by WSP July 2023.

Datum: NAD83
Projection: UTM Zone 15N

**FIRST MINING
GOLD****SPRINGPOLE GOLD PROJECT****Simulated Co-Disposal Facility Seepage
Pathway for Post-closure Model**

PROJECT N°: ONS2104

FIGURE: 6-10

SCALE: 1:15,000

DATE: September 2024

0 125 250 500 750 1,000
Metres

7.0 SENSITIVITY ANALYSIS

Sensitivity analysis was done to examine how variation in parameters affects the results for variants that were expected to result in increased seepage bypass from the CDF or increased groundwater inflow rates to the open pit. It should be noted, however, that it is equally probable for most variants that conditions exist that would result in reduced environmental effects. For example, the in situ bedrock may have lower hydraulic conductivity than simulated in the base case (i.e., calibrated value), which would result in decreased seepages and open pit inflows. A series of 12 model sensitivity variants were simulated for EoMO (Section 7.1) and post-closure (Section 7.2) conditions to assess the sensitivity of simulation outputs to key model inputs. Detailed model outputs assessed as part of the sensitivity analysis were generally selected based on the simulation case. For example, detailed seepage distributions for the CDF south cell were assessed for variant 6, where the permeability of south cell tailings was increased. In addition to the 11 3D model sensitivity variants, a series of model runs was conducted using specially prepared 2D cross sectional model, representing the south cell during post-closure conditions, to assess the sensitivity of CDF seepages to the embankment liner effectiveness (i.e., permeability). A summary of the simulated variants is given in Table 7-1. The location and orientation of the fault introduced for sensitivity variants 3 and 10 is given in Figure 7-1

7.1 End of Mine Operations (Variants 0 to 5)

The main output of interest for EoMO sensitivity cases was the effect of simulated input parameters on the groundwater–surface water balance (primarily the effects on the simulated open pit groundwater inflow rate). Sensitivity parameters were thus selected for parameters expected to yield the greatest changes in open pit inflows. The resulting simulated water budgets for variants 0 to 5 are given below in Table 7-2. As with the previously reported groundwater budgets, values in this table represent net water budgets, which include losing and gaining components. The open pit represents a gaining only feature in this case.

Open pit inflow rates in Table 7-2 range from 3,034 m³/d (base case) to 10,630 m³/d (variant 4). The least sensitive parameter in this table is the lake bed sediments K value (variant 5). This is due to the thickest zones of the lake bed sediments being removed as part of open pit development and the Springpole Lake dikes being placed at locations of minimal sediment depth (i.e., flows from the lake to the open pit are forced through bedrock). The extent of the low RQD zone has the greatest effect on the simulated open pit inflow rate, which basically acts to shorten the hydraulic distance between Springpole Lake and Birch Lake from the open pit, thereby increasing flows. This is similar in concept to variant 1 (host bedrock hydraulic conductivity), although the effect on simulated flows is less.

7.2 Post-closure (Variants 6 to 10)

Post-closure sensitivity variants focused primarily on the simulated seepages from the north and south cells of the CDF. Detailed particle tracking was, therefore, conducted on an individual basis depending on the simulation case. In addition to the simulated CDF seepages, groundwater budgets were also analyzed for each of the hydrological nodes to assess the effects on groundwater–surface water interactions.

The simulated water budgets for post-closure sensitivity variants 6 to 10 are given in Table 7-3. Values in Table 7-3 show that there is generally minor sensitivity of the simulated post-closure water budgets to the selected parameters for the post-closure conditions. The largest deviation between these sensitivity variants is the amount of groundwater discharge to the pit area for variant 10. This is due to the influence of the east–west trending SW-2 fault in this simulation, which diverts more flow in the south cell area towards the open pit area. This is supported by the head contours presented in Figure 7-2, which show a deflection in computed head contours towards the simulated fault.

Seepage analyses were conducted for sensitivity variants 6 to 10 in the same manner described in Section 6.0. Detailed particle tracking was done for select variants for south cell (variants 6, 8 and 10) and north cell (6 and 8) based on their anticipated response. A summary of the overall seepages for all post-closure variants is given in Table 7-4.

For the south cell, results presented in Table 7-4 show that the total seepage is most sensitive to the permeability of tailings within the south cell (variant 8). The total amount of bypass, however, is most sensitive to the presence of the potential east-west trending bedrock structure underlying the south cell (variant 10), which results in a total south cell bypass of 24% (compared to the base case value of 9%). Variant 6 shows that an increase in the hydraulic conductivity of CDF area shallow bedrock predicts a slightly less, although similar, amount of total seepage and bypass compared to variant 8. As would be anticipated, variants 7 and 9 show minimal effect on the amounts of total seepage and bypass for the south cell; overburden is of limited prevalence (variant 7), and the applied north cell recharge has limited influence on south cell seepage (variant 9). The simulated south cell seepage distributions for sensitivity variants 6, 8 and 10 are given in Table 7-5.

South cell simulated seepage rates to hydrological nodes 4, 5, 6 and 8 in Table 7-5 are all similar between variants; however, variant 8 shows an increase in seepage to node 7 to approximately 16 m³/d, largely a result of, and only representing a small portion of, the increase in total seepage of 343 m³/d compared to the base case (i.e., 866 m³/d versus 523 m³/d). The largest deviation in Table 7-5 is the increase in seepage bypass reporting to the open pit area in variant 10, which shows an increase to 91 m³/d compared to the base case value of 19 m³/d. This is due to the presence of the east-west trending bedrock structure (with increased permeability) that is introduced to the model for this variant, which allows increased hydraulic connection to the open pit area.

North cell seepage results in Table 7-4 show that the total amount of seepage bypass from the north cell is most sensitive to the applied infiltration to the north cell (variant 9), where a 50% increase in infiltration yields a 37% increase in bypass seepage (i.e., the majority of the excess infiltration flows towards the perimeter dam toes / ditches). This is because the excess infiltration flows preferentially laterally within the tailings above the bedrock towards the perimeter dams, rather than percolates into the bedrock. Simulated north cell seepage distributions for sensitivity variants 6 and 9 are given in Table 7-6. Variant 9 shows that the increase in seepage bypass is fairly evenly distributed across the hydrological nodes.

7.3 South Cell Embankment Liner Effectiveness (Variant 11)

A simplified 2D cross sectional model was prepared to simulate the effects of varying south cell embankment liner performance (Variant 11). The simulated cross section is shown in Figure 7-3. Hydraulic conductivity values for model layers were set equal to the 3D predictive model values (Table 5-4). Similar to the 3D models, a constant head boundary condition was applied along the tailings surface (assumed head of 480 m), a seepage node was applied at the downstream-side toe, seepage nodes were applied to a depth of 1 m at a distance of 60 m from the downstream-side toe to simulate the effects of perimeter ditches, and constant head nodes were applied approximately 300 m from the downstream toe at a head of 390 m to simulate Springpole Lake.

Manufacturer documentation specifications for a representative GCL indicate a maximum hydraulic conductivity of 5×10^{-11} m/s (Terrafox 2023). To test the effect of liner permeability on predicted seepage rates, five simulations were run with liner permeabilities ranging from completely impermeable to 5×10^{-11} m/s. Because numerical element size in the cross sectional model is considerably larger than the GCL, effective permeabilities for the liner were computed based on the model liner layer thickness (2 m), assumed in situ GCL hydrated thickness of 10 mm, and the in situ GCL permeability (up to 5×10^{-11} m/s) so that the simulated fluxes through the liner were equivalent.

A summary of the 2D simulations is provided in Table 7-7. Simulated flows from the model are expressed in cubic metres per day per metre ($\text{m}^3/\text{d}/\text{m}$; i.e., volumetric flow per unit width). The inflow column indicates the total seepage inflow to the model at the tailings surface boundary condition. The capture field represents the combined quantity of seepage flow discharging to the dam toe and perimeter collection ditch (though it should be noted that the majority of capture flow is predicted to discharge at the dam toe for all simulated cases). Finally, the bypass field represents the amount of seepage discharging to the receiver.

Results in Table 7-7 illustrate several key insights:

- As the simulated liner permeability increases, the overall seepage inflow to the model increases.
- The majority of incremental seepage flow increases are captured (at the dam toe).
- There is a negligible increase in seepage bypass between cases, despite the overall increase in seepage inputs. Seepage flows that pass through the liner, entering the permeable dams, have a very strong tendency to discharge at the dam toe. The simulated bypass from the impermeable to maximum liner permeability cases shows only an approximate 5% increase.

Thus, degradation, imperfections, or otherwise increased permeability of the liner is likely to result in increased seepage flows to the perimeter dams (and subsequently the perimeter ditches), with only minimal increase in seepage predicted to bypass the collection ditches and discharge to surface water receivers (and the open pit during operations). The 2D model result findings show that flows entering the perimeter dams tend to discharge at the dam toes is consistent with the 3D model simulations, which show that the preferred pathway of seepage is into the perimeter dams and to subsequently discharge at the dam toes.

Two-dimensional simulations were also conducted to assess the effect of introducing a liner at the base of the CDF south cell on amount of seepage emanating from the south cell, which are discussed under separate cover in WSP 2023. Results from this modelling indicate that the incorporation of a basal liner to the CDF south cell (i.e., in addition to the liner along the embankments) results in a minimal decrease in seepage bypass compared to the case with the liner only on the dam embankments.

Table 7-1: Sensitivity Simulation Variants

Simulation ID	Model Configuration	Sensitivity Parameter	Parameter Change
Variant 0	End of mine operations	Groundwater recharge	Increase by 50%
Variant 1	End of mine operations	Other host rock K	Increase $\times 3.2$ (half-order)
Variant 2	End of mine operations	CDF rock K	Increase $\times 3.2$ (half-order)
Variant 3 ⁽¹⁾	End of mine operations	E-W fault SW-2	Introduced to model ⁽¹⁾
Variant 4	End of mine operations	Low RQD zone extent	Increase extent by 200 m
Variant 5	End of mine operations	Lake bed sediment K	Increase $\times 3.2$ (half-order)
Variant 6	Post-closure	CDF shallow rock K	Increase $\times 3.2$ (half-order)
Variant 7	Post-closure	Overburden K	Increase $\times 5.9$ (to geometric mean)
Variant 8	Post-closure	South cell tailings K	Increase $\times 3.2$ (half-order)
Variant 9	Post-closure	North cell recharge	Increase to 300 mm/yr
Variant 10 ⁽¹⁾	Post-closure	E-W fault SW-2	Introduced to model ⁽¹⁾
Variant 11	2D south cell post-closure	Liner K	Impermeable to manufacturer specific upper limit ⁽²⁾

Notes:

(1) Fault SW-2 simulated as an approximately 40 m width feature with a hydraulic conductivity of 2×10^{-6} m/s (i.e., the same as the low RQD zone). This superseded bedrock layers from surface to the bottom of the model.

(2) Manufacturer specifications for the liner indicate a maximum liner permeability of 5×10^{-11} m/s (TerraFix 2023).

ID = identification; E-W = east-west.

Table 7-2: Simulated Groundwater Budgets for End of Mine Operations Sensitivity Analysis

Variant	Hydrological Node Groundwater Budget (m ³ /d) ⁽²⁾								
	1	2	3	4	5	6	7	8	Open Pit
EoMO⁽¹⁾	-235	-49	-13	42	-657	-2	134	566	3,034
0	-189	-10	9	54	-503	57	155	853	3,162
1	-751	-294	-129	37	-2,368	-245	107	367	6,628
2	-271	-49	-13	53	-985	-135	162	615	4,161
3	-236	-50	-14	54	-826	-3	127	460	3,524
4	-473	-87	-17	39	-7,308	-206	108	482	10,630
5	-238	-50	-15	38	-790	-11	114	562	3,095

Notes:

(1) Base case model.

(2) Sign convention taken with respect to surface water (+ = gaining; - = losing).

Table 7-3: Simulated Groundwater Budgets for Post-closure Sensitivity Analysis

Variant	Hydrological Node Groundwater Budget (m ³ /d) ⁽²⁾								
	1	2	3	4	5	6	7	8	Pit Area
Post-closure⁽¹⁾	54	-2	-9	38	628	164	113	641	280
6	54	-2	-9	42	645	172	124	656	316
7	52	-8	-16	50	649	177	122	651	298
8	54	-2	-9	42	631	163	117	642	294
9	54	-2	-9	40	630	166	118	645	278
10	54	-1	-9	39	628	162	114	641	362

Notes:

(1) Base case model.

(2) Sign convention taken with respect to surface water (+ = gaining; - = losing).

Table 7-4: Summary of Post-closure Variant Seepages

Variant	South Cell Seepage (m ³ /d)			North Cell Seepage (m ³ /d)		
	Total	Capture	Bypass	Total	Capture	Bypass
Post-closure ⁽¹⁾	523	475	48	947	855	92
6	790	746	44	947	835	112
7	545	491	54	947	827	120
8	866	814	52	947	866	81
9	509	463	46	1,423	1,297	126
10	526	404	122	947	844	103

Note:

(1) Base case model.

Table 7-5: Simulated South Cell Seepages for Model Variants (post-closure)

Variant	Total (m ³ /d)	Capture (m ³ /d)	Bypass (m ³ /d)	Hydrological Node South Cell Seepage (m ³ /d)					
				4	5	6	7	8	Pit Area
Post-closure ⁽¹⁾	523	475	48	5	24	0	0	0	19
6	790	746	44	5	21	0	2	0	15
8	866	814	52	5	18	0	16	0	13
10	526	404	122	4	22	0	0	0	91

Note:

(1) Base case model.

Table 7-6: Simulated North Cell Seepages for Model Variants (post-closure)

Variant	Total (m ³ /d)	Capture (m ³ /d)	Bypass (m ³ /d)	Hydrological Node North Cell Seepage (m ³ /d)					
				4	5	6	7	8	Pit Area
Post-closure ⁽¹⁾	947	855	92	0	0	19	26	26	21
6	947	835	112	0	0	22	34	28	29
9	1,423	1,297	126	3	3	23	32	38	26

Note:

(1) Base case model.

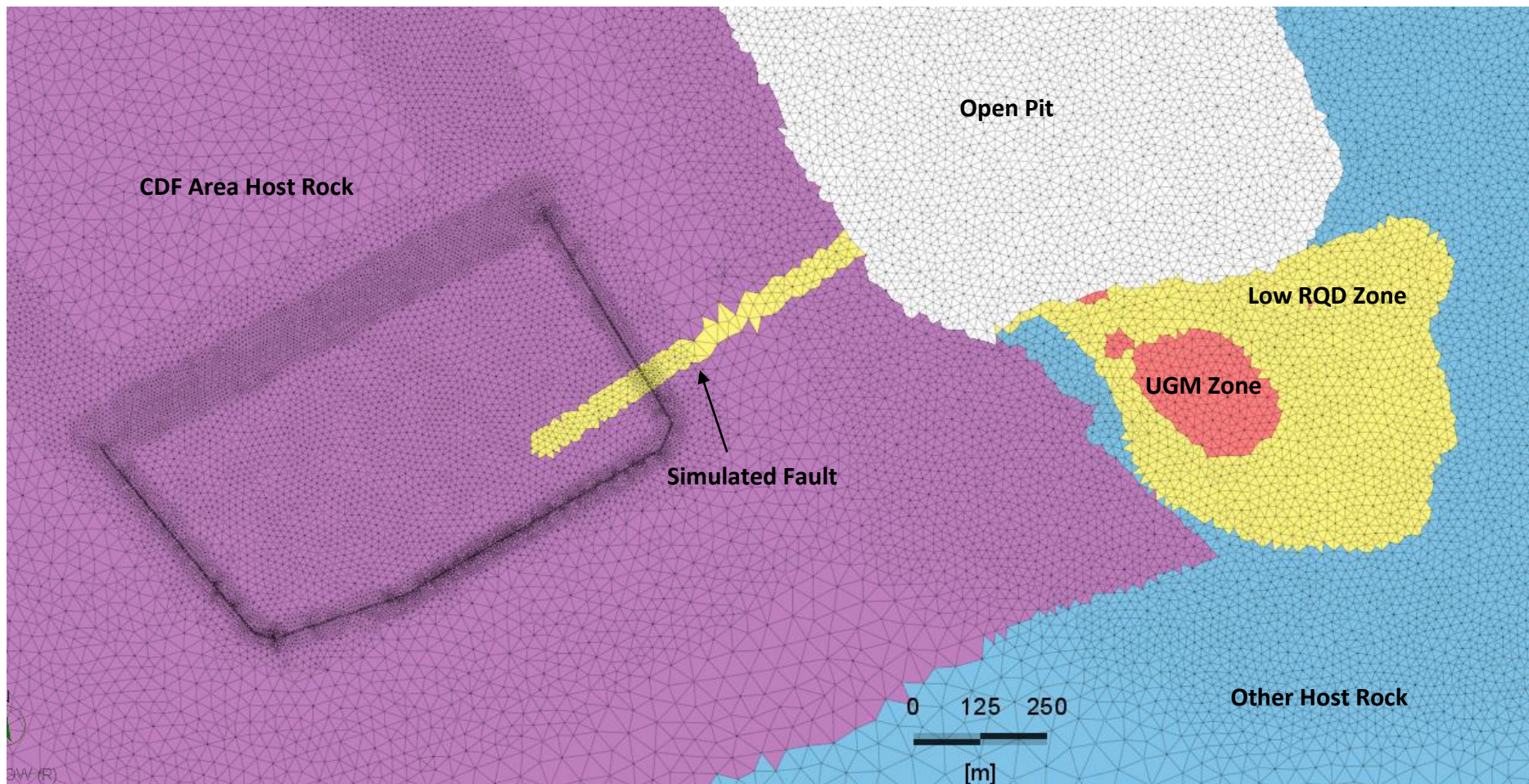
Table 7-7: 2D Model Simulated Flows for Variant 11

Liner Hydraulic Conductivity (m/s)		Flows (m ³ /d/m)		
In situ	Model Value ⁽¹⁾	Inflow	Capture	Bypass
0 (impermeable)	Inactive	0.360	0.341 (95%) ⁽²⁾	0.0199 (5%)
5.0×10^{-12}	1.0×10^{-9}	0.618	0.598 (97%)	0.0202 (3%)
1.0×10^{-11}	2.0×10^{-9}	0.804	0.783 (97%)	0.0204 (3%)
3.0×10^{-11}	6.0×10^{-9}	1.255	1.234 (98%)	0.0210 (2%)
5.0×10^{-11}	1.0×10^{-8}	1.447	1.426 (98%)	0.0210 (2%)

Notes:

(1) Model values computed based on in situ hydraulic conductivity, thickness (10 mm) and numerical grid layer thickness (2 m) to maintain equivalency for simulated fluxes.

(2) Percentages for capture and bypass calculated as proportion of total inflow.



**FIRST MINING
GOLD**



Figure No: 7-1

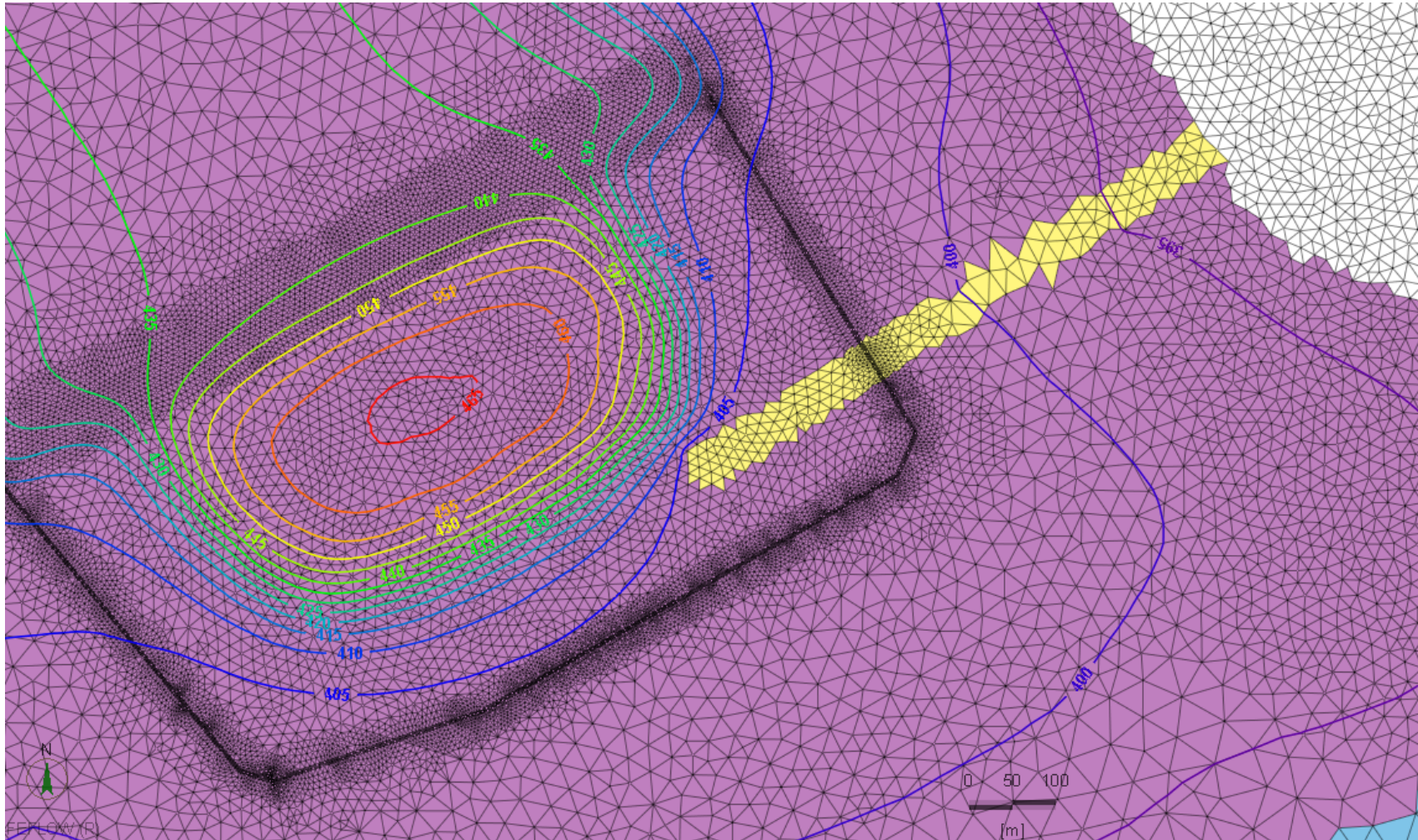
Project No: ONS2104

Date: 29-Jun-23

Rev: 0

Springpole Gold Project – 2023 Hydrogeological Modelling Report

E-W Fault SW-2 Location for Sensitivity Simulations



**FIRST MINING
GOLD**



Figure No: 7-2

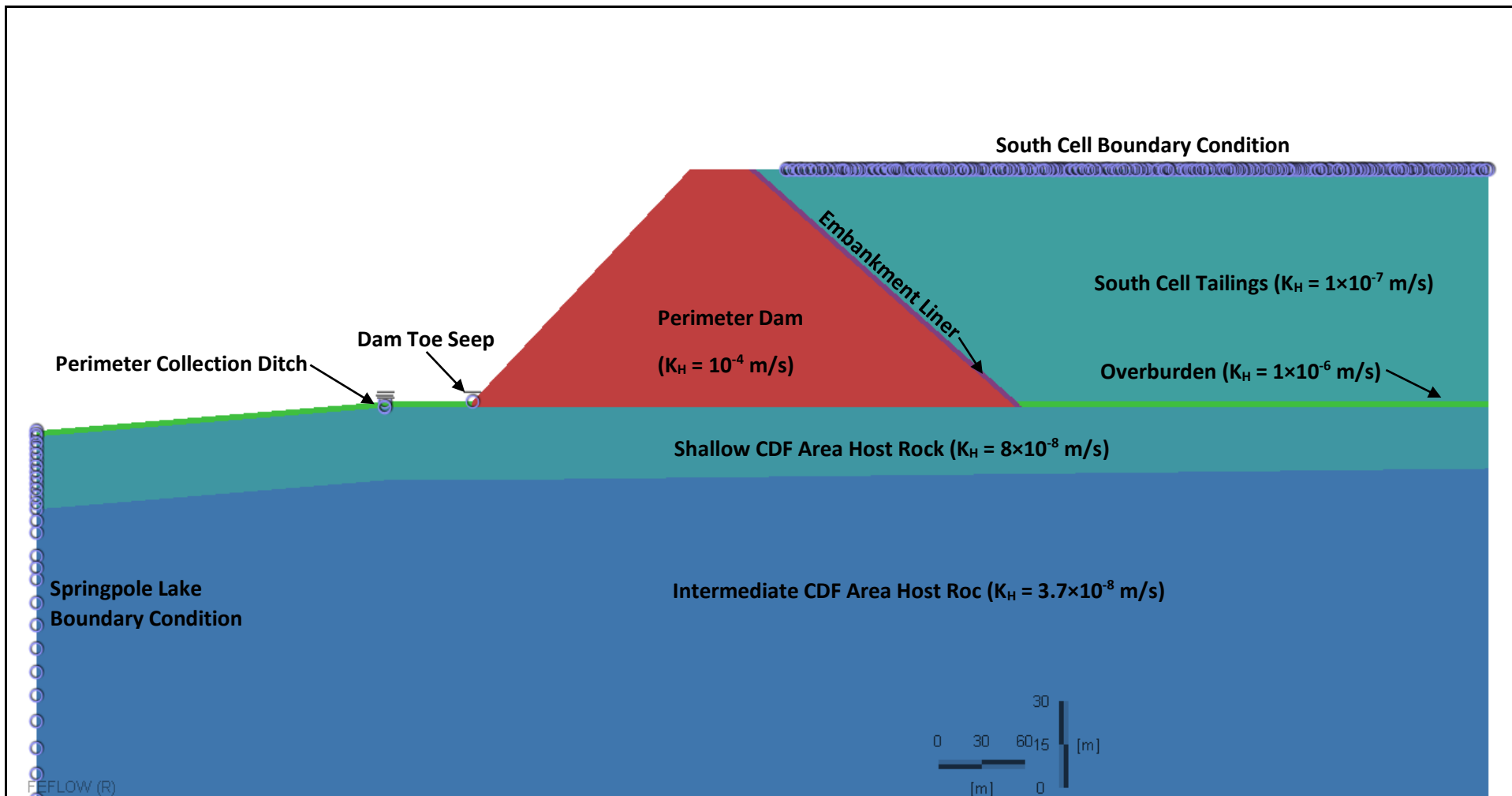
Project No: ONS2104



Date: 29-Jun-23

Rev: 0

Springpole Gold Project – 2023 Hydrogeological Modelling Report

Variant 10 Shallow Bedrock Head Contours (masl)



 FIRST MINING GOLD	Figure No: 7-3	Springpole Gold Project – 2023 Hydrogeological Modelling Report
	Project No: ONS2104	
	Date: 29-Jun-23	2D Model for Variant 11 Simulations
	Rev: 0	

8.0 SUMMARY AND CONCLUSIONS

A numerical groundwater flow model has been developed and calibrated to simulate existing conditions at the proposed Springpole Gold Project site using information gathered as part of baseline characterization activities.

Following model calibration, the groundwater flow model was used to conduct predictive simulations for two phases of the mine life, representing EoMo and post-closure conditions, to estimate effects of mine infrastructure / operation on the surrounding groundwater environment. In addition to base case simulations for each phase, a suite of sensitivity simulations was run to assess the implications of parameter uncertainty for key model inputs on the estimated effects with outputs.

Simulations for the EoMO focused on the estimation of groundwater inflow rates to the dewatered open pit and the overall effects on groundwater–surface interactions (i.e., groundwater budgets). Sensitivity was only run for variants that were expected to result in a higher environmental impact. Based on these simulations:

- Overall, simulated seepage bypass rates (i.e., fugitive seepage) from the CDF to nearby surface water receivers are very low in comparison to the overall water balance for the primary receivers (i.e., Springpole Lake and Birch Lake). Simulated seepage rates for these features are generally in the tens of cubic metres per day range, which represent only a small fraction of the overall water budgets for these large lakes.
- The simulated groundwater inflow rate to the open pit for the base-case is 3,034 m³/d. This ranges from 3,095 to 10,612 m³/d in sensitivity analyses, with the greatest value corresponding to the case where the low RQD zone is increased in spatial extent by 200 m.
- Water budget analysis shows that the largest sources of water to open pit inflows are Springpole Lake and Birch Lake, which represent the closest major surface water features (i.e., boundary conditions). The largest relative changes in groundwater budgets are generally for the smaller lakes / ponds proximal to the open pit. These effects on groundwater budgets are expected to be relatively short term and rebound readily as the open pit refills after closure.

Simulations for conditions post-closure (i.e., long after mine closure) focused on the estimation of seepage rates emanating from the CDF to surrounding surface water features. Based on these simulations:

- For the base case model, approximately 90% of the seepages from both the north and south cells of the CDF discharge at the downstream toes of the perimeter CDF dams (i.e., “capture,” which would subsequently runoff to the perimeter collection ditches). The remaining approximately 10% (i.e., “bypass”) discharges to the various surface water receivers surrounding the CDF. In all post-closure variants, the total amount of seepage bypass was less than 225 m³/d, which represents only a small fraction of the overall water balance for Birch and Springpole lakes.
- The north cell seepage is driven by the applied north cell infiltration rate of 200 mm/yr. The primary receiver of the 10% of north cell bypass is Birch Lake (i.e., nodes 6 to 8). The amount of north cell bypass is most sensitive to the applied north cell infiltration, where a 50% increase in infiltration yields a 37% increase in bypass.

- Seepage from the south cell is driven by the constant head boundary condition applied at its top surface (representing assumed shallow groundwater depth conditions). Similar to the north cell, approximately 91% of the total seepage from the south cell discharges to the perimeter dam toes (and subsequently the perimeter ditches) in the base-case simulation. Sensitivity analysis for the south cell shows that the total seepage is most sensitive to the assumed permeability of tailings in the south cell. The total amount of bypass, however, is most sensitive to the presence of a potential east-west trending bedrock structure underlying the south cell (corresponding to a topographic lineament, simulated as a zone of increased permeability for sensitivity analysis), which results in an increase from 9% to 24% bypass.
- Sensitivity analysis of the performance of the south cell embankment liner was conducted to assess varying liner performance, corresponding to a range of assumed liner permeabilities in a 2D cross sectional model. Simulation results showed that, while increasing liner permeability results in increased total seepage, the total amount of bypass increases only very minorly since seepage penetrating / exfiltrating the liner enters the dams and subsequently discharges at the toe of the dam and would be captured by the perimeter ditches.

Numerical groundwater model simulations presented in this report thus further emphasize that the primary factor of hydrogeological interest for the Project is the hydraulic conditions of bedrock at site. Specifically:

1. The hydraulic conductivity of bedrock surrounding the open pit (represented conceptually by both / either of the extent of the low RQD zone or the overall hydraulic conductivity of the other host bedrock zone) has the most influence on the simulated groundwater inflow rate to the open pit and the effects on groundwater–surface water balance.
2. The hydraulic conductivity of bedrock immediately underlying the CDF influences the total rate of seepage emanating from the south cell. Changes in the assumed hydraulic conductivity of shallow bedrock exert a similar level of control on predicted seepage rates as changes in the assumed hydraulic properties of the tailings themselves.

9.0 CLOSING

This hydrogeological modelling report was prepared for First Mining Gold Corp. by WSP. The quality of information, conclusions and scheduling estimates contained here is consistent with the level of effort involved in WSP's services and based on 1) information available at the time of preparation; 2) data supplied by outside sources; and 3) the assumptions, conditions and qualifications set forth in this report.

Yours sincerely,

WSP Canada Inc.

Prepared by:

Prepared by:

Keenan Lamb, M.Sc.E., P.Eng.
Hydrogeological Engineer

Brad Markham, MSc., P.Geo.
Principal Geoscientist

Reviewed by:

Simon Gautrey, M.Sc., M.B.A., P.Geo., F.G.C., BCES
Senior Hydrogeological Engineer

10.0 REFERENCES

- Anderson, M., Woessner, W. and Hunt, R. 2015. Applied Groundwater Modeling – Simulation of Flow and Advective Transport- 2nd Edition. Academic Press. San Diego CA. August 2015.
- Diersch, H. 2014. FEFLOW - Finite element modeling of flow, mass and heat transport in porous and fractured media. Springer.
- Seequent Limited (Seequent). 2020. User Manual for Leapfrog Works Version 3.1.
- Singer, S.N., and Cheng, C.K., 2002. An Assessment of the Groundwater Resources of Northern Ontario. Hydrogeology of Ontario Series – Report 2.
- SRK Consulting (SRK). 2013. Technical Memorandum Structural Model of the Springpole Project. Project #2CG026.002. December 16, 2013.
- SRK Consulting (SRK)., 2024. Springpole Gold Project- 2022 Geotechnical and Hydrogeological Testing Program – Factual Report.. CAPR001609. April 2024.
- Terrafix Geosynthetics Inc. (Terrafix). 2023. Bentofix SRNWL. Thermal Lock Geosynthetic Clay Liners. <https://terrafixgeo.com>
- Wels, C., Mackie, D., and Scibek, J. 2012. Guidelines for Groundwater Modelling to Assess Impacts of Proposed Natural Resource Development Activities. British Columbia Ministry of Environment – Water Protection and Sustainability Branch. April 2012.
- Wood Environment & Infrastructure Americas (Wood). 2022. Hydrogeological Modelling Report – Springpole Gold Project. ONS2104. 2022.
- WSP Canada Inc. (WSP). 2023. Technical Decision Memorandum – Co-Disposal Facility (CDF) Liner Requirement. SP-EM-TDM-001-A. OMGM2215.200. June 27, 2023.
- WSP Canada Inc. (WSP). 2024. 2021 - 2023 Hydrogeological Field Program Report. Project No. ONS2104. 2024.